Centro de Investigación y de Estudios
Avanzados del Instituto Politécnico Nacional

Physics Department

Effective field theories in lepton flavor violating processes

Presented by
Bibiana Marcela Marín Ochoa

In Partial Fulfilment of the Requirements for the Degree
Doctor of Science in the Specialty of Physics

Advisor: **Dr. Pablo Roig Garcés**

Mexico City May 2022

A mis padres, Guillermo y Luz Elena,
por todo y por tanto.

Agradecimientos

Primero a mis padres, Luz Elena y Guillermo, por su amor y motivación constante, además de cuidar de Melissa miestras estuve fuera del país. A mi compañero de vida, Frank, por su paciencia y su amor, y por convertirse en mi soporte emocional. A mis hermanas, Mariluz e Ivonne, y por supuesto a mi amada sobrina, Carolina, quienes siempre estuvieron presentes para brindarme su apoyo y compañía. A Melissa, cuya simple existencia ilumina mi vida.

A mi asesor Pablo Roig por su paciencia y el tiempo invertido en mi formación acádemica, así como, por su compromiso y dedicación para con sus estudiantes. A Alejandro Ibarra de quien he obtenido muchos conocimientos, los cuales indudablemente han contribuido en mi desarrollo y formación profesional. A Iván Heredia y Eduard de la Cruz, por todas las enriquecedoras pláticas y discusiones respecto a mis trabajos, y por brindarme su punto de vista experimental siempre tan neccesario.

A mis sinodales, Eduard de la Cruz, Iván Heredia, Gerardo Hernández Tomé, Josué De Santiago, y Marco Arroyo, por su paciencia y tiempo invertido en la revisión de esta tesis.

A mis compañeros y amigos, a quienes conocí en mis años en el Cinvestav. Con ellos compartí la experiencia del posgrado, me mostraron un poco de la cultura méxicana, y cuya amistad hizo más grata y fructífera toda esta experiencia.

A los profesores, secretrias, personal de apoyo, y a toda la comunidad del Cinvestav, cuya labor y dedicacion me permitieron concluir satisfactoriamente con esta etapa de mi vida.

Por último, agradezco al pueblo de México por el apoyo económico recibido a través de la beca de CONACYT para mis estudios de doctorado, así como, los proyectos CB-250628 (CONACYT) y Cátedra Marcos Moshinsky 2020 (Fundación Marcos Moshinsky), sin los cuales este trabajo no hubiera podido realizarse.

Abstract

The original version of the Standard Model (SM) where only massless left-handed (L) neutrinos are present, predicts the conservation of lepton flavor. Neutrino oscillations undoubtedly imply Lepton Flavor Violation (LFV), although, for the charged sector, no lepton flavor violating process has been observed so far. Consequently, there is a strong experimental program searching for any kind of charged LFV (cLFV) observation that would lead to New Physics (NP) beyond the SM.

In the first work included in this thesis, we analyzed the flavor violating decays $\ell_i \to \ell_j \chi$, where χ is a massive gauge boson, which has not been described satisfactorily so far for ultralight χ. Observables like the decay rate exhibited an unphysical divergence in the limit of massless χ, associated with its longitudinal polarizations. We first analyze these processes from an Effective Field Theories (EFTs) framework, exhibiting the possible divergences in the limit $m_\chi \to 0$ which are however cancelled in any theory with underlying local gauge invariance. We then present two explicit models where the LFV is generated either at tree level or at one loop. We show that, because of gauge symmetry, finiteness of observables is ensured in the massless χ limit. Finally, we discuss the most salient phenomenological consequences and their relevance in the searches for this kind of decays.

In the second work, we perform an analysis of the cLFV processes $\ell_i \to \ell_j \gamma\gamma$, in an EFT approach. We build an effective Lagrangian that describes the local interaction of two charged leptons of different flavors and two photons. We show that in the scenario where only the double photon emission is allowed at tree level, loop corrections can still induce large branching ratios for $\ell_i \to \ell_j \gamma$. Through the correlation between the two processes, we show that the loop corrections can induce large rates for $\ell_i \to \ell_j \gamma$ deriving in indirect upper limits for $\ell_i \to \ell_j \gamma\gamma$. We find that our bounds are orders of magnitude better than the current limits for these processes. Finally, we demonstrate that searches for these channels are well-motivated from the theoretical point of view, showing that both these single and double-photon processes have similar probabilities within two Higgs doublet models, strengthening the case for the $\ell_i \to \ell_j \gamma\gamma$ searches.

Resumen

La versión original del Modelo Estándar, donde solo aparecen neutrinos izquierdos no masivos, predice la conservación del sabor leptónico. Las oscilaciones de neutrinos implican sin lugar a dudas violación del sabor leptónico, sin embargo, hasta ahora, no se ha observado violación de sabor leptónico en el sector cargado. En consecuencia, existe un sólido programa experimental que busca cualquier tipo de observación de violación de sabor leptónico en el sector cargado, que conduzca a una nueva física más allá del Modelo Estándar.

En el primer trabajo de esta tesis analizamos las desintegraciones que violan sabor $\ell_i \to \ell_j \chi$, donde χ es un bosón de gauge masivo, el cual, hasta ahora, no ha sido descrito satisfactoriamente para χ ultraligero. Los observables como la tasa de decaimiento exhibían una divergencia no física en el límite $m_\chi \to 0$. Presentamos entonces dos modelos explícitos donde la violación del sabor leptónico es generada a nivel árbol o a un loop. Mostramos que, gracias a la simetría gauge local, se asegura la finitud de los observables en el límite de χ sin masa. Finalmente, discutimos las consecuencias fenomenológicas más destacadas y su relevancia en las búsquedas de este tipo de desintegraciones.

En el segundo trabajo, realizamos un análisis de los procesos que violan el sabor leptónico en el sector cargado $\ell_i \to \ell_j \gamma\gamma$, en un enfoque de teoría de campos efectiva. Construimos un Lagrangiano efectivo que describe la interacción local entre dos leptones cargados de diferente sabor y dos fotones. Mostramos que en el escenario donde solamente la emisión de doble fotón es permitida a nivel árbol, las correcciones de loop pueden aún inducir probabilidades grandes para $\ell_i \to \ell_j \gamma$ derivando en límites superiores indirectos para $\ell_i \to \ell_j \gamma\gamma$. Encontramos que nuestros límites son órdenes de magnitud mejores que los límites actuales para estos procesos. Finalmente, discutimos que las búsquedas de estos canales están bien motivadas teóricamente, mostrando que tanto los procesos con un solo fotón como los procesos con dos fotones tienen probabilidades similares en los modelos de dos dobletes de Higgs, fortaleciendo así las búsquedas de $\ell_i \to \ell_j \gamma\gamma$.

Contents

Chapter 1

Introduction

Our understanding of modern elementary particle physics is based on the Standard Model, whose theoretical formulation was developed in the 1960s and 1970s [1–3]. In the minimal version of the SM massless neutrinos are assumed, so lepton flavor conservation is an automatic consequence of gauge invariance and the renormalizability of the SM Lagrangian.

Our understanding of neutrinos has changed dramatically at the end of the XX century. Thanks to the observations of neutrino oscillation [4–6] from Super-kamiokande and Sudbury Neutrino Observatory, which were confirmed later by other experiments, we have learned that neutrinos produced in a well-defined flavor eigenstate can be detected, after propagating a macroscopic distance, as a different flavor eigenstate. The simplest interpretation of this phenomenon is that the neutrinos have mass and that the neutrinos mix, *i.e.* the neutrino flavor eigenstates are different from neutrino mass eigenstates.

The discovery of neutrino oscillations implies that all so-called lepton flavor violating processes are also allowed, raising the possibility of the LFV on the charged sector. The rates for such processes, however, cannot be estimated model-independently and, hence, are expected to provide non-trivial information regarding the nature of NP. In the minimal extensions of the SM with massive neutrinos, cLFV processes have rates suppressed by a factor $(\Delta m^2_\nu/M^2_W)^2$ due to a Glashow–Iliopolous–Maiani (GIM)-like mechanism. For a difference of the neutrino mass squared of $\Delta m^2_\nu \sim 10^{-3}$ eV^2, the expected branching ratios are as small as $\sim 10^{-54,-55}$, so experiments cannot probe these signals. The situation changes drastically in other theoretical scenarios, which can predict branching ratios close to the present experimental upper bounds, and therefore they could be accessible and tested by current and future experiments.

The first search for lepton flavor violation with $\mu^+ \to e^+\gamma$ decay was made by Hincks and Pontecorvo in 1947 using cosmic-ray muons [7]. Its negative result set an upper limit of less than 10%. The searches were significantly improved when muons became artificially produced at accelerators, so in 1955, the upper limits of $\mathrm{BR}(\mu \to e\gamma) < 2 \times 10^{-5}$ and $\mathrm{BR}(\mu^-\mathrm{Cu} \to e^-\mathrm{Cu}) < 5 \times 10^{-4}$ [8] were set at the Columbia University Nevis cyclotron. Nowadays, we count on a strong

experimental program interested in the search for signals of LFV in charged leptons. The best upper limits for these types of processes are of the order of 10^{-13} from radiative muon decay, 10^{-12} for $\mu \to e$ conversion in nuclei, 10^{-8} in τ decays, $10^{-5,-7}$ in Z decays, and $10^{-3,-4}$ in Higgs decays. These upper bounds will be improved in future experiments, where we can expect the sensitivity to reach $\mathcal{O}(10^{-9}) - \mathcal{O}(10^{-10})$ in Belle-II for tau modes, $\mathcal{O}(10^{-14})$ in muon decays from the upgrade of MEG, and $\mathcal{O}(10^{-16})$ for the $\mu - e$ conversion.

The physics associated with searches for the LFV in charged-lepton processes could be sensitive to new particles and interactions beyond the SM of particle physics. Further, this issue is intimately related to the understanding of the origin of neutrino masses, which remains unknown. These processes may also play a key role in our understanding of the seesaw mechanism, grand unified theories, and the physics behind the matter-antimatter asymmetry of the universe. Future studies of LFV in charged leptons phenomena undoubtedly provide unique, complementary information on the existence of NP, even beyond the discovery of neutrino oscillations.

In this thesis, we are interested in different scenarios of cLFV. In the first work, we analyzed the LFV decay $\ell_i \to \ell_j \chi$, with χ a spin-one boson. We focused on the ultralight regime, where a naive EFT approach generates an unphysical divergence in the limit $m_\chi \to 0$. We show simple and complementary models that, thanks to the gauge symmetry, ensure the finiteness of observables in the massless χ limit. In the second work, we perform an analysis of the $\ell_i \to \ell_j \gamma\gamma$ decay, using an effective Lagrangian that describes the local interaction between two leptons, ℓ_i, and ℓ_j, and two photons. By means of this effective Lagrangian, the $\ell_i \to \ell_j \gamma$ decay is induced at one-loop level. Through the correlations between both processes, we derive an indirect upper bound for the double photon emission that improves current direct limits. Besides, we discuss an appealing UV completion -two Higgs doublet models- in which the two-photon processes can indeed provide more significant NP signatures than the single-photon ones. We hope that this observation triggers increased experimental efforts in these searches by the MEG-II and Belle-II collaborations.

This thesis is organized as follows. In Chapter 2, we give a short summary of the Electroweak (EW) sector of the SM, as well as, some generalities of EFT. In Chapter 3, LFV in the charged sector is discussed, and we present the current status of its searches. Chapters 4 and 5 are the heart of the thesis. In the former, we developed a detailed analysis of the decay rate $\ell_i \to \ell_j \chi$, focusing on the light χ case. In the latter, we performed an EFT analysis of the LFV decay $\ell_i \to \ell_j \gamma\gamma$, setting the strongest (indirect) upper limit on its branching ratio. In Chapter 6, future prospects, and final conclusions are briefly discussed.

Chapter 2

The Architecture of the Electroweak Theory

2.1 Overview

The Standard Model [1–3] is a gauge quantum field theory, mathematically self-consistent and renormalizable, which describes strong, weak, and electromagnetic interactions, mediated by the exchange of gauge bosons: $W^{\pm}$, Z, γ and eight gluons, associated with the group generators. The SM is based on the internal symmetries of the unitary product group $SU(3)_C \otimes SU(2)_L \otimes U(1)_Y$, with $8 + 3 + 1 = 12$ generators. The subscripts have no group-theoretic significance, but they denote colour (C), left-chiral nature (L) and weak hypercharge (Y).

The $SU(3)_C$ factor describes the theory of strong interactions or Quantum Chromodynamics (QCD). It is an unbroken gauge theory, non-chiral, and acts on the color indices of the left-handed (L)- and right-handed (R)-chiral quarks. In contrast, the EW theory, $SU(2)_L \otimes U(1)_Y$, is a chiral theory, in the sense that the L- and R- fermionic fields behave differently under the gauge group. Then, mass terms for fermions are not allowed in the EW gauge-symmetric limit and their masses will be generated by means of the Spontaneous Symmetry Breaking (SSB).

The fundamental particles in the SM are organized into fermions and bosons. The fermions are the building blocks of matter with a half-integral spin. The fermion content is divided into two groups: quarks and leptons, and they at the same time, are organized in three families with different masses, where the heavier families are unstable and decay into the lightest. On the other hand, the bosons have an integral spin and are the mediators of interactions. The gluons, photons, and the $W^{\pm}$ and Z are the force-carrying bosons of the SM and are vector fields, while the Higgs boson is a scalar field. Moreover, the photon and the gluons are massless, while the Z, the $W^{\pm}$ and the Higgs are massive. The last particles discovered were the $W^{\pm}$ and Z bosons at CERN by the UA1 and UA2 collaborations in 1983 [9,10], the top quark by the CDF and DØ experiments at Fermilab in 1995 [11,12], the tau neutrino in 2000 by the DONUT collaboration from Fermilab [13], and the Higgs boson in 2012 by CMS and ATLAS collaborations from CERN [14,15].

The EW theory is extremely well tested experimentally, to the level of 0.1%, which is possible

because we have very precise measurements in lepton–lepton collisions, further it can be reliably calculated in perturbation theory. On the other hand, QCD requires hadronic processes which are known experimentally with less accuracy and are also theoretically subject to larger uncertainties. Nonetheless, the SM is the most precise theory in the history of physics and has been enormously successful. Our confidence in it is well-founded by its ability to accurately describe the bulk of our present-day data, and of its enormous success in predicting new phenomena.

Despite its impressive phenomenological success, there are well-founded reasons to believe that the SM is not the end of the story. We do not understand yet, for instance, the existence of dark matter, the baryon asymmetry of the universe, gravity itself at the quantum level, and the nature and origin of neutrino masses.

There is then experimental evidence that, although strictly speaking does not contradict the SM, represents a strong hint for physics beyond the SM. Just to mention one, the convincing evidence of neutrino oscillations from both solar and atmospheric experiments, showing that neutrinos have masses and lepton flavor is not a conserved symmetry. The existence of the lepton flavor violation opens a very interesting window to unknown phenomena which represent the core of this thesis, so in the next chapter we will discuss about it.

We will focus below on the EW sector of the SM which is the theoretical framework of this thesis. In Section 2.2, we will present the gauge structure, the SSB mechanism, and the weak charged and neutral currens. Finally, in Section 2.3, we will also briefly discuss some generalities of effective field theories, which will be a recurrent technique used to approach the analyses presented in this work.

2.2 Electroweak theory

As the EW theory is a renormalizable gauge theory, it suffices to specify the gauge symmetry group, the scalar and fermion fields, the transformations of the fields under the action of the gauge group and a renormalizable Lagrangian (and finally if the vacuum shares the whole symmetry of the Lagrangian, or only a subgroup of it). Before presenting the EW Lagrangian, let us point out that fermions can be described in terms of Dirac spinors, ψ, that combine two independent components with left and right chirality respectively, $\psi_L = (1-\gamma^5)\psi/2$ and $\psi_R = (1+\gamma^5)\psi/2$. The EW theory is a chiral theory, where the L- and R-chirality components of fermions transform under inequivalent representations of the gauge group, then to describe the EW interactions, we should consider separately the L- and R-fermions fields.

As mentioned previously, the fermionic matter content is given by leptons (ℓ) and quarks (q), and their corresponding antiparticles, which are organized in a three family structure, and

represented by $SU(2)_L$ doublets, for the L-fields; and by singlets for R-fermions:

$$\chi^{\ell}_{mL} \equiv \begin{pmatrix} \nu^0_m \\ \ell^0_m \end{pmatrix}_L , \quad \ell^0_{mR} \quad \text{and}$$
$$\chi^{q}_{mL} \equiv \begin{pmatrix} U^0_m \\ D^0_m \end{pmatrix}_L , \quad U^0_{mR} , \quad D^0_{mR} .$$

There is no experimental evidence for the existence of the R neutrinos, ν^0_{mR}, and they are not necessary for the consistency of the SM, so they are not included in the theory. The subscript $m = 1\,, 2\,, 3$ is a label of family, and the superscripts '0' refer to the fact that these fields are weak eigenstates, and after SSB, these will become mixtures of mass eigenstate fields.

Three of the four gauge bosons are massive. Masses will be implemented in the EW theory by the Higgs mechanism [16,17], by which the gauge symmetry has been broken by the vacuum, which triggers the SSB of the EW group $SU(2)_L \otimes U(1)_Y$ to the electromagnetic subgroup $U(1)_{QED}$. The boson associated with this subgroup, $U(1)_{QED}$, remains massless, being the photon (γ). Then, the minimal formulation of the EW theory requires introducing a complex scalar doublet

$$\phi = \begin{pmatrix} \phi^+ \\ \phi^0 \end{pmatrix} , \tag{2.1}$$

where ϕ^+ is a charged scalar field, and ϕ^0 is a neutral scalar field.

The group $SU(2)_L \otimes U(1)_Y$ is generated by three isospin operators, $I_{1\,,2\,,3}$, associated with a triplet of vector fields, W^a_μ, and a hypercharge generator Y, described by the singlet field B_μ, where:

$$W^a_{\mu\nu} = \partial_\mu W^a_\nu - \partial_\nu W^a_\mu + g\epsilon_{abc} W^b_\mu W^c_\nu, \quad \text{with} \quad a, b, c = 1, 2, 3,$$
$$B_{\mu\nu} = \partial_\mu B_\nu - \partial_\nu B_\mu,$$

and ϵ_{abc} are the structure constants of the $SU(2)_L$ group, which coincide with the Levi-Civita tensor, and g is its gauge coupling constant. The abelian $U(1)_Y$ gauge boson has no self-interactions and we will identify its coupling constant as g'. Taking into account the field strength tensors defined above, the Lagrangian associated to the dynamics of gauge bosons, invariant under gauge transformations is:

$$\mathcal{L}_{gauge} = -\frac{1}{4}\sum_{a=1}^{3} W^a_{\mu\nu} W^{\mu\nu,a} - \frac{1}{4} B_{\mu\nu} B^{\mu\nu}. \tag{2.2}$$

The $SU(2)_L$ and $U(1)_Y$ representations are chiral, so no fermion mass terms are allowed. Therefore the interaction term for fermionic fields consists entirely of gauge-covariant kinetic

energy terms

$$\mathcal{L}_f = \sum_{m=1}^{3} \Big(\overline{\chi}^{\ell}_{mL} i\gamma^\mu D_\mu \chi^{\ell}_{mL} + \overline{\chi}^{q}_{mL} i\gamma^\mu D_\mu \chi^{q}_{mL} + \overline{\ell}^{0}_{mR} i\gamma^\mu D_\mu \ell^{0}_{mR} + \overline{U}^{0}_{mR} i\gamma^\mu D_\mu U^{0}_{mR} + \overline{D}^{0}_{mR} i\gamma^\mu D_\mu D^{0}_{mR} \Big) \,, \tag{2.3}$$

and the fermion gauge covariant derivatives, D_μ, become:

$$D_\mu \chi^{q}_{mL} = \left(\partial_\mu + i\frac{g}{2}\tau_a W^a_\mu + i\frac{g'}{6} B_\mu \right) \chi^{q}_{mL} \,, \qquad D_\mu \chi^{\ell}_{mL} = \left(\partial_\mu + i\frac{g}{2}\tau_a W^a_\mu - i\frac{g'}{2} B_\mu \right) \chi^{\ell}_{mL} \,,$$
$$D_\mu U^{0}_{mR} = \left(\partial_\mu - i\frac{2g'}{3} B_\mu \right) U^{0}_{mR} \,, \qquad D_\mu \ell^{0}_{mR} = \left(\partial_\mu - ig' B_\mu \right) \ell^{0}_{mR} \,,$$
$$D_\mu D^{0}_{mR} = \left(\partial_\mu + i\frac{g'}{3} B_\mu \right) D^{0}_{mR} \,,$$

where τ_a are the three Pauli matrices.

Now it is time to discuss the scalar sector. As we pointed out before, the masses of the $W^\pm$ and Z gauge bosons, as well as those of the fermions, are generated by means of the Higgs mechanism, introducing the scalar doublet, ϕ, defined in Eq. (2.1), and building the following Lagrangian,

$$\mathcal{L}_h = (D_\mu \phi)^\dagger (D_\mu \phi) - V(\phi), \tag{2.4}$$

where the Higgs potential is given by

$$V(\phi) = \mu^2 \phi^\dagger \phi + \lambda (\phi^\dagger \phi)^2 \,,$$

and the gauge covariant derivative is

$$D_\mu = \partial_\mu + i\frac{g}{2}\tau_a W^a_\mu + i\frac{g'}{2} B_\mu \,. \tag{2.5}$$

The Higgs potential has been constructed in such a way that its vacuum expectation value is not null, so the vacuum stability requires $\lambda > 0$. On the other side, $\mu^2 < 0$ to realize the SSB and thus generate the masses of the gauge bosons. The vacuum must be electrically neutral so in the complex scalar doublet, the charged part, ϕ^+, must have a zero value in the vacuum, while, the neutral part, ϕ^0, can have a nonzero value in the vacuum. To satisfy that the potential has not a trivial minimum, we must have the following relation for the vacuum expectation value

$$\langle \phi \rangle = \frac{1}{\sqrt{2}} \begin{pmatrix} 0 \\ v \end{pmatrix}, \quad \text{with} \quad v \equiv \sqrt{\frac{-\mu^2}{\lambda}}.$$

The Higgs doublet, ϕ, can be conveniently written in the unitary gauge as

$$\phi(x) = \frac{1}{\sqrt{2}}\begin{pmatrix} 0 \\ v + H(x) \end{pmatrix},$$

where $H(x)$ is a Hermitian scalar field, associated with a scalar and neutral particle, the physical Higgs boson.

The last piece to build the Lagrangian of the EW theory is the term that gives us the couplings between the Higgs field and the fermions, necessary to generate the mass of the fermions, through SSB is the Yukawa Lagrangian, which has the form

$$\mathcal{L}_y = -\sum_{m,n=1}^{3}\left[\Gamma^d_{mn}\overline{\chi}^q_{mL}\phi D^0_{nR} + \Gamma^u_{mn}\overline{\chi}^q_{mL}\tilde{\phi}U^0_{nR} + \Gamma^{\ell m}\overline{\chi}^\ell_{mL}\phi\ell^0_{nR}\right] + \text{h.c.}, \tag{2.6}$$

with $\tilde{\phi} = \begin{pmatrix} \phi^{0\dagger} \\ -\phi^- \end{pmatrix}$ and $\Gamma^d_{mn}, \Gamma^u_{mn}, \Gamma^\ell_{mn}$ are 3×3 matrices (3 for the number of families), which will determine the fermions masses and mixings. As we have pointed out before, there are no R neutrinos in the SM so that we do not have neutrino masses, however neutrino oscillations [4,5,18] constitute undeniable evidence that neutrinos have mass. The SM should account for that, therefore, we must extend the SM to include a mechanism for the mass generation of neutrinos, nevertheless, this is still an open question in particle physics.

Finally, putting all the pieces together, given in the Eqs. (2.2), (2.3), (2.4) and (2.6), we have that the EW model is described by the following Lagrangian [1]

$$\mathcal{L}_{EW} = \mathcal{L}_{gauge} + \mathcal{L}_f + \mathcal{L}_h + \mathcal{L}_y\,.$$

2.2.1 The Higgs and the Yukawa sectors

The existence of fermion and vector boson masses is evidence that the SM gauge invariance should be spontaneously broken. In particular, one has SSB when the ground state of the system is not symmetric. It is then the system itself that "spontaneously" breaks the symmetry.

One can in principle define the fermionic mass term as $m(\bar{\psi}_L\psi_R + \bar{\psi}_R\psi_L) = m\bar{\psi}\psi$, but this is not allowed by the gauge symmetry. Then, in the exact $SU(2)_L \otimes U(1)_Y$ symmetry, no gauge-invariant fermion mass term can be written, consequently the fermions are forced to be massless. To give rise to a mass term it needs to break the gauge symmetry. In the unitary gauge, after the SSB, the Yukawa Lagrangian takes the simpler form

$$\mathcal{L}_y = -\left(1 + \frac{H}{v}\right)\left[\overline{D}^0_L M_D D^0_R + \overline{U}^0_L M_U U^0_R + \overline{\ell}^0_L M_\ell \ell^0_R\right] + \text{h.c.}\,, \tag{2.7}$$

[1] Gauge fixing and ghosts terms are not discussed here.

where $D_L^0 = (d_{1L}^0\ d_{2L}^0\ d_{3L}^0)^T$ and $D_R^0 = (d_{1R}^0\ d_{2R}^0\ d_{3R}^0)^T$ are 3-component column vectors, with an analogous definition for U_R^0, U_L^0, ℓ_R^0 and ℓ_L^0. The fermionic mass term will be defined through fermion mass matrices, not necessarily diagonal, M_D, M_U and M_ℓ,

$$M_D = \Gamma^d_{mn}\frac{v}{\sqrt{2}}\,, \quad M_U = \Gamma^u_{mn}\frac{v}{\sqrt{2}}\,, \quad M_\ell = \Gamma^\ell_{mn}\frac{v}{\sqrt{2}}\,.$$

As a consequence of the absence of Yukawa couplings in the neutrinos sector, the SSB does not generate masses for neutrinos, then, there will no be mixtures in the lepton sector, and M_ℓ will be a diagonal matrix. On the other side, to be able to identify the physical particle content, the matrices M_D and M_U will be diagonalized by means of rotations in the flavor eigenspace to recast the Lagrangian in terms of the mass eigenstates

$$U^0_{L,R} = V^U_{L,R}U_{L,R}, \quad D^0_{L,R} = V^D_{L,R}D_{L,R}\,,$$

and the diagonal mass matrices for the quark sector, are:

$$M_U^d \equiv \mathrm{diag}(m_u, m_c, m_t) = V_L^{U\dagger}M_U V_R^U\,, \quad M_D^d \equiv \mathrm{diag}(m_d, m_s, m_b) = V_L^{D\dagger}M_D V_R^D\,,$$

where $V_L^{U,D}$ and $V_R^{U,D}$ are unitary transformations on the L- and R- fermion fields and they are not unique. $U_{L,R} \equiv (u_{L,R}\ \ c_{L,R}\ \ t_{L,R})^T$ and $D_{L,R} = (d_{L,R}\ \ s_{L,R}\ \ b_{L,R})^T$ are 3-component column vectors.

In the SSB, the gauge vector associated with each broken generator gets a longitudinal component and a mass. Let us now see the effects on the Higgs Lagrangian after SSB. The vector boson masses arise from the $(D_\mu\phi)^\dagger(D_\mu\phi)$ term in the Higgs Lagrangian. Applying the covariant derivative on $\langle\phi\rangle$

$$D_\mu\langle\phi\rangle = i\frac{v}{2\sqrt{2}}\begin{pmatrix} g\left(W_\mu^1 - iW_\mu^2\right) \\ gW_\mu^3 - g'B_\mu \end{pmatrix} = i\frac{v}{2\sqrt{2}}\begin{pmatrix} \sqrt{2}gW_\mu^+ \\ \sqrt{g^2+g'^2}Z_\mu \end{pmatrix}, \tag{2.8}$$

where we have defined

$$W_\mu^\pm = \frac{1}{\sqrt{2}}\left(W_\mu^1 \mp iW_\mu^2\right) \quad \text{and}$$

$$\begin{pmatrix} A_\mu \\ Z_\mu \end{pmatrix} = \begin{pmatrix} \cos\theta_w & \sin\theta_w \\ -\sin\theta_w & \cos\theta_w \end{pmatrix}\begin{pmatrix} B_\mu \\ W_\mu^3 \end{pmatrix},$$

thereby $Z_\mu \equiv \cos\theta_w W_\mu^3 - \sin\theta_w B_\mu$ and $A_\mu \equiv \cos\theta_w B_\mu + \sin\theta_w W_\mu^3$, being θ_w the weak mixing angle defined by $\tan\theta_W = g'/g$, $0 \le \theta_w \le \pi/2$. The $W^\pm$ are the charged gauge bosons that will mediate the charged current interactions and Z is a massive Hermitian vector boson that will mediate the neutral current interaction.

In the unitary gauge, the Higgs Lagrangian in eq. (2.4) becomes

$$\mathcal{L}_h = \frac{1}{2}\left(\partial_\mu H\right)^2 + \frac{g^2 v^2}{4} W_\mu^\dagger W^\mu + \frac{g^2 v^2}{8\cos^2\theta_w} Z_\mu Z^\mu + \frac{g^2 v}{2} W_\mu^\dagger W^\mu H + \frac{g^2 v}{4\cos^2\theta_w} Z_\mu Z^\mu H + \frac{g^2}{4} W_\mu^\dagger W^\mu H^2 + \frac{g^2}{8\cos^2\theta_w} Z_\mu Z^\mu H^2 - V(\phi)\,, \tag{2.9}$$

where the Higgs potential reads

$$V(\phi) = -\frac{\mu^4}{4\lambda} - \mu^2 H^2 + \lambda v H^3 + \frac{\lambda}{4} H^4\,. \tag{2.10}$$

After the SSB, the Lagrangian (2.9) includes the mass terms of the Higgs, the $W^\pm$, and the Z bosons, and also describes the interactions between the Higgs and the gauge bosons. It also contains the kinematical term and the self-interactions of the Higgs boson. The fourth vector boson, A, the photon, does not get a mass term, as the corresponding generator is not broken.The explicit form for the masses of the Higgs, the $W^\pm$, and the Z bosons are:

$$M_W = \frac{gv}{2}\,, \quad M_Z = \frac{gv}{2\cos\theta_w}\,, \quad \text{and} \quad M_H = \sqrt{-2\mu^2}\,.$$

2.2.2 The Weak Charged Current (WCC) and the Weak Neutral Current (WNC)

Using the previously obtained expressions, we can recast the fermionic sector on the EW Lagrangian in terms of the mass eigenstates

$$\mathcal{L}_f + \mathcal{L}_y = \mathcal{L}_\psi - \frac{g}{2\sqrt{2}}\left(J_W^\mu W_\mu^- + J_W^{\mu\dagger} W_\mu^+\right) - \frac{gg'}{\sqrt{g^2+g'^2}} J_Q^\mu A_\mu - \frac{\sqrt{g^2+g'^2}}{2} J_Z^\mu Z_\mu,$$

with $\mathcal{L}_\psi$ the kinetic energy term for fermions, and the other terms describe the gauge interactions between the fermions and the vector bosons.

The $W^\pm$ terms are the charged current interaction, J_W^μ, in the weak eigenstate basis is given by

$$J_W^\mu = \sum_{m=1}^{3}\left[\overline{\ell}_m^0 \gamma^\mu \left(1-\gamma^5\right)\nu_m^0 + \overline{D}_m^0 \gamma^\mu \left(1-\gamma^5\right) U_m^0\right]\,. \tag{2.11}$$

Rewriting the charged currents in terms of mass eigenstates

$$J_W^\mu = 2\overline{\ell}_L \gamma^\mu V_\ell^\dagger \nu_L + 2\overline{D}_L \gamma^\mu V_q^\dagger U_L\,, \tag{2.12}$$

where $V_q = V_L^{U\dagger} V_L^D \equiv V_{CKM}$ is the matrix that describes the transitions between quarks of type

U and D, and is known as the Cabibbo-Kobayashi-Maskawa (CKM) matrix [19, 20]. The CKM matrix involves three mixing angles and one observable Charge-Parity (CP)-violating phase. It highlights the fact that this phase is the only source of CP-violation in the EW theory which was first detected in the neutral kaons system, and more sizeable signals of CP-violation have been recently established at the B factories. V_ℓ is the analogous leptonic mixing matrix, since we are assuming that neutrinos are massless, $V_\ell = I$ with I the identity matrix. Thus, no mixing matrix is obtained for leptons as it is for quarks. The 3-component column vectors U_L and D_L were previously defined, and $\ell_L \equiv (e_L \ \mu_L \ \tau_L)^T$ and $\nu_L \equiv (\nu_{eL} \ \nu_{\mu L} \ \nu_{\tau L})^T$.

The neutral currents in the EW Lagrangian are J_Q^μ and J_Z^μ, with J_Q^μ the usual QED current, given by

$$J_Q^\mu = \frac{2}{3}\overline{U}\gamma^\mu U - \frac{1}{3}\overline{D}\gamma^\mu D - \overline{\ell}\gamma^\mu \ell \,.$$

We note that $\overline{U}\gamma^\mu U = \overline{U}_L\gamma^\mu V_L^{U\dagger}V_L^U U_L + \overline{U}_R\gamma^\mu V_R^{U\dagger}V_R^U U_R = \overline{U}^0_L\gamma^\mu U^0_L + \overline{U}^0_R\gamma^\mu U^0_R = \overline{U}^0\gamma^\mu U^0$, similarly for D and ℓ, then J_Q^μ takes the same form on both bases, the mass eigenstate basis, and the weak eigenstate basis. Consequently, J_Q^μ is flavor diagonal and family universal.

Finally, the term that accompanies the Z boson, is a new ingredient predicted by the $SU(2) \otimes U(1)$ unification, the weak neutral current

$$J_Z^\mu = \overline{U}_L\gamma^\mu U_L - \overline{D}_L\gamma^\mu D_L + \overline{\nu}_L\gamma^\mu \nu_L - \overline{\ell}_L\gamma^\mu \ell_L - 2\sin^2\theta_w J_Q^\mu \,.$$

Note that, analogously to the electromagnetic current, the weak neutral current takes the same form both on the mass eigenstate basis and the weak eigenstate, therefore there are no flavour-changing neutral currents at tree level in the SM.

2.3 Effective Field Theory (EFT)

A remarkable fact about nature is that interesting physics occurs on all energy scales. In a first approximation for describing whatever physical process, we can set to infinity (zero) all scales that are much larger (smaller) than the energy scale of interest. In this limit, physics at scales much different from the scale of interest becomes irrelevant and can be neglected; if needed, its effect can be reintroduced in perturbation theory. To this day, this strategy is one of the first steps when modeling a physical phenomenon.

EFTs are an approximate description of physics at a given energy scale Λ in terms of their corresponding degrees of freedom, which explicitly implement the strategy outlined above and turn it into a precise, quantitative framework. The EFTs are the appropriate theoretical tool to describe low-energy physics, where "low" is defined with respect to Λ. If it is properly formulated, all physical theories could be effective theories. Next, we will discuss briefly the basic ideas and

methods of EFTs, for a more detailed discussion see [21–25].

The theoretical basis behind the construction of EFTs can be formulated in terms of theorem of Weinberg [26]: "*To any given order in perturbation theory, and for a given set of asymptotic states, the most general possible Lagrangian containing all terms allowed by the assumed symmetries will yield the most general S-matrix elements consistent with analyticity, perturbative unitarity, cluster decomposition, and assumed symmetry principles*".

An EFT is completely specified by three ingredients: degrees of freedom, symmetries, and expansion parameters. The degrees of freedom and symmetries should include the most relevant parameters to describe the physical system at the energy scale of interest, where the best option is to choose the most economical description. Expansion parameters are small quantities controlling the impact that the physics we choose to neglect could potentially have on the degrees of freedom we choose to keep. In perturbation theory, the observables are calculated as a series in these small parameters, then for this strategy to work, the expansion parameters must be chosen carefully.

To construct an EFT implements a Taylor expansion on an expansion parameter E/Λ ($E << \Lambda$), where each term in the expansion contributes to the effective Lagrangian, $\mathcal{L}_{eff}$. We can expand $\mathcal{L}_{eff}$ as a string of operators with different energy dimensions:

$$\mathcal{L}_{eff} = \mathcal{L}_{\leq D} + \mathcal{L}_{\leq D+1} + \mathcal{L}_{\leq D+2} + \dots ,$$

with D the dimension of spacetime. The effective Lagrangian must be constructed taking into account the symmetries and degrees of freedom adequate to the energy scale of interest. Noteworthy, only the first term is renormalizable in the "classical" sense, however, the renormalizability is not an issue since, at a given order in the energy expansion, the low-energy theory is specified by a finite number of couplings; this allows for an order-by-order renormalization. Since the EFT has an infinite number of terms, for the $\mathcal{L}_{eff}$ to be useful we must establish a criterion for ignoring most of them.

The effective Lagrangian can be written as a sum of operators, $\mathcal{L}_{eff} = \mathcal{L}_0 + \sum_i c_i \mathcal{O}_i$, where $\mathcal{L}_0$ is the low energy (classically) renormalizable Lagrangian, the operators constructed $\mathcal{O}_i$ are organized according to their dimensions, d_i, where $[\mathcal{O}_i] = d_i$, and the effective couplings $c_i \propto \Lambda^{-(d_i-4)}$ hide the information on any heavy degrees of freedom. At low energy, the behavior of the different operators is determined by their dimensions, thereby, the relation to the $\mathcal{O}_i$ and c_i with d_i, allows us to classify the operators according to their dimension as: relevant if $d_i < 4$, marginal if $d_i = 4$, and irrelevant if $d_i > 4$.

The operators called relevant give rise to effects that become large at energies much smaller than the scale of interest. In a four-dimensional relativistic field theory, the number of possible relevant operators are the unit operator for $d = 0$, the boson mass terms for $d = 2$, the fermion

mass terms ($\psi\overline{\psi}$) and cubic scalar interactions (ϕ^3) for $d = 3$.

In contrast, the irrelevant operators have dimensions greater than four, and their effects are suppressed by powers of E/Λ, thus are small at low energies. Here irrelevant does not mean that they are not important, but rather that these operators are weak at low energies.

Operators of dimension four are called marginal. They should be considered at all energy scales since due to quantum corrections they are in an insecure position and almost always change from marginal to either relevant or irrelevant.

If there is a large gap between the energy where one is doing experiments and the energy scale of NP (*i. e.* $E \ll \Lambda$), the effects induced by irrelevant operators are always suppressed by powers of E/Λ, then the EFT will only consist of marginal and relevant operators and is called (classically) renormalizable.

It is important to highlight that an EFT is a different theory from the full theory. The full theory must be a renormalizable field theory, while, the EFT could be a (classically) non-renormalizable field theory[2], then it has a different divergence structure from the full theory. An EFT is constructed to correctly reproduce the low-energy effects and is useful only for computing results to a certain order in E/Λ.

[2]The symmetry that enables the organization of the EFT in a power expansion warrants its renormalizability order by order in this expansion.

Chapter 3

Charged lepton flavor violation

3.1 Overview

The Standard Model of elementary particle physics describes the fundamental fermions: quarks and leptons, grouped by mass eigenstates in three generations

$$\begin{array}{rcccc} \text{First generation} & u\,, & d\,, & \nu_1\,, & e \\ \text{Second generation} & c\,, & s\,, & \nu_2\,, & \mu \\ \text{Third generation} & t\,, & b\,, & \nu_3\,, & \tau\,. \end{array}$$

Individual quarks and leptons are assigned a quantum number called flavor. The electron, muon, and tau flavors are assigned to the charged leptons. Such as we presented in Section 2.2.2, flavor is conserved at the tree level by all neutral current interactions, mediated by Z, and γ, but is violated in the quark sector by charged current weak interactions mediated by $W^{\pm}$ bosons. Unlike the quark sector, in the lepton sector the flavor is conserved, as a consequence of assuming massless neutrinos. However, unlike other conservation laws in the SM, lepton flavor conservation is not associated with any conserved current.

The discovery of neutrino oscillations [4, 5, 18] qualifies as the first evidence of NP beyond the SM. Its implication of nonvanishing neutrino masses and the non-conservation of neutrino flavor, open the door to the search for cLFV processes. Aside for neutrino oscillations, no other lepton flavor violating process has been observed up to this day, so the question of whether similar violations occur in the charged lepton sector is still open [27]. The search for LFV in charged leptons will probably be the most interesting goal of flavor physics during the next few years.

This chapter presents the current status of cLFV searches. In Section 3.2 we describe the flavor changing in the original version of the SM. In Section 3.3 we present a short summary of neutrino oscilations and its implications. In Section 3.4 and 3.5 we describe the muon and tau decay searches, respectively, focusing mainly in the status and the future perspective. Finally, in

Section 3.6 we present the summary and outlook on cLFV processes.

3.2 Flavor changing in the Standard Model

In the absence of interactions that lead to nonzero neutrino masses, individual lepton-flavor numbers are expected to be conserved. At the tree level of the SM Lagrangian, the charged fermions have three gauge interactions, with the photon, the $W^{\pm}$ and Z bosons, and also the Higgs interaction, as we described in Section 2.2. So in the SM the flavor is only violated in charged current weak interactions.

In the case of quarks, flavor mixing is induced, since after the SSB in the Yukawa sector (see Eq. (2.7)), the unitary matrices for the left-handed up-type quark and the left-handed down-type quark are generally different. As we see in the second term of the Eqs. (2.11) and (2.12), where the V_{CKM} represents the flavor mixing matrix for the quark sector.

Conversely, in the lepton sector, the charged lepton mass matrix in Eq. (2.7) is fully diagonalised by unitary transformations on the lepton doublet fields and the lepton singlet fields. As we can observe in the first term in Eqs. (2.11) and (2.12), as a result of having assumed massless neutrinos, V_ℓ is the identity matrix, then the charged current weak interaction for leptons remains diagonal. In the mass eigenstates, the lepton flavors can be defined for each generation, and are thus conserved.

Due to mixing among generations of fermions, charged current loop effects can induce flavor changing neutral current weak interactions at the quantum level. On the quark side, such loop-induced effects lead to small but observable transitions, for instance, in $K_L^0 \to \mu^+\mu^-$ decay where we have $s \to d$ transitions. The rare leptonic decay of the neutral Kaon was extremely important in unveiling the existence of charm via the GIM-mechanism [28] . More recently, the measurement of $b \to s\gamma$ transitions in the search for $B_s \to \mu^+\mu^-$ has been at the forefront of (low-energy) supersymmetry constraints. Contrarily, on the charged lepton side, searches for flavor changing neutral current effects have, so far, yielded null results, even so, have important historical significance. The nonobservation of $\mu \to e\gamma$ [7], as well as the tau decays $\tau \to \mu\gamma$ and $\tau \to e\gamma$, helped establish the muon and tau as elementary leptons. The constrain on $\mathrm{BR}(\mu \to e\gamma)$ below $\sim 10^{-5}$, were also used to propose the existence of a second neutrino (the ν_μ) [29–31]. The introduction of the ν_μ was needed to suppress flavor changing neutral current charged lepton interactions, which was completely analogous to the GIM-mechanism introduction of charm to suppress strangeness changing neutral currents.

3.3 Neutrino Masses and Mixing

In the last decades, a variety of neutrino oscillation experiments proved beyond any doubt that neutrino flavors, *i.e.*, individual lepton flavor numbers, are not conserved [4–6]. From these phenomena it is concluded that: *i)* neutrino masses are nonzero, and distinct and *ii)* the weakly interacting flavor neutrinos ν_e, ν_μ, and ν_τ are nontrivial superpositions of the so-called mass eigenstate neutrinos ν_1, ν_2, and ν_3, where these superpositions are described by a 3×3 unitary mixing matrix, via

$$\begin{pmatrix} \nu_e \\ \nu_\mu \\ \nu_\tau \end{pmatrix} = U_{PMNS} \begin{pmatrix} \nu_1 \\ \nu_2 \\ \nu_3 \end{pmatrix} , \tag{3.1}$$

with U_{PMNS} the Pontecorvo–Maki–Nakagawa–Sakata (PMNS) neutrino mixing matrix [31]. The PMNS matrix is most commonly parameterized by three mixing angles (θ_{12}, θ_{13} and θ_{23}) and a single phase angle called δ related to CP violations [1], in which case the matrix can be written as:

$$U_{PMNS} = \begin{pmatrix} c_{12}c_{13} & s_{12}c_{13} & s_{13}e^{-i\delta} \\ -s_{12}c_{23} - c_{12}s_{23}s_{13}e^{i\delta} & c_{12}c_{23} - s_{12}s_{23}s_{13}e^{i\delta} & s_{23}c_{13} \\ s_{12}s_{23} - c_{12}c_{23}s_{13}e^{i\delta} & -c_{12}s_{23} - s_{12}c_{23}s_{13}e^{i\delta} & c_{23}c_{13} \end{pmatrix} ,$$

where $c_{ij} \equiv \cos\theta_{ij}$, $s_{ij} \equiv \sin\theta_{ij}$, $i, j = 1, 2, 3$. From a combination of solar, reactor, atmospheric, and accelerator neutrino oscillation results [32–42], we now know (roughly) the values of all three mixing angles, as well as the two independent mass-squared differences, and recently, the CP-phase [41]

$$\begin{aligned} |\Delta m^2_{32}| &= |m^2_3 - m^2_2| \simeq 2.5 \times 10^{-3}\ \text{eV}^2 , \\ \Delta m^2_{21} &= m^2_2 - m^2_1 \simeq 7.53 \times 10^{-5}\ \text{eV}^2 , \\ \sin^2\theta_{12} &\simeq 0.307 , \\ \sin^2\theta_{23} &\simeq 0.546 , \\ \sin^2\theta_{13} &\simeq 0.0220 , \\ \delta &\simeq 1.36\pi , \end{aligned}$$

where normal mass ordering was assumed for the limit on the CP-phase. Given the current precision of neutrino oscillation experiments and the fact that neutrino oscillations are only sensitive to mass-squared differences, two possible arrangements of the neutrino masses are allowed [43]:

[1] This is not the only parameterization and is different in the case of neutrinos that have Majorana mass.

normal ordering, *i.e.* $m_1 < m_2 \ll m_3$ and inverted ordering, *i.e.* $m_1 \simeq m_2 \gg m_3$. Neutrino mass ordering remains unconstrained.

In the minimal extension of the SM modified by the presence of the neutrino mass term, the neutrino oscillation induces $\mu \to e\gamma$ to one-loop. Assuming that the neutrinos have Dirac mass terms, $\nu_\beta = \sum_i U_{\beta i}\nu_i$, $\beta = e\,,\mu\,,\tau$ and $i = 1\,,2\,,3$, as we describe in Eq. (3.1), one finds [44]

$$\mathrm{BR}(\mu \to e\gamma) \sim \frac{3\alpha}{32\pi}\left|\sum_{k=1,3} U_{\mu k}U_{ek}^{*}\frac{\Delta m_{\nu k}^{2}}{M_W^2}\right|^2 \sim 10^{-54}\,, \tag{3.2}$$

where $U_{\beta k}$, with $\beta = e\,,\mu\,,\tau$, are the elements of the PMNS matrix, α is the fine-structure constant, and M_W is the W-boson mass. Similar small rates are expected for $\mu \to eee$, $\mu \to e$ conversion, and rare processes involving taus, for instance: $\mathrm{BR}(Z \to \ell_i^{\pm}\ell_j^{\mp}) \sim 10^{-54}$ [45], $\mathrm{BR}(H \to \ell_i^{\pm}\ell_j^{\mp}) \sim 10^{-55}$ [46], $\mathrm{BR}(\mu \to 3e) \sim 10^{-54}$, and $\mathrm{BR}(\tau \to 3\ell) \sim 10^{-55}$ [47]. These tiny branching ratios are due to the cLFV being a flavor-changing neutral current process and such processes being subject to the GIM-mechanism. As a result of the extremely small mass differences compared to the weak scale ($M_W \sim 80.4$ GeV), we have an accidental approximate lepton flavor conservation.

Unlike the charged fermions, where conservation of electric charge allows only Dirac-type mass terms, one can write two kinds of Lorentz invariant mass terms for the neutrino, Dirac and Majorana masses. This new state has also raised many other issues [48–50], in addition to those already mentioned: neutrino mass ordering and Majorana or Dirac fermions nature, they go together. For instance: *i)* massive Dirac neutrinos can have nonzero magnetic dipole moments, and massive Dirac and Majorana neutrinos can have nonzero transition dipole moments; and *ii)* the heavier neutrinos decay into lighter ones, like charged fermions.

The newest addition to the standard model paradigm, neutrino oscillations, demands to extend it to include a mechanism for the mass generation of neutrinos. There are several ways to reconcile this with the SM, the fact that neutrinos have masses and explain its smallness. One of the simplest, considering Dirac neutrinos, is to add right-handed neutrinos to the SM, so in the Yukawa Sector (Eq. (2.6)) we will have analogous terms to the other leptons. The smallness of the neutrino masses can be possibly understood using the Weinberg gauge-invariant operator [51]. After the spontaneous symmetry breaking, when the Higgs acquires its vacuum expectation value, that operator represents the neutrino Majorana mass. The most popular physics model explanation of the smallness of neutrino mass is the seesaw mechanism [52, 53], which postulates the existence of heavy ν_R. There are, however, other possible scenarios to generate mechanisms for neutrino masses (see *e.g.* [43, 54]).

3.4 cLVF in muon framework

Searches for $\mu \to e\gamma$ date back to the late 1940's. By the early 1960's the nonobservation to BR($\mu \to e\gamma$) above 10^{-6} was among the most pressing arguments in favor of the so-called 'two-neutrino hypothesis' and the postulate that there were two lepton flavors, each accompanied by a conserved lepton-flavor number.

Experimentally, a $\mu \to e\gamma$ event is characterized by a simple two-body final state, the electron and photon, which are emitted back to back in the rest frame of the decaying muon. The main background in its search comes from two decays $\mu \to e\nu\overline{\nu}$ and $\mu \to e\nu\overline{\nu}\gamma$. The first is an accidental coincidence of a positron from the standard Michel decays of muons, and a relatively high energy γ ray from radiative muon decays or annihilation of positrons in material. The second from radiative muon decays is strongly suppressed by reasonably good energy and momentum measurements at a rate more than an order of magnitude smaller than the accidental background. The present best upper limit on the BR($\mu^+ \to e^+\gamma$) is 4.2×10^{-13} at 90% CL [55], which was established by the MEG (Mu to E Gamma) experiment at the Paul Scherrer Institute. The upgrade of the MEG Experiment hopes to reach a sensitivity of 6×10^{-14} [56], which will improve the current upper limits on $\mu \to e\gamma$.

Along with $\mu \to e\gamma$ decays, two other rare muon processes provide the most stringent current bounds on cLFV, and promise the highest near-future sensitivity to these phenomena: $\mu \to 3e$ decays, and $\mu \to e$ conversion in nuclei. The present upper limit on the BR($\mu^+ \to e^-e^+e^+$) $< 1.0 \times 10^{-12}$ at 90% CL [57], was obtained by the SINDRUM experiment in 1988. The most stringent bound for $\mu \to e$ conversion in nuclei is BR(μAu $\to e$Au) $< 7 \times 10^{-13}$ at 90% CL [58], where the $\mu \to e$ conversion rate is usually defined as BR($\mu N \to eN$) $\equiv \sigma(\mu N \to eN)/\sigma(\mu N \to$ all captures).

In the $\mu^+ \to e^+e^-e^+$ decay one searches for two positrons and one electron coming from a common vertex and with a total energy equal to the muon mass $E_{tot} \sim 105.6$ MeV. The backgrounds are very similar to the case of the $\mu^+ \to e^+\gamma$ search [57]. There is a prompt background due to the allowed muon decay $\mu^+ \to e^+e^-e^+\overline{\nu}_\mu\nu_e$ [59], which becomes serious when the two neutrinos have very little energy. The total energy of the three particles closely resembles the Michel spectrum due to the fact that the three leptons behave roughly as the single electron of the ordinary muon decay [60]. In contrast, the spectra of individual lepton energies are quite different from the normal spectrum [61]. The other background comes from an accidental overlay from Michel positrons that coincide with e^+e^- pairs from γ conversions or from other Michel positrons that undergo Bhabha scattering. The upper limit from SINDRUM collaboration dates back to 1988, the Mu3e experiment aims to search for the cLFV decay $\mu^+ \to e^+e^-e^+$ with a final estimated sensitivity to the signal decay of 2.3×10^{-15} [62].

The muon-to-electron conversion, $\mu N \to eN$, is the spontaneous conversion of a muon to an electron without the emission of neutrinos, within the Coulomb potential of an atomic nucleus: it is therefore only possible for negative muons [58, 63, 64]. Experimentally, the signal for $\mu \to e$ conversion in nuclei is a monochromatic electron, whose energy lies just beyond the kinematical end-point of Michel electrons produced by muon decay in orbit, so from an experimental point of view, this process is very attractive. One of the major backgrounds is muon decay in orbit from a muonic atom, in which the e^- endpoint energy is the same as the energy of the signal. Another important source of noise is the beam-related background, where the most significant of these is radiative pion capture. Experimentally, in the long-run, it is widely anticipated that $\mu \to e$ conversion in nuclei will provide the ultimate sensitivity to cLFV, with rates below 10^{-18} or lower [65].

Other cLFV processes involving muons and electrons include rare kaon decays like $K_L \to \mu^\pm e^\mp$, $K \to \pi\mu^\pm e^\mp$ [66], muonimum–antimuonium oscillations, $\mu^+e^- \leftrightarrow \mu^-e^+$ [67], and recently, $B^0 \to \mu^\pm e^\mp$ [68] among others (see *e.g.* [69]).

3.5 cLVF in tau framework

Unlike μ, decays which are sensitive only to new leptonic interactions, the τ can decay into many final states involving hadrons, due to its relatively large mass, $m_\tau \sim 1777$ MeV [41]. These characteristics make the tau an experimental escenario particularly interesting, playing a special role in the search for NP.

From an experimental point of view some difficulties arise: the τ lepton has a much shorter lifetime (2.9×10^{-13} s instead of 2.2×10^{-6} s for the muon [41]) and is not as copiously produced as muons are, not to mention the fact that it is impossible to produce tau "beams". Tau samples must be obtained at proton or electron accelerators, operating in an energy range where the production cross section is large, with little background, and their decay must be measured with large detectors with good particle identification and tracking capabilities, as well as excellent calorimetry and hermeticity in order to constrain the kinematics. Until now, the best limits come from the B-flavour factories, whose luminosity and asymmetric beam energy enhance the capability of reconstructing tau decays.

Experimentally, LFV τ decays can be conveniently classified as $\tau^\pm \to \ell^\pm\gamma$,$\tau^\pm \to \ell_1^\pm\ell_2^+\ell_3^-$, and $\tau^\pm \to \ell^\pm X^0$, where ℓ is either an electron or a muon and where X^0 represents a hadronic system. In the searches by B-factories, X^0 has been categorized in three ways: *i)* X^0 corresponds to a pseudoscalar meson, *e.g.* π^0, η, K_S^0; *ii)* X^0 corresponds to a neutral vector meson, *e.g.* ω, $K^*(892)$, ϕ; and *iii)* X^0 is a pair of oppositely charged mesons, $X^0 = X_1^+X_2^-$, where $X_{1(2)}^\pm = \pi^\pm$ or $K^\pm$. Actually the B-Factories have explored LFV τ decays until $\mathcal{O}(10^{-7}) - \mathcal{O}(10^{-8})$ sensitivities [70],

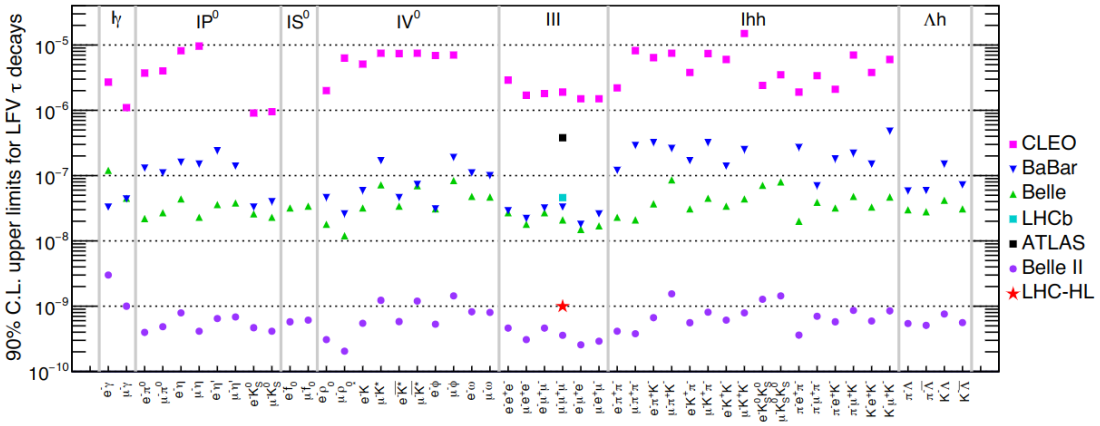

Figure 3.1: *Summary plot for τ LFV decays; projections of the Belle-II bounds were performed by the Belle-II collaboration assuming* 50 ab^{-1} *of integrated luminosity [71].*

see Fig. 3.1.

The golden channels for τ modes are $\tau^{\pm} \to \ell^{\pm}\gamma$ and $\tau^{\pm} \to \ell_1^{\pm}\ell_2^{+}\ell_3^{-}$. The better upper limits of the radiative decays $\tau \to \ell\gamma$ are $\text{BR}(\tau^{\pm} \to e^{\pm}\gamma) < 3.3 \times 10^{-8}$ at 90% CL from BaBar [72] and recently, Belle-II Collaboration reported $\text{BR}(\tau^{\pm} \to \mu^{\pm}\gamma) < 4.2 \times 10^{-8}$ at 90% CL [73]. Both Belle [74] and BaBar [75] have the strongest results on searches for $\tau^{\pm} \to \ell_1^{\pm}\ell_2^{+}\ell_3^{-}$. Unlike μ, the τ lepton allows for six different leptonic decays $\tau^{\pm} \to (e^{\pm}e^{+}e^{-}, \mu^{\pm}\mu^{+}\mu^{-}, e^{\pm}e^{-}\mu^{+}, e^{\pm}\mu^{-}e^{+}, \mu^{\pm}e^{-}\mu^{+}, \mu^{\pm}\mu^{-}e^{+})$, where the best upper limit at 90% CL is $\text{BR}(\tau^{\pm} \to \ell_1^{\pm}\ell_2^{+}\ell_3^{-}) \lesssim \mathcal{O}(10^{-8})$. In the near future, in the end of Belle-II would be able to probe branching ratios down to $\mathcal{O}(10^{-9})$ [76], for an integrated luminosity of 50 ab^{-1}.

Other cLFV processes involving taus include neutral meson decays like $J/\psi \to \ell^{\pm}\tau^{\mp}$ [77] and $B^0 \to \ell^{\pm}\tau^{\mp}$ [78, 79], among others.

Last but not least, there are also processes in which we have an invisible boson instead of the X^0 above, which is one of the main topics studied in this thesis.

3.6 Summary and outlook

The discovery of neutrino oscillations reveals that charged-lepton flavor violating phenomena must occur. Naive massive-neutrino expectations are that the rates for cLFV processes are absurdly small thanks to the GIM-mechanism and the fact that neutrino masses are tiny compared to the weak scale. So theoretical predictions on the branching ratio of cLFV processes are $\mathcal{O}(10^{-54}) - \mathcal{O}(10^{-55})$.

BaBar and Belle experiments have set upper bounds for cLFV processes $\mathcal{O}(10^{-8})$ for branching ratios in tau decays. The B-factories on the horizon will see the experiments reach $\mathcal{O}(10^{-9})$ –

$\mathcal{O}(10^{-10})$. Meanwhile, for μ sector has probed $\mathcal{O}(10^{-12}) - \mathcal{O}(10^{-13})$. Later we can expect the sensitivity to reach $\mathcal{O}(10^{-14})$, and for the $\mu - e$ conversion front, we hope to see $\mathcal{O}(10^{-16})$. Other cLFV scenarios with experimental activity include neutral boson decays like $H \to \ell_i^{\pm}\ell_j^{\mp}$ [80, 81] and $Z \to \ell_i^{\pm}\ell_j^{\mp}$ [82, 83].

Finally, cLFV phenomena may play a key role in our understanding of the physics behind neutrino masses, grand unified theories, and the physics behind the matter–antimatter asymmetry of the universe. So, even if the LHC fails to detect any new degrees of freedom at the TeV scale, future studies of cLFV phenomena will provide unique, complementary information about new (or old) physics.

Chapter 4

Flavor violating ℓ_i decay into ℓ_j and a light gauge boson

4.1 Overview

The observation of neutrino oscillations constitutes undeniable evidence for lepton flavor violation, although, for the charged sector, no lepton flavor violating process has been observed so far. The SM predictions for cLFV processes have a strong suppression by a GIM-like mechanism [28, 84], then any observation of cLFV would imply the existence of NP.

Recently, interest has been aroused in physics at the low energy frontier (for a review, see [85]). This possibility may lead to new lepton flavor violating decays, such as $\ell_i \to \ell_j \chi$, with χ an invisible boson. For the muon sector, the TWIST collaboration [86], set the limit $\mathrm{BR}(\mu \to e\chi) < 8.1 \times 10^{-6}$ at 90% C.L., and for $m_\chi = 0$ the best upper limit is $\mathrm{BR}(\mu^+ \to e^+\chi) < 2.5 \times 10^{-6}$ from Jodidio *et al.* [87]. For the tau flavor, the ARGUS collaboration obtained $\mathrm{BR}(\tau \to e\chi) < 2.7 \times 10^{-3}$ and $\mathrm{BR}(\tau \to \mu\chi) < 5 \times 10^{-3}$ at 95% C.L. [88]. Further, the light boson χ could lead to the three-body lepton flavor violating decay $\ell_i \to 3\ell_j$, when χ is off-shell, resulting into complementary constraints on this scenario. For the muon mode, the best upper limit comes from SINDRUM Collaboration (1988) [57], and for tau channels the current limits come from Belle and BaBar Collaborations (2010) [74, 75], as show in Table 4.1.

On an EFT framework, the first description for the cLFV decay $\ell_i \to \ell_j \chi$ is through the Lagrangian $\mathcal{L}_{\text{eff}} = g\bar{\ell}_i \gamma^\rho \chi_\rho \ell_j + \text{h.c.}$, with χ_ρ the 4-potential associated to the $U(1)_\chi$ symmetry [1]. Due to the emission of the longitudinal component of the gauge boson, we have terms proportional to g^2/m_χ^2 into the rate for $\ell_i \to \ell_j \chi$. At first sight, observables diverge as $m_\chi \to 0$, preventing the matching of the effective theory to the well studied $\ell_i \to \ell_j \gamma$ decay. Moreover, the decays into several gauge bosons $\ell_i \to \ell_j \chi \cdots \chi$, could also contribute overwhelmingly to the total decay width, reminding the "hyperphoton catastrophe" for the electron decay into a neutrino and an ultralight photon [91–93]. Exhaustive studies have been developed, if χ is a scalar or pseudoscalar

[1] The general case for either spin 0 or 1 was studied preliminary in my Master Thesis [89], see also [90]. Therein, however, our approach did not yield a physical $m_\chi \to 0$ limit.

boson, see *e.g.* [94–109], then we will focus on the scenario where χ is a gauge boson.

In this Chapter we are going to present a detailed analysis of the decay rate $\ell_i \to \ell_j \chi$, focusing on the light χ case [110–112]. We will show that in the limit $m_\chi \to 0$, the decay rate for $\ell_i \to \ell_j \chi$ is finite and well matched to its analogous $\ell_i \to \ell_j \gamma$ decay channel. In Section 4.2 we present the most general effective interaction leading to the decay $\ell_i \to \ell_j \chi$ in terms of form factors. In Sections 4.3 and 4.4 we present two gauge invariant and renormalizable models where the process $\mu \to e\chi$ is generated, respectively, at tree level and at the one-loop level. We calculate the decay rate for $\mu \to e\chi$ and $\mu \to 3e$. In Section 4.5 we extend to three flavors the two models presented in Sections 4.3 and 4.4. Finally, we conclude in Section 4.6. Sections are based on our article [113] and Section 4.5 in our proceedings contribution to the TAU 2021 Conference.

4.2 Effective theory

In a first approximation, we developed the description of $\ell_i \to \ell_j \chi$ decay, in an EFT framework. Here i, j are lepton flavor indices and χ is a light gauge boson with $m_\chi \ll m_i$. Under this framework, the most general transition amplitude is given by:

$$M = \overline{u}(p_j)\Gamma^\alpha(p_i, p_j)u(p_i)\epsilon^*_\alpha(p_\chi)\,,$$

where the four-momenta p_i, p_j and p_χ are associated to ℓ_i, ℓ_j, and χ, respectively. The function $\Gamma^\alpha(p_i, p_j)$ is a linear combination of the possible vector forms, parameterized as a function of six

Decay Mode	BR (90%CL)
$\mu^+ \to e^+e^-e^+$	1.0×10^{-12}
$\tau^- \to e^-e^+e^-$	2.7×10^{-8}
$\tau^- \to e^-\mu^+\mu^-$	2.7×10^{-8}
$\tau^- \to \mu^-e^+\mu^-$	1.7×10^{-8}
$\tau^- \to \mu^-e^+e^-$	1.8×10^{-8}
$\tau^- \to e^-\mu^+e^-$	1.5×10^{-8}
$\tau^- \to \mu^-\mu^+\mu^-$	2.1×10^{-8}

Table 4.1: *Current experimental upper limits on BR (90%CL) for the $\ell_i \to 3\ell_j$ cLFV decays.*

dimensionless scalar form factors $F_k(p_\chi^2)$, $G_k(p_\chi^2)$, $k = 1, 2, 3$, as:

$$\Gamma^\alpha = \left(\gamma^\alpha - \frac{\not{p}_\chi p_\chi^\alpha}{p_\chi^2}\right) F_1(p_\chi^2) + i\frac{\sigma^{\alpha\beta}p_{\chi\beta}}{m_i+m_j}F_2(p_\chi^2) + \frac{2p_\chi^\alpha}{m_i+m_j}F_3(p_\chi^2) + \left(\gamma^\alpha - \frac{\not{p}_\chi p_\chi^\alpha}{p_\chi^2}\right)\gamma^5 G_1(p_\chi^2) + i\frac{\sigma^{\alpha\beta}\gamma^5 p_{\chi\beta}}{m_i+m_j}G_2(p_\chi^2) + \frac{2p_\chi^\alpha}{m_i+m_j}\gamma^5 G_3(p_\chi^2)\,, \tag{4.1}$$

where $\sigma_{\alpha\beta} = \frac{i}{2}[\gamma^\alpha, \gamma^\beta]$. If the gauge boson was a photon and the fermions were identical, some physical insight into these form factors can be obtained by considering their non-relativistic limits. The form factor $F_1(p_\chi^2)$ appears with the bilinear involving γ^α and it is associated with the charge of the fermion, so $F_1(0) \equiv Q_f$. The forms factors $F_2(0)$ and $G_2(0)$ are known as the magnetic dipole and electric dipole moments. The magnetic dipole moment is defined as:

$$\mu \equiv \frac{1}{2m}\left(Q_f + F_2(0)\right)\,,$$

where the contribution that is proportional to the charge of the particle, Q_f, is called the Dirac contribution to the magnetic moment, and the other contribution involving $F_2(0)$ is called the anomalous magnetic moment. The electric dipole moment can be identified as $d \equiv -G_2(0)/2m$. The form factor $G_1(0)$ is a pure (unobservable) quantum effect, called the anapole moment of the fermion [114].

Before presenting the decay rate, we should explain how some of the terms in Eq. (4.1) will vanish. The conservation of the $U(1)_\chi$ charge requires the form factor $F_3(p_\chi^2)$ to vanish. Moreover, the Ward identities imply that $p_\chi^\alpha \cdot \epsilon_\alpha^*(p_\chi) = 0$, so the contributions proportional to p_χ^α vanish for all p_χ^2. Finally, the decay rate can be written as a function of four form factors and reads

$$\Gamma(\ell_i \to \ell_j \chi) = \frac{\lambda^{1/2}[m_i^2, m_j^2, m_\chi^2]}{16\pi m_i}\left[\left(1-\frac{m_j}{m_i}\right)^2\left(1-\frac{m_\chi^2}{(m_i-m_j)^2}\right)\left(2\left|F_1(m_\chi^2) - F_2(m_\chi^2)\right|^2 + \left|F_1(m_\chi^2)\frac{(m_i+m_j)}{m_\chi} - F_2(m_\chi^2)\frac{m_\chi}{(m_i+m_j)}\right|^2\right) + \left(1+\frac{m_i}{m_j}\right)^2\left(1-\frac{m_\chi^2}{(m_i+m_j)^2}\right)\left(2\left|G_1(m_\chi^2) - G_2(m_\chi^2)\frac{(m_i-m_j)}{(m_i+m_j}\right|^2 + \left|G_1(m_\chi^2)\frac{(m_i-m_j)}{m_\chi} + G_2(m_\chi^2)\frac{m_\chi}{(m_i+m_j)}\right|^2\right)\right]\,, \tag{4.2}$$

where $\lambda[m_i^2, m_j^2, m_\chi^2]$ is the usual Källén function, and m_i, m_j, and m_χ denote the masses of the leptons ℓ_i and ℓ_j, and the gauge boson χ, respectively.

Note that the decay rate does not have interference terms between the form factors $F_k(p_\chi^2)$ and

$G_k(p_\chi^2)$, because in a one-to-two-body process like this, all kinematic is fixed and V-A interferences cancel out. We highlight also the fact that the terms proportional to $1/m_\chi$ associated with the emission of the longitudinal component of the vector boson are accompanied just by the form factors F_1 and G_1.

To all appearances the rate has an unphysical divergence in the limit $m_\chi \to 0$ on account of the term coming from the emission of the longitudinal component of the vector boson. Therefore, in an EFT approach, great care should be taken when considering decays into ultralight gauge bosons, since in a gauge invariant and renormalizable theory, the $\ell_i \to \ell_j \chi$ rate must be finite and continuously matched to the result from $\ell_i \to \ell_j \gamma$ [44, 115, 116].

We present below two specific models in which the cLFV interaction is generated either at tree level or at the one-loop level. We will show explicitly that, as a result of gauge invariance, the decay rate is finite and well behaved in the limit $m_\chi \to 0$. For the sake of the discussion, we have restricted the analysis to the two-generation case, although for completeness, we will present the extension to three generations in Section 4.5.

4.3 $\mu \to e\chi$ at tree level

We present first a model that generates the $\mu \to e\chi$ decay at tree level. In this model, the cLFV interaction will be generated by means of the bases change mechanism where we rotate the fields from the flavor eigenstate basis to the mass eigenstate basis. With the aim of generating this interaction, we need to allow for generation dependent charges under $U(1)_\chi$. Once the ingredients of the model have been presented, we will develop this mechanism in detail.

The particle content of the model, and the corresponding spins and charges under $SU(2)_L \otimes U(1)_Y \otimes U(1)_\chi$, are summarized in Table 4.2. Here ϕ_{jk}, $i, j = 1, 2$ denote complex scalar fields, doublets under $SU(2)_L$, with hypercharge Y_{jk} and charge under $U(1)_\chi$ equal to $q_{\phi_{jk}}$. We denote the SM $SU(2)_L$ lepton doublets and singlets, as:

$$L_{L_i} = \begin{pmatrix} \nu_{L_i} \\ \ell_{L_i} \end{pmatrix}, \quad \text{and} \quad e_{R_i}\,, \quad i = 1\,, 2\,,$$

respectively. Further, they have a generation independent hypercharge, Y_L and Y_e. It should be noted that the model is anomalous at it stands, but it can be made anomaly-free by adding heavy particles with suitable charges, without modifying the discussion that follows.

The kinetic Lagrangian of the model is written as

$$\mathcal{L}_{\text{kin}} = \sum_{j=1}^{2} i \left(\overline{L}_j \not{D} L_j + \overline{e}_{R_j} \not{D} e_{R_j} \right) + \sum_{j,k=1}^{2} (D_\mu \phi_{jk})^\dagger (D^\mu \phi_{jk}) \,, \tag{4.3}$$

	L_1	L_2	e_{R_1}	e_{R_2}	ϕ_{11}	ϕ_{12}	ϕ_{21}	ϕ_{22}
spin	1/2	1/2	1/2	1/2	0	0	0	0
$SU(2)_L$	2	2	1	1	2	2	2	2
$U(1)_Y$	$-1/2$	$-1/2$	-1	-1	Y_{11}	Y_{12}	Y_{21}	Y_{22}
$U(1)_\chi$	q_{L_1}	q_{L_2}	q_{e_1}	q_{e_2}	$q_{\phi_{11}}$	$q_{\phi_{12}}$	$q_{\phi_{21}}$	$q_{\phi_{22}}$

Table 4.2: *Spins and charges under $SU(2)_L \otimes U(1)_Y \otimes U(1)_\chi$ of the particles of the model described in Section 4.3, leading to the decay $\mu \to e\chi$ at tree level. All fields are assumed to be singlets under $SU(3)_C$.*

where D_μ denotes the covariant derivative, given by

$$\begin{aligned} D_\mu &= \partial_\mu + igW_\mu^a T_a + ig'YB_\mu + ig_\chi q\chi_\mu \quad \text{for the } SU(2)_L \text{ doublets}\,, \\ D_\mu &= \partial_\mu + ig'YB_\mu + ig_\chi q\chi_\mu \quad \text{for the } SU(2)_L \text{ singlets}\,, \end{aligned} \tag{4.4}$$

with g, g' and g_χ the coupling constants of $SU(2)_L$, $U(1)_Y$ and $U(1)_\chi$ respectively.

We also assume $Y_{jk} = 1/2$. Then, for j, k such that $q_{\phi_{jk}} = q_{L_j} - q_{e_k}$ the following Yukawa couplings arise in the Lagrangian:

$$-\mathcal{L}_{\text{Yuk}} = \sum_{j,k=1}^{2} y_{jk}\overline{L}_j \phi_{jk} e_{R_k} + \text{h.c.} \tag{4.5}$$

We also assume that the doublet scalars acquire a vacuum expectation value for some i, j, $\langle\phi_{jk}\rangle = v_{jk}$. To keep the discussion general, we consider that the charges of the particles allow all Yukawa couplings, and that all ϕ_{jk} acquire a vacuum expectation value; the different subcases follow straightforwardly by setting the corresponding y_{jk} and/or v_{jk} to zero.

Applying the covariant derivative over the scalar field and considering that $\langle\phi_{jk}\rangle \neq 0$, mass terms for the bosons arise, thus

$$m_\chi^2 = g_\chi^2(q_{\phi_{11}}^2 v_{11}^2 + q_{\phi_{12}}^2 v_{12}^2 + q_{\phi_{21}}^2 v_{21}^2 + q_{\phi_{22}}^2 v_{22}^2)\,. \tag{4.6}$$

Furthermore, since ϕ_{jk} have charge under $SU(2)_L \otimes U(1)_Y$, their expectation value would also contribute to the Z and W masses. Since we are assuming $m_\chi \ll m_\mu$, this contribution can be safely neglected.

The expectation value of the doublet scalars generates a mass term for the charged leptons,

$-\mathcal{L}_{\rm mass} \supset \overline{e}_{L_j} M_{jk} e_{R_k} + \text{h.c.}$, with

$$M = \begin{pmatrix} y_{11}v_{11} & y_{12}v_{12} \\ y_{21}v_{21} & y_{22}v_{22} \end{pmatrix} . \tag{4.7}$$

We now rotate the fields to express the Lagrangian in the mass eigenstate basis:

$$\begin{pmatrix} e_L \\ \mu_L \end{pmatrix} = \begin{pmatrix} \cos\theta_L & \sin\theta_L \\ -\sin\theta_L & \cos\theta_L \end{pmatrix} \begin{pmatrix} e_{L_1} \\ e_{L_2} \end{pmatrix} , \qquad \begin{pmatrix} e_R \\ \mu_R \end{pmatrix} = \begin{pmatrix} \cos\theta_R & \sin\theta_R \\ -\sin\theta_R & \cos\theta_R \end{pmatrix} \begin{pmatrix} e_{R_1} \\ e_{R_2} \end{pmatrix} , \tag{4.8}$$

so that $-\mathcal{L}_{mass} \supset \overline{e}_L m_e e_R + \overline{\mu}_L m_\mu \mu_R + \text{h.c.}$. Here θ_L and θ_R are the mixing angles and the 2×2 matrices are unitary transformations on the L- and R- leptons, and we are going to refer to them as V_L and V_R, respectively. It should be noted that $MM^\dagger = V_L M_\ell^2 V_L^\dagger$ and $M^\dagger M = V_R M_\ell^2 V_R^\dagger$, with $M_\ell \equiv \text{diag}(m_e, m_\mu) = V_L^\dagger M V_R$. Using these relations, we can find the mixing angles and the lepton masses as a function of v_{jk} and y_{jk}, as follow

$$\begin{aligned} MM^\dagger &= \begin{pmatrix} y_{11}^2 v_{11}^2 + y_{12}^2 v_{12}^2 & y_{11}v_{11}y_{21}v_{21} + y_{22}v_{22}y_{12}v_{12} \\ y_{11}v_{11}y_{21}v_{21} + y_{22}v_{22}y_{12}v_{12} & y_{22}^2 v_{22}^2 + y_{21}^2 v_{21}^2 \end{pmatrix} \\ &= \begin{pmatrix} m_e^2 \cos^2\theta_L + m_\mu^2 \sin^2\theta_L & (-m_\mu^2 + m_e^2)\sin\theta_L\cos\theta_L \\ (-m_\mu^2 + m_e^2)\sin\theta_L\cos\theta_L & m_\mu^2\cos^2\theta_L + m_e^2\sin^2\theta_L \end{pmatrix} , \\ \text{Tr}[MM^\dagger] &= m_e^2 + m_\mu^2 = y_{11}^2 v_{11}^2 + y_{12}^2 v_{12}^2 + y_{21}^2 v_{21}^2 + y_{22}^2 v_{22}^2 , \\ \text{Det}[MM^\dagger] &= m_e^2 m_\mu^2 = (y_{11}v_{11}y_{22}v_{22} - y_{12}v_{12}y_{21}v_{21})^2 , \end{aligned} \tag{4.9}$$

similar expressions are found using $M^\dagger M = V_R M_\ell^2 V_R^\dagger$. From the off diagonal inputs of the matrices in Eq. (4.9) we can find $\sin 2\theta_L$ and assuming that $m_\mu \gg m_e$, it follows that

$$\begin{aligned} m_\mu^2 &\simeq y_{11}^2 v_{11}^2 + y_{12}^2 v_{12}^2 + y_{21}^2 v_{21}^2 + y_{22}^2 v_{22}^2 , \\ m_e^2 &\simeq \frac{(y_{11}v_{11}y_{22}v_{22} - y_{12}v_{12}y_{21}v_{21})^2}{y_{11}^2 v_{11}^2 + y_{12}^2 v_{12}^2 + y_{21}^2 v_{21}^2 + y_{22}^2 v_{22}^2} , \\ \sin 2\theta_L &\simeq -2\frac{y_{11}v_{11}y_{21}v_{21} + y_{12}v_{12}y_{22}v_{22}}{y_{11}^2 v_{11}^2 + y_{12}^2 v_{12}^2 + y_{21}^2 v_{21}^2 + y_{22}^2 v_{22}^2} , \\ \sin 2\theta_R &\simeq -2\frac{y_{11}v_{11}y_{12}v_{12} + y_{21}v_{21}y_{22}v_{22}}{y_{11}^2 v_{11}^2 + y_{12}^2 v_{12}^2 + y_{21}^2 v_{21}^2 + y_{22}^2 v_{22}^2} . \end{aligned} \tag{4.10}$$

Finally, we recast the kinetic Lagrangian Eq. (4.3) in terms of the mass eigenstates. We find flavor violating terms of the form

$$-\mathcal{L} \supset \overline{e}_R i g_{e\mu}^{RR} \gamma^\rho \chi_\rho \mu_R + \overline{e}_L i g_{e\mu}^{LL} \gamma^\rho \chi_\rho \mu_L + \text{h.c.} , \tag{4.11}$$

with

$$g_{e\mu}^{RR} = g_\chi(q_{e_1} - q_{e_2}) \sin\theta_R \cos\theta_R \ ,$$
$$g_{e\mu}^{LL} = g_\chi(q_{L_1} - q_{L_2}) \sin\theta_L \cos\theta_L \ . \tag{4.12}$$

Clearly, if the $U(1)_\chi$ charges are generation independent, the flavor violation is absent at tree-level (as is the case for the photon and Z flavor violating couplings). Further, if the interaction eigenstates are aligned to the mass eigenstates, the tree-level flavor violation is also absent. This happens in particular for some choices of the expectation values of the fields ϕ_{ij}, for example, when $v_{ii} = 0$, but $v_{12}, v_{21} \neq 0$.

Comparing to the general form of the lepton flavor violating interaction vertex, Eq. (4.1), one can identify

$$F_1 = \frac{1}{2}(g_{e\mu}^{RR} + g_{e\mu}^{LL}) \ ,$$
$$G_1 = \frac{1}{2}(g_{e\mu}^{RR} - g_{e\mu}^{LL}) \ , \tag{4.13}$$

while all other form factors vanish at tree-level. The rate for $\mu \to e\chi$ then reads:

$$\Gamma(\mu \to e\chi) = \frac{m_\mu}{32\pi}\left(\left|g_{e\mu}^{LL}\right|^2 + \left|g_{e\mu}^{RR}\right|^2\right)\left(2 + \frac{m_\mu^2}{m_\chi^2}\right)\left(1 - \frac{m_\chi^2}{m_\mu^2}\right)^2 \ , \tag{4.14}$$

where we have neglected the electron mass against the muon mass. In a naive analysis, the term proportional to $1/m_\chi^2$ could lead to an unphysical divergence in the limit $m_\chi \to 0$. However, if the gauge and fermion masses arise as a consequence of the spontaneous breaking of the $U(1)_\chi$ symmetry, the limit $m_\chi \to 0$ requires $v_{jk} \to 0$ for all i, j (which in turn implies $m_\mu \to 0$), or $g_\chi \to 0$ (which in turn implies $g_{e\mu}^{LL}, g_{e\mu}^{RR} \to 0$). One can explicitly check from Eqs. (4.6), (4.10) and (4.12) that indeed when $m_\chi \to 0$ the term $(|g_{e\mu}^{LL}|^2 + |g_{e\mu}^{RR}|^2)\, m_\mu^2/m_\chi^2$ is finite (as expected from the Goldstone boson equivalence theorem [117–120]), and depends on a function of the Yukawa couplings, the gauge coupling, and the charges and vacuum expectation values of the fields ϕ_{jk}. [2]

We consider a particular case, where it is exhibited that in the limit of an ultralight boson, the decay rate is finite and well-behaved. We assume that the Yukawa couplings satisfy $y_{22} \gg y_{11} \gg y_{12}, y_{21}$ and all $v_{jk} = v$, so that the mass matrix M is almost diagonal, and $q_{\phi_{jk}} = Q$. The

[2] An analogous behaviour occurs in the top decay $t \to bW^+$. The decay rate is $\Gamma(t \to bW^+) \sim m_t^3/M_W^2$ and naively diverges when $M_W \to 0$. However, since both masses arise as a consequence of the SSB of the EW symmetry, $\Gamma(t \to bW^+) \sim m_t y_t^2/g^2$ and is finite.

relevant parameters of the model after the spontaneous breaking of the gauge symmetries are:

$$\begin{aligned} m_\mu^2 \simeq y_{22}^2 v^2, \qquad m_e^2 \simeq y_{11}^2 v^2, \qquad m_\chi^2 \simeq 4 g_\chi^2 Q^2 v^2 \ , \\ \sin 2\theta_L \simeq -2\frac{y_{12}}{y_{22}}, \qquad \sin 2\theta_R \simeq -2\frac{y_{21}}{y_{22}} \ . \end{aligned} \tag{4.15}$$

From Eq. (4.14) it follows that the rate for $\mu \to e\chi$ in the limit $m_\chi \to 0$ is finite, just as expected, and it is given by

$$\Gamma(\mu \to e\chi)\Big|_{m_\chi \to 0} \simeq \frac{m_\mu}{32\pi} \frac{g_\chi^2}{y_{22}^2} \left(2 + \frac{y_{22}^2}{4 g_\chi^2 Q^2}\right) \left(1 - \frac{4 g_\chi^2 Q^2}{y_{22}^2}\right)^2 \left[y_{12}^2 (q_{L_1} - q_{L_2})^2 + y_{21}^2 (q_{e_1} - q_{e_2})^2\right] . \tag{4.16}$$

We point out that the rate is maximal when $Q g_\chi / y_{22} \to 0$, and zero when $Q g_\chi / y_{22} \simeq 1/2$, which corresponds to $m_\chi / m_\mu \simeq 1$, *i.e.* when the phase space available for the decay closes. For most values of g_χ / y_{22}, the prefactor is $\sim 10^{-3}$, and therefore the rate can only be suppressed by invoking small couplings y_{12}, y_{21}, or by postulating intergenerational universality of the $U(1)_\chi$ charges. In the latter case, the process $\mu \to e\chi$ could be generated at the one loop level, as we will discuss in the next section.

A complementary probe of the e-μ flavor violation is the three-body decay $\mu^- \to e^- e^+ e^-$, which is generated in this model at tree-level via the exchange of a virtual χ. This process is generated through a flavor violating interaction vertex described in Eq. (4.11) and a flavor conserving interaction vertex of the form:

$$-\mathcal{L} \supset \bar{e}_R i g_{ee}^{RR} \gamma^\rho \chi_\rho e_R + \bar{e}_L i g_{ee}^{LL} \gamma^\rho \chi_\rho e_L \ , \tag{4.17}$$

where

$$\begin{aligned} g_{ee}^{RR} &= g_\chi \left(q_{e_2} \sin^2\theta_R + q_{e_1} \cos^2\theta_R\right) \ , \\ g_{ee}^{LL} &= g_\chi \left(q_{L_2} \sin^2\theta_L + q_{L_1} \cos^2\theta_L\right) \ . \end{aligned} \tag{4.18}$$

Note that, if the $U(1)_\chi$ charges are generation independent, the flavor conserving interaction is still present, just as it must be. Using the interaction Lagrangians in Eqs. (4.17) and (4.11), we

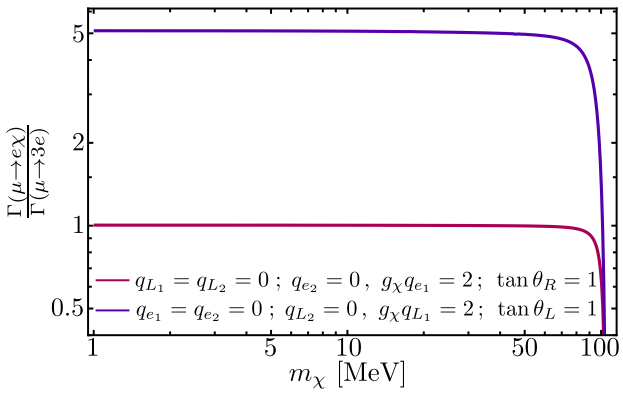

Figure 4.1: *Ratio of rates of* $\mu \to e\chi$ *and* $\mu \to 3e$ *as a function of* m_χ *for the tree-level model presented in Section 4.3, for the cases described in the text* $q_{L_i} = 0$, $q_{e_2} = 0$, $g_\chi q_{e_1} = 2$, *and* $\tan\theta_R = 1$ *(magenta line); and* $q_{e_i} = 0$, $q_{L_2} = 0$, $g_\chi q_{L_1} = 2$, *and* $\tan\theta_L = 1$ *(blue line).*

find that the corresponding differential decay rate reads:

$$\frac{\mathrm{d}^2\Gamma(\mu\to 3e)}{\mathrm{d}s\ \mathrm{d}t} = \frac{1}{128\pi^3 m_\mu^3}\Bigg[(|g_{ee}^{LL}|^2|g_{e\mu}^{RR}|^2 + |g_{ee}^{RR}|^2|g_{e\mu}^{LL}|^2)\left(\frac{t(m_\mu^2-t)}{(m_\chi^2-s)^2+m_\chi^2\Gamma_\chi^2} + \frac{s(m_\mu^2-s)}{(m_\chi^2-t)^2+m_\chi^2\Gamma_\chi^2}\right)$$
$$+\left(|g_{ee}^{LL}|^2|g_{e\mu}^{LL}|^2 + |g_{ee}^{RR}|^2|g_{e\mu}^{RR}|^2\right)\left(\frac{(s+t)\left(m_\mu^2-s-t\right)\left(4\Gamma_\chi^2 m_\chi^2 + (s+t-2m_\chi^2)^2\right)}{((m_\chi^2-s)^2+m_\chi^2\Gamma_\chi^2)((m_\chi^2-t)^2+m_\chi^2\Gamma_\chi^2)}\right)\Bigg]\,, \tag{4.19}$$

where Γ_χ is the total width of the χ-boson, and the Mandelstam variables $s \equiv (p_\mu - p_{e_1})^2$ and $t \equiv (p_\mu - p_{e_2})^2$, with p_{e_1} and p_{e_2} the electron momenta, and which are kinematically restricted to be in the range:

$$0 \le t \le (m_\mu^2 - s) \quad \text{and} \quad 0 \le s \ \le m_\mu^2\,. \tag{4.20}$$

We focus in what follows in a scenario where 1 MeV $\lesssim m_\chi \lesssim m_\mu$. In this mass range, the dominant decay channels are $\chi \to e^-e^+\,, \overline{\nu}_{L_1}\nu_{L_1}\,, \overline{\nu}_{L_2}\nu_{L_2}$. Using the electron interaction vertex from Eq. (4.17) and the neutrino interaction vertex from Eq. (4.3), we find that the total decay width is:

$$\Gamma_\chi = \frac{m_\chi}{24\pi}\left(|g_{ee}^{LL}|^2 + |g_{ee}^{RR}|^2 + |g_\chi q_{L_1}|^2 + |g_\chi q_{L_2}|^2\right)\,. \tag{4.21}$$

We show in Fig. 4.1 the ratio between $\Gamma(\mu \to e\chi)$ and $\Gamma(\mu \to 3e)$ as a function of m_χ, for a representative case where χ couples only to the right-handed leptons (*i.e.* $q_{L_1} = q_{L_2} = 0$; and $q_{e_2} = 0$, $g_\chi q_{e_1} = 2$, and $\tan\theta_R = 1$) or when χ couples only to the left-handed leptons (*i.e.* $q_{e_1} = q_{e_2} = 0$; and $q_{L_2} = 0$, $g_\chi q_{L_1} = 2$, and $\tan\theta_L = 1$). In the former case, the ratio is $\simeq 1$, and in the latter it is $\simeq 5$; with a mild sensitivity to the concrete choices of the charges and mixing angles. This result can be understood using the narrow width approximation (NWA), which holds

when χ is produced close to the mass shell. Under this approximation, one can replace in the propagators:

$$\frac{1}{(x-m_\chi^2)^2+m_\chi^2\Gamma_\chi^2} \to \frac{\pi}{m_\chi\Gamma_\chi}\delta(x-m_\chi^2)\,, \tag{4.22}$$

where x is any Mandelstam variable. Under this approximation, the decay rate for $\mu \to 3e$ reads:

$$\begin{aligned}\Gamma(\mu\to 3e) \simeq \frac{m_\mu}{32\pi}\frac{\left(|g_{e\mu}^{LL}|^2+|g_{e\mu}^{RR}|^2\right)\left(|g_{ee}^{LL}|^2+|g_{ee}^{RR}|^2\right)}{|g_{ee}^{LL}|^2+|g_{ee}^{RR}|^2+|g_\chi q_{L_1}|^2+|g_\chi q_{L_2}|^2}\left(2+\frac{m_\mu^2}{m_\chi^2}\right)\left(1-\frac{m_\chi^2}{m_\mu^2}\right)^2 \\ + \frac{m_\chi}{64\pi}\left(|g_{ee}^{LL}|^2|g_{e\mu}^{LL}|^2+|g_{ee}^{RR}|^2|g_{e\mu}^{RR}|^2\right)\frac{m_\chi}{m_\mu}\left(1-2\frac{m_\chi^2}{m_\mu^2}\right)\,.\end{aligned} \tag{4.23}$$

It should be noted that the term in the second row is subdominant for the light boson, but as m_χ becomes larger, the ratio becomes sensitive to the underlying model parameters, although this sensitivity is suppressed by a factor m_χ^2/m_μ^2, and is hence typically weak, in agreement with the numerical results of Fig. 4.1. Using Eqs. (4.14) and (4.23) for the two representative scenarios analyzed, we can reproduce the result $\Gamma(\mu \to e\chi)/\Gamma(\mu \to 3e) \simeq 1$ or $\simeq 5$. Further, like the decay rate for $\mu \to e\chi$ the Eq. (4.23) apparently diverges, but is in fact finite since m_μ and m_χ are both generated after the breaking of the $U(1)_\chi$ symmetry.

Given the current experimental limits on $\mathrm{BR}(\mu \to e\chi)$ and $\mathrm{BR}(\mu \to 3e)$, the most stringent constraints on the model will stem from the latter process [3]. For the case $m_\chi \ll m_\mu$, and using the upper limit $\mathrm{BR}(\mu \to 3e)$ from SINDRUM, one finds very stringent constraints on the strength of the effective couplings. Concretely, when $q_{L_i} = 0$, one finds $|g_{e\mu}^{RR}|/m_\chi \lesssim 1.6\times10^{-16}/\mathrm{MeV}$. This limit on the effective parameters can in turn be translated into limits on the Yukawa couplings, $U(1)_\chi$-charges and gauge coupling, and expectation values of the scalar doublets ϕ_{ij}, with the restriction of reproducing the correct muon mass $m_\mu \simeq 105$ MeV. Let us finish this section noting that the rare muon decay $\mu \to e\gamma$ could occur in this model at the one loop level. However, the strong constraints from the tree-level decay $\mu \to 3e$ preclude the observation of this process.

4.4 $\mu \to e\chi$ at the one loop level

Now we turn to a renormalizable model with generation-independent $U(1)_\chi$ charges, where the process $\mu \to e\chi$ is generated at one-loop level. Lepton flavor is now violated through a new Dirac fermion, ψ, and a new complex scalar, η, which does not acquires a vacuum expectation value. The particle content of the model and its spins and charges under $SU(2)_L \otimes U(1)_Y \otimes U(1)_\chi$, are listed in Table 4.3. Here L_i and e_{R_i}, with $i = 1\,,2$ are SM $SU(2)_L$ lepton doublets and

[3] We note that the on-shell χ decays into e^+e^- with a decay length $L_\chi \simeq 7.9\times10^{-10}\mathrm{m}\,(m_\chi/\mathrm{MeV})^{-2}g^{-2}$, where g is a combination of couplings, *cf.* Eq. (4.21), and therefore the decay occurs inside the detector.

	L_1	L_2	e_{R_1}	e_{R_2}	ϕ	ψ	η
spin	1/2	1/2	1/2	1/2	0	1/2	0
$SU(2)_L$	2	2	1	1	2	1	1
$U(1)_Y$	$-1/2$	$-1/2$	-1	-1	$+1/2$	Y_ψ	Y_η
$U(1)_\chi$	q_L	q_L	q_e	q_e	q_ϕ	q_ψ	q_η

Table 4.3: *Spins and charges under $SU(2)_L \otimes U(1)_Y \otimes U(1)_\chi$ of the particles of the model described in Section 4.4, leading to the decay $\mu \to e\chi$ at the one loop level. All fields are assumed to be singlets under $SU(3)_C$.*

singlets, respectively. The doublet scalar ϕ has hypercharge $+1/2$ and its $U(1)_\chi$-charge satisfies that $q_\phi = q_L - q_e$, such that the Yukawa coupling $y_{jk}\overline{L}_j e_{R_k}\phi + \text{h.c.}$ is allowed. The new fields ψ and η are singlets under $SU(2)_L$, with hypercharges Y_ψ and Y_η, and $U(1)_\chi$-charges q_ψ and q_η, respectively.

As required by $U(1)_\chi$-charge conservation, $q_e = q_\psi + q_\eta$. We assume $Y_e = Y_\psi + Y_\eta$, for the Yukawa couplings $y_i \overline{e}_{R_i}\psi\eta$ to be allowed. We also assume that ϕ acquires a non-zero vacuum expectation value, generating so mass for the boson χ: $m_\chi = g_\chi q_\phi \langle\phi\rangle$ [4]. Further, a mass matrix for the charged leptons is generated, of the form Eq. (4.7). Let us note that if η acquires an expectation value, a mixing between e_{R_i} and ψ is generated, and the mass matrix becomes instead 3×3. The analysis in that case would be analogous, although we disregard that possibility for simplicity and assume that $\langle\eta\rangle = 0$.

The Lagrangian in terms of the mass eigenstates, $e_{L,R}$ and $\mu_{L,R}$, that describes the interaction with the massive gauge boson χ has the form

$$\begin{aligned}\mathcal{L} \supset \quad & -ig_\chi q_L \left(\overline{e}_L\gamma^\nu e_L + \overline{\mu}_L\gamma^\nu\mu_L + \overline{\nu}_{L1}\gamma^\nu\nu_{L1} + \overline{\nu}_{L2}\gamma^\nu\nu_{L2}\right)\chi_\nu - ig_\chi q_e\left(\overline{e}_R\gamma^\nu e_R + \overline{\mu}_R\gamma^\nu\mu_R\right)\chi_\nu \\ & -ig_\chi q_\psi\overline{\psi}\gamma^\nu\psi\chi_\nu - iq_\eta g_\chi\left[\eta^*(\partial^\nu\eta) - (\partial^\nu\eta^*)\eta\right]\chi_\nu\,, \end{aligned} \tag{4.24}$$

as well as a Yukawa coupling to the right-handed leptons:

$$\mathcal{L} \supset h_e\overline{e}_R\eta\psi + h_\mu\overline{\mu}_R\eta\psi + \text{h.c.} \tag{4.25}$$

The process $\mu \to e\chi$ is generated in this model at the one-loop level, with ψ and η into the

[4] In this simple model, m_μ, m_e and m_χ are all proportional to $\langle\phi\rangle$. However, one can completely uncorrelate the fermion masses and the gauge boson masses by imposing $q_\phi = 0$ and by postulating the existence of another scalar field, whose expectation value contributes to m_χ, but not to the fermion masses.

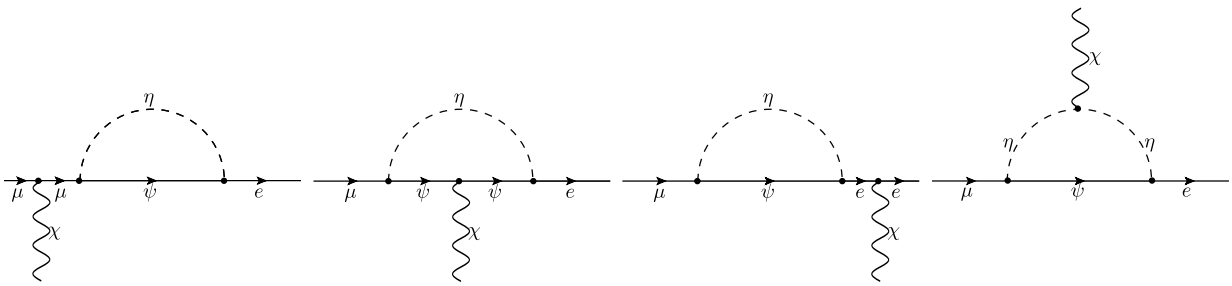

Figure 4.2: *One loop diagrams contributing to the decay* $\mu \to e\chi$.

loop, as we shown in Fig. 4.2. For this specific model, the form factors are finite and read:

$$\begin{aligned} F_1(m_\chi^2) = \quad G_1(m_\chi^2) &= \frac{g_\chi h_e h_\mu}{384\pi^2}\frac{m_\chi^2}{M_\eta^2}\left[q_\eta \mathcal{F}_{1\eta}\Big(\frac{M_\psi^2}{M_\eta^2}\Big) + q_\psi \mathcal{F}_{1\psi}\Big(\frac{M_\psi^2}{M_\eta^2}\Big)\right], \\ F_2(m_\chi^2) = -G_2(m_\chi^2) &= \frac{g_\chi h_e h_\mu}{384\pi^2}\frac{m_\mu^2}{M_\eta^2}\left[q_\eta \mathcal{F}_{2\eta}\Big(\frac{M_\psi^2}{M_\eta^2}\Big) + q_\psi \mathcal{F}_{2\psi}\Big(\frac{M_\psi^2}{M_\eta^2}\Big)\right], \end{aligned} \tag{4.26}$$

from where the form factors satisfy that $F_1 = G_1$ and $F_2 = -G_2$. We also find that the form factor F_1 (and G_1) is proportional to m_χ^2/M_η^2, while F_2 (and G_2) is proportional to m_μ^2/M_η^2. Further, one finds that $F_1 m_\mu/m_\chi \propto m_\chi m_\mu/M_\eta^2$, and $F_2 m_\chi/m_\mu \propto m_\chi m_\mu/M_\eta^2$.

The functions $\mathcal{F}_{1\eta(\psi)}$ and $\mathcal{F}_{2\eta(\psi)}$ in Eq. (4.26) are given by

$$\begin{aligned} \mathcal{F}_{1\eta}(x) &= \frac{-2 + 9x - 18x^2 + x^3\,(11 - 6\ln x)}{3\,(1-x)^4}, \\ \mathcal{F}_{1\psi}(x) &= \frac{16 - 45x + 36x^2 - 7x^3 + 6\,(2-3x)\ln x}{3\,(1-x)^4}, \\ \mathcal{F}_{2\eta}(x) &= \frac{1 - 6x + 3x^2(1 - 2\ln x) + 2x^3}{(1-x)^4}, \\ \mathcal{F}_{2\psi}(x) &= \frac{-2 - 3x(1 + 2\ln x) + 6x^2 - x^3}{(1-x)^4}, \end{aligned} \tag{4.27}$$

which are regular at $x = 1$ as we show in Fig. 4.3, where we represent the absolute value as a function of x.

Using the relation found between the form factors, the decay rate in Eq. (4.2), neglecting the electron mass, can be recast as

$$\Gamma(\mu \to e\chi) \simeq \frac{m_\mu}{8\pi}\left(1 - \frac{m_\chi^2}{m_\mu^2}\right)^2 \left[\left|F_1(m_\chi^2)\frac{m_\mu}{m_\chi} - F_2(m_\chi^2)\frac{m_\chi}{m_\mu}\right|^2 + 2\left|F_1(m_\chi^2) - F_2(m_\chi^2)\right|^2\right]. \tag{4.28}$$

In this decay rate, the term proportional to $1/m_\chi^2$ from the emission of the longitudinal polarization cancels with the factors m_χ^2 implicit in the form factors F_1 and G_1, thus the rate for $\mu \to e\chi$ is finite and well-behaved in the limit $m_\chi \to 0$. As $M_\eta, M_\psi \gg m_\mu$, it follows that the rate in the limit $m_\chi \to 0$ will depend mostly on the form factors F_2 and G_2, and can be well approximated by:

$$\Gamma(\mu \to e\chi)\Big|_{m_\chi \to 0} \simeq \frac{g_\chi^2\ |h_e|^2 |h_\mu|^2}{(768)^2\ \pi^5} \frac{m_\mu^5}{M_\eta^4} \left[q_\eta \mathcal{F}_{2\eta}\left(\frac{M_\psi^2}{M_\eta^2}\right) + q_\psi \mathcal{F}_{2\psi}\left(\frac{M_\psi^2}{M_\eta^2}\right) \right]^2 . \tag{4.29}$$

Nevertheless, the form factors F_1 and G_1 generate a sizable contribution to the rate when $m_\chi/m_\mu \gtrsim 0.1$.

We show in Fig 4.4 the branching ratio for $\mu \to e\chi$ for two representative choices of charges, $q_\eta = 1$ and $q_\psi = 0$ (left panel) and $q_\eta = 0$ and $q_\psi = 1$ (right panel), and three choices of the masses of the particles in the loop: $M_\psi = 750$ GeV and $M_\eta = 500$ GeV (blue line), $M_\psi = M_\eta = 500$ GeV (purple line), and $M_\psi = 500$ GeV and $M_\eta = 750$ GeV (red line). These values are compatible with the current searches for exotic charged particles [121, 122]. We have also taken for concreteness $h_e h_\mu = 1$ and $g_\chi = 1$, although the scaling of the rates with the Yukawa couplings is straightforward. The solid lines show the full result calculated using Eq. (4.28), while the dashed lines assume $F_1 = G_1 = 0$. As apparent for the plot, while for $m_\chi \ll m_\mu$ the form factors F_1 and G_1 can be neglected, they modify the rate when $m_\chi/m_\mu \gtrsim 0.1$, especially close to the threshold. We also show the current upper limit BR$(\mu \to e\chi)$ from the TWIST collaboration [86].

The process $\mu \to 3e$ is generated in this toy model also at the one-loop level, through χ-penguin and box diagrams. The χ-penguins are similar to the diagrams shown in Fig. 4.2, plus a fermionic line $e^- e^+$ coupled to the off-shell χ-boson, while the box diagrams have the fields ψ and η into the loop, and the leptons in the external legs. It should be noted that the χ-penguin

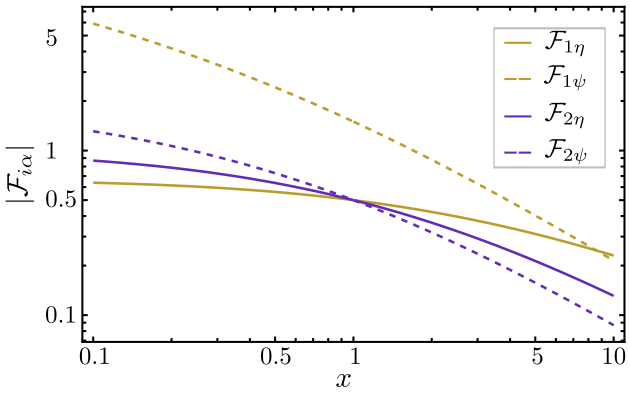

Figure 4.3: *Moduli of the functions $\mathcal{F}_{i\alpha}(x)$, with $i = 1, 2$ and $\alpha = \eta, \psi$, as defined in Eq. (4.27).*

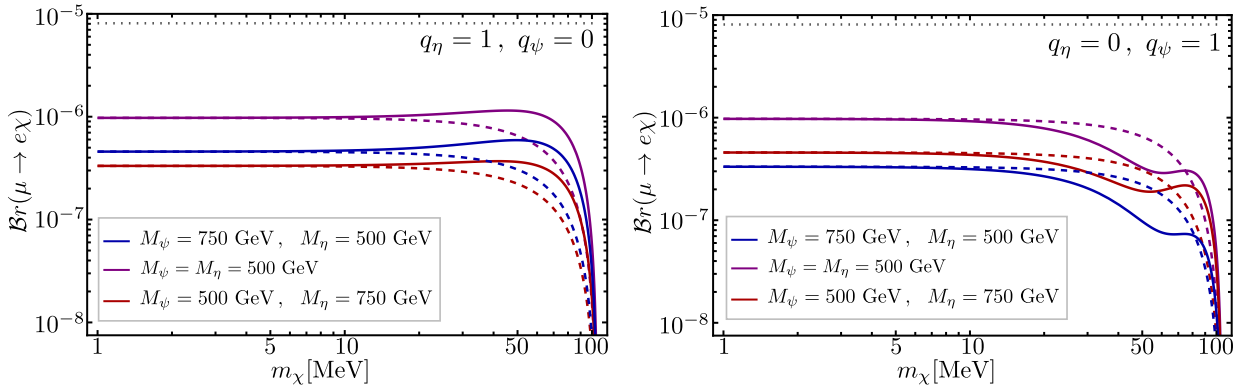

Figure 4.4: *Branching ratio of the process $\mu \to e\chi$ as a function of m_χ for the one loop model presented in Section 4.4, assuming $q_\eta = 1$ and $q_\psi = 0$ (left plot), and $q_\eta = 0$ and $q_\psi = 1$ (right plot); in both cases it was assumed $h_e h_\mu = 1$ and $g_\chi = 1$. The solid lines show the full result obtained from Eq. (4.28), while the dashed lines neglect the contribution from F_1. The grey dotted line indicates the current upper limit on* $\mathrm{BR}(\mu \to e\chi)$ *from the TWIST collaboration.*

diagrams are proportional to $h_e^2 h_\mu^2 g_\chi^4$ and the box diagramas to $h_e^6 h_\mu^2$. Assuming $h_e \ll g_\chi$, the decay will be dominated by the χ-penguin diagrams [5], with doubly differential rate given by:

$$\begin{aligned}\frac{\mathrm{d}^2\Gamma(\mu \to 3e)}{\mathrm{d}s\ \mathrm{d}t} \simeq & \frac{g_\chi^2}{32\pi^3 m_\mu^5}\Bigg[\frac{1}{\left(m_\chi^2 - s\right)^2 + m_\chi^2\Gamma_\chi^2}\Bigg(|q_e|^2(m_\mu^2 - s - t)\Big(m_\mu^2 s\big|F_1(m_\chi^2) - F_2(m_\chi^2)\big|^2 + \\ & t\ \left(|F_1(m_\chi^2)|m_\mu^2 - |F_2(m_\chi^2)|s\right)\Big) + |q_L|^2\ t\Big(\big|F_1(m_\chi^2)m_\mu^2 - F_2(m_\chi^2)s\big|^2 - \\ & t\ \left(|F_1(m_\chi^2)|^2 m_\mu^2 - |F_2(m_\chi)|^2 s\right)\Big)\Bigg) + t \leftrightarrow s\ + \\ & \frac{2|q_e|^2(m_\mu^2 - s - t)\left(m_\chi^2(\Gamma_\chi^2 + m_\chi^2 - s - t) + s\ t\right)}{\left(\left(m_\chi^2 - s\right)^2 + m_\chi^2\Gamma_\chi^2\right)\left(\left(m_\chi^2 - t\right)^2 + m_\chi^2\Gamma_\chi^2\right)} \\ & \Big(m_\mu^2(s+t)(|F_1(m_\chi^2)|^2 - F_1(m_\chi^2)F_2(m_\chi^2)) + |F_2(m_\chi^2)|^2 s\ t\Big)\Bigg]\,, \end{aligned} \tag{4.30}$$

where $s \equiv (p_\mu - p_{e_1})^2$ and $t \equiv (p_\mu - p_{e_2})^2$, with kinematic limits given in eq. (4.20), and Γ_χ the total decay width of χ. Similarly to Section 4.3, the dominant decay modes are $\chi \to e^- e^+, \overline{\nu}_{L_1}\nu_{L_1}, \overline{\nu}_{L_2}\nu_{L_2}$, with width:

$$\Gamma_\chi = \frac{g_\chi^2\ m_\chi}{24\pi}\Big(|q_e|^2 + 3|q_L|^2\Big)\,. \tag{4.31}$$

[5] Unless there is a strong hierarchy between the loop particles box contributions are subleading [123].

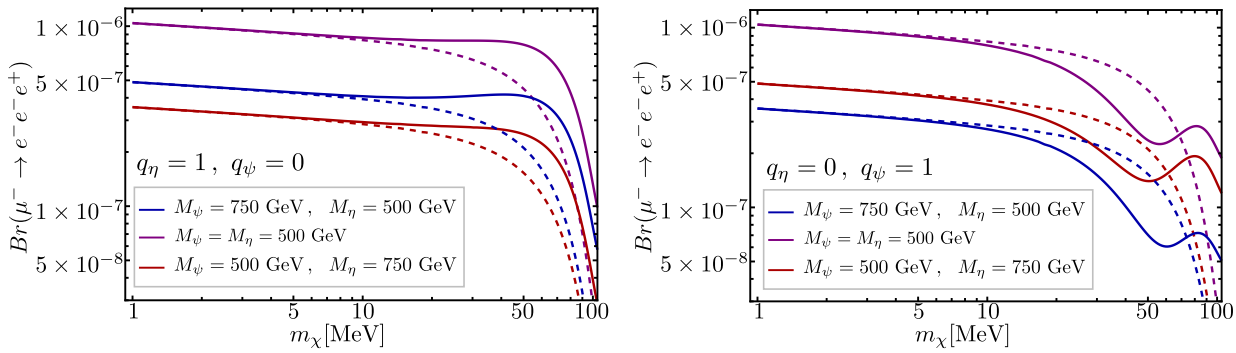

Figure 4.5: *Same as Fig. 4.4, but for the process* $\mu \to 3e$*, assuming* $q_L = 1 + q_e$*.*

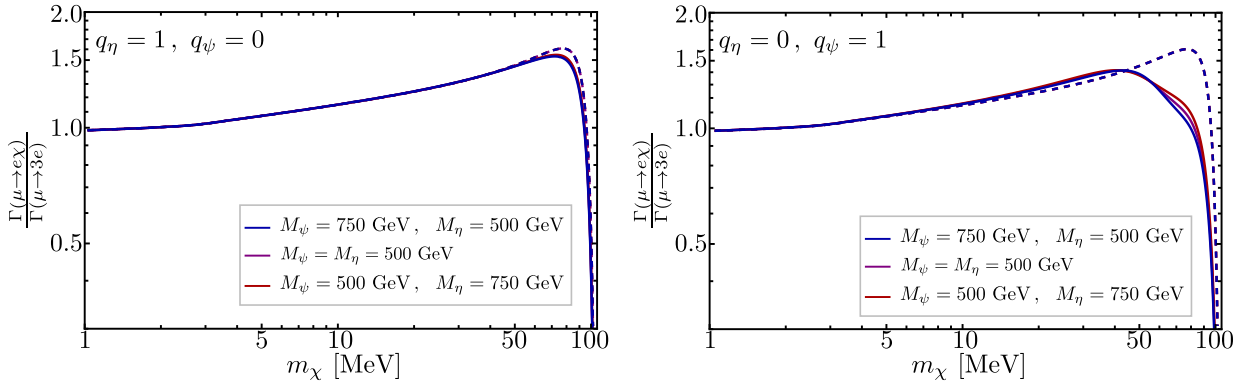

Figure 4.6: *Same as Fig. 4.4, but for the ratio of rates* $\Gamma(\mu \to e\chi)/\Gamma(\mu \to 3e)$*, assuming* $q_L = 1 + q_e$*.*

We show in Fig. 4.5, the branching ratio for $\mu \to 3e$ for the same choices of q_η and q_ψ as in Fig. 4.4, and adopting $q_L = 1 + q_e$ (with $q_e = q_\psi + q_\eta$), using the full result Eq. (4.30) (solid lines) or setting the form factors $F_1 = G_1 = 0$ (dashed lines). As for $\mu \to e\chi$, the form factors can be neglected when $m_\chi \ll m_\mu$, and only contribute to the rate when $m_\chi/m_\mu \gtrsim 0.1$. In Fig. 4.6 we show the ratio of rates $\Gamma(\mu \to e\chi)/\Gamma(\mu \to 3e)$ as a function of m_χ for each of the cases analyzed. We find that the ratio is ~ 1. As in Section 4.3, this result can be understood analytically employing the narrow width approximation. Using the NWA, close to the mass shell, the decay

rate for χ-penguin contribution for $\mu \to 3e$ reads

$$\Gamma(\mu \to 3e) \simeq \frac{m_\mu}{4\pi} \frac{|q_e|^2 + |q_L|^2}{|q_e|^2 + 3|q_L|^2} \left(1 - \frac{m_\chi^2}{m_\mu^2}\right)^2 \left[\left|F_1(m_\chi^2)\frac{m_\mu}{m_\chi} - F_2(m_\chi^2)\frac{m_\chi}{m_\mu}\right|^2 + 2|F_1(m_\chi^2) - F_2(m_\chi^2)|^2\right]$$
$$+ \frac{g_\chi^2 |q_e|^2}{16\pi} \frac{m_\chi^2}{m_\mu} \left(1 - 2\frac{m_\chi^2}{m_\mu^2}\right) \left(2\left(|F_1(m_\chi^2)|^2 - F_1(m_\chi^2)F_2(m_\chi^2)\right) + |F_2(m_\chi^2)|^2 \frac{m_\chi^2}{m_\mu^2}\right) . \tag{4.32}$$

As well as in the analogous expression in the tree level model in Eq. (4.23), the term in the second row is subdominant for the light boson, but the ratio becomes most sensitive to the model parameters as the mass of the χ-boson grows. Also in this scenario one finds an apparent divergence when $m_\chi \to 0$, however the factor $1/m_\chi$ in the rate is cancelled by the factor m_χ implicitly contained in the form factor F_1. As a result, in the limit $m_\chi \to 0$ the rate for $\mu \to 3e$ is finite and comparable to the rate for $\mu \to e\chi$, quite independently of the masses and charges of the particles in the loop.

Given that the current limits on the processes $\mu \to 3e$ and $\mu \to e\chi$, we expect the former to yield the strongest limits on this scenario. This is apparent from Fig. 4.5: the three choices of parameters are allowed by the current constraints on $\mu \to e\chi$, but several orders of magnitude above the SINDRUM limit $\mathrm{BR}(\mu \to 3e) < 1.0 \times 10^{-12}$.

4.5 Extension to three flavors

In this Section we present the extension to three generations of the models discussed in Sections 4.3 and 4.4 [124]. The conclusions obtained remain valid, and the discussion will not modify in the three generation case. However, we will perform an analysis of the tau modes and so complete the picture. The tau decays case is specially interesting given the Belle(-II) efforts (see for instance [125, 126]) in this direction [6].

4.5.1 $\ell_i \to \ell_j \chi$ at tree level

First we perform the extension to three-generation the model described in Section 4.3, which generates the cLFV interaction at tree level. Table 4.4 summarizes the model's particle content and corresponding spins and charges under $SU(2)_L \otimes U(1)_Y \otimes U(1)_\chi$.

The kinetic Lagrangian in Eq. (4.3) and the Yukawa interaction in Eq. (4.5) are still valid with the obvious extension to three generations. Further, the boson mass that arises after the breaking

[6] Private discussions with the Belle-II group at Cinvestav and with Denis Epifanov are acknowledged.

	L_i	e_{R_i}	ϕ_{ij}
spin	1/2	1/2	0
$SU(2)_L$	2	1	2
$U(1)_Y$	$-1/2$	-1	Y_{ij}
$U(1)_\chi$	q_{L_i}	q_{e_i}	$q_{\phi_{ij}}$

Table 4.4: *Spins and charges under $SU(2)_L \otimes U(1)_Y \otimes U(1)_\chi$ of the particles of the model described in Section 4.3, extended to three generations in Section 4.5.1. All fields are assumed to be singlets under $SU(3)_C$ and the subscripts i, $j = 1\,,2\,,3$.*

of the $U(1)_\chi$ symmetry reads

$$m_\chi^2 = g_\chi^2 \sum_{i,j} q_{\phi_{ij}}^2 v_{ij}^2 \,. \tag{4.33}$$

As we previously explained, we need to rotate the fields in flavor eigenstate basis to the mass eigenstate basis in order to find the flavor violating contributions. So, for the three generation case

$$M = \begin{pmatrix} y_{11}v_{11} & y_{12}v_{12} & y_{13}v_{13} \\ y_{21}v_{21} & y_{22}v_{22} & y_{23}v_{23} \\ y_{31}v_{31} & y_{32}v_{32} & y_{33}v_{33} \end{pmatrix} \,, \tag{4.34}$$

and the unitary transformations now are written as

$$V_R = \begin{pmatrix} c_{12_R}c_{13_R} & s_{12_R}c_{13_R} & s_{13_R}e^{-i\delta_{13_R}} \\ -s_{12_R}c_{23_R} - c_{12_R}s_{23_R}s_{13_R}e^{-i\delta_{13_R}} & c_{12_R}c_{23_R} - s_{12_R}s_{23_R}s_{13_R}e^{-i\delta_{13_R}} & s_{23_R}c_{13_R} \\ s_{12_R}s_{23_R} - c_{12_R}c_{23_R}s_{13_R}e^{-i\delta_{13_R}} & -c_{12_R}s_{23_R} - s_{12_R}c_{23_R}s_{13_R}e^{-i\delta_{13_R}} & c_{23_R}c_{13_R} \end{pmatrix} \,, \tag{4.35}$$

where we have defined $s_{jk_R} \equiv \sin\theta_{jk_R}$ and $c_{jk_R} \equiv \cos\theta_{jk_R}$. The unitary transformation V_L is defined analogously to V_R in eq. (4.35), substituting $\theta_{jk_R} \to \theta_{jk_L}$. Finally, following an analogous

procedure to that described in Section 4.3, and using $M_\ell \equiv \text{diag}(m_e, m_\mu, m_\tau)$, it follows that

$$
\begin{aligned}
m_\tau^2 \simeq & y v_{11}^2 + y v_{12}^2 + y v_{13}^2 + y v_{21}^2 + y v_{22}^2 + y v_{23}^2 + y v_{31}^2 + y v_{32}^2 + y v_{33}^2 \,, \\
m_\mu^2 \simeq & \frac{1}{m_\tau^2}\Big(y v_{21}^2 \left(y v_{12}^2 + y v_{13}^2 + y v_{32}^2 + y v_{33}^2\right) + y v_{31}^2 \left(y v_{12}^2 + y v_{13}^2 + y v_{22}^2 + y v_{23}^2\right) + \\
& y v_{11}^2 \left(y v_{22}^2 + y v_{23}^2 + y v_{32}^2 + y v_{33}^2\right) + y v_{23}^2 \left(y v_{12}^2 + y v_{32}^2\right) + y v_{13}^2 \left(y v_{22}^2 + y v_{32}^2\right) + \\
& y v_{33}^2 \left(y v_{12}^2 + y v_{22}^2\right) - 2 y v_{21} y v_{22} y v_{31} y v_{32} - 2 y v_{21} y v_{23} y v_{31} y v_{33} - 2 y v_{22} y v_{23} y v_{32} y v_{33} - \\
& 2 y v_{12} y v_{13} \left(y v_{22} y v_{23} + y v_{32} y v_{33}\right) - 2 y v_{11} \left(y v_{12} y v_{21} y v_{22} + y v_{12} y v_{31} y v_{32} + \right. \\
& \left. y v_{13} y v_{21} y v_{23} + y v_{13} y v_{31} y v_{33}\right)\Big) \,, \\
m_e^2 \simeq & \frac{1}{m_\tau^2 m_\mu^2} \big(y v_{31} (y v_{13} y v_{22} - y v_{12} y v_{23}) + y v_{32} (y v_{11} y v_{23} - y v_{13} y v_{21}) + \\
& y v_{33} (y v_{12} y v_{21} - y v_{11} y v_{22})\big)^2 \,,
\end{aligned}
\tag{4.36}
$$

where $y v_{jk} \equiv y_{jk} v_{jk}$, and we have assumed without loss of generality in the considered phenomenology that the CP-violating phase $\delta_{13_{R(L)}} = 0$ and employed that $m_\tau \gg m_\mu \gg m_e$. So, after rotating Eq. (4.3) to the mass eigenstate basis the flavor violating terms have the form

$$
-\mathcal{L} \supset \overline{\ell}_{i_R} i g_{ij}^{RR} \gamma^\rho \chi_\rho \ell_{j_R} + \overline{\ell}_{i_L} i g_{ij}^{LL} \gamma^\rho \chi_\rho \ell_{j_L} + \text{h.c.} \,,
\tag{4.37}
$$

with

$$
\begin{aligned}
g_{e\mu}^{RR} =& g_\chi \left(c_{12_R} s_{12_R} \left(c_{13_R}^2 q_{e_1} + c_{23_R}^2 (q_{e_3} s_{13_R}^2 - q_{e_2}) + s_{23_R}^2 (q_{e_2} s_{13_R}^2 - q_{e_3}) \right) + \right. \\
& \left. c_{23_R} s_{23_R} (q_{e_3} - q_{e_2}) s_{13_R} \cos(2\theta_{12_R}) \right) \,, \\
g_{e\tau}^{RR} =& g_\chi c_{13_R} \left(c_{23_R} s_{23_R} (q_{e_3} - q_{e_2}) s_{12_R} + c_{12_R} s_{13_R} \left(q_{e_1} - c_{23_R}^2 q_{e_3} - s_{23_R}^2 q_{e_2} \right) \right) \,, \\
g_{\mu\tau}^{RR} =& g_\chi \left(c_{23_R} s_{23_R} (q_{e_2} - q_{e_3}) c_{12_R} + s_{12_R} s_{13_R} \left(q_{e_1} - c_{23_R}^2 q_{e_3} - s_{23_R}^2 q_{e_2} \right) \right) \,.
\end{aligned}
\tag{4.38}
$$

The effective couplings $g_{e\tau}^{LL}$, $g_{e\mu}^{LL}$, and $g_{\mu\tau}^{LL}$, are defined analogously to the right couplings in Eq. (4.38), substituting $\theta_{jk_R} \to \theta_{jk_L}$ and $q_{e_j} \to q_{L_j}$. Here θ_{jk_R} and θ_{jk_L} are mixing angles which can be written as a function of vacuum expectation values, v_{jk}, and Yukawa couplings, y_{jk}, as in the two-generation case. We note that all $g_{ij}^{LL/RR}$ vanish for intergenerational universality of the $U(1)_\chi$ charges, thus forbiding the $\ell_i \to \ell_j \chi$ decays in this tree-level model.

In the three-generation case, in addition to decays of type $\ell_i^- \to \ell_j^- \ell_j^+ \ell_j^-$, we can generate processes of type $\ell_i^- \to \ell_j^- \ell_k^+ \ell_j^-$ and $\ell_i^- \to \ell_j^- \ell_j^+ \ell_k^-$. For concreteness we will only analyze here the decay $\ell_i^- \to \ell_j^- \ell_j^+ \ell_j^-$ (results are similar for the other charge channels). This process is generated through a flavor violating interaction vertex described in eq. (4.37) and a flavor conserving

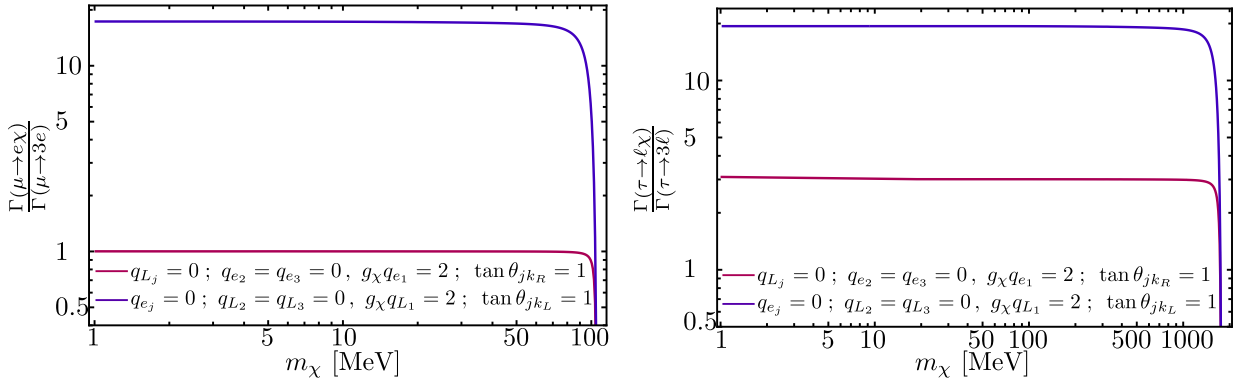

Figure 4.7: $\Gamma(\mu\to e\chi)/\Gamma(\mu\to 3e)$ *(left plot) and* $\Gamma(\tau\to\ell\chi)/\Gamma(\tau\to 3\ell)$ *with* $\ell=e\,,\mu$ *(right plot) as a function of* m_χ *for the tree-level model, for the cases described in the text* $q_{L_j}=0$, $q_{e_2}=q_{e_3}=0$, $g_\chi q_{e_1}=2$, *and* $\tan\theta_{jk_R}=1$ *(magenta line); and* $q_{e_j}=0$, $q_{L_2}=q_{L_3}=0$, $g_\chi q_{L_1}=2$, *and* $\tan\theta_{jk_L}=1$ *(blue line).*

interaction vertex of the form:

$$-\mathcal{L}\supset\bar{\ell}_{i_R}ig^{RR}_{ii}\gamma^\rho\chi_\rho\ell_{i_R}+\bar{\ell}_{i_L}ig^{LL}_{ii}\gamma^\rho\chi_\rho\ell_{i_L}\,, \tag{4.39}$$

where

$$\begin{aligned}
g^{RR}_{ee}&=g_\chi\left(c^2_{12_R}c^2_{13_R}q_{e_1}+\left(c_{23_R}s_{12_R}+c_{12_R}s_{13_R}s_{23_R}\right)^2q_{e_2}+\left(c_{12_R}c_{23_R}s_{13_R}-s_{12_R}s_{23_R}\right)^2q_{e_3}\right)\,,\\
g^{RR}_{\mu\mu}&=g_\chi\left(c^2_{13_R}s^2_{12_R}q_{e_1}+\left(c_{12_R}c_{23_R}-s_{12_R}s_{13_R}s_{23_R}\right)^2q_{e_2}+\left(c_{23_R}s_{12_R}s_{13_R}+c_{12_R}s_{23_R}\right)^2q_{e_3}\right)\,,\\
g^{RR}_{\tau\tau}&=g_\chi\left(s^2_{13_R}q_{e_1}+c^2_{13_R}\left(s^2_{23_R}q_{e_2}+c^2_{23_R}q_{e_3}\right)\right)\,,
\end{aligned} \tag{4.40}$$

and the left couplings, g^{LL}_{ee}, $g^{LL}_{\mu\mu}$, and $g^{LL}_{\tau\tau}$, are obtained with obvious substitutions in eq. (4.40).

We focus again in the scenario where 1 MeV $\lesssim m_\chi\lesssim m_i$. For $m_i=m_\mu$, the dominant decay channels are $\chi\to e^-e^+,\overline{\nu}_{L_1}\nu_{L_1},\overline{\nu}_{L_2}\nu_{L_2},\overline{\nu}_{L_3}\nu_{L_3}$. Then, the total decay width of the χ-boson is:

$$\Gamma_\chi=\frac{m_\chi}{24\pi}\left(|g^{LL}_{ee}|^2+|g^{RR}_{ee}|^2+|g_\chi q_{L_1}|^2+|g_\chi q_{L_2}|^2+|g_\chi q_{L_3}|^2\right)\,, \tag{4.41}$$

and for $m_i=m_\tau$ the decays $\chi\to\mu^-\mu^+,\mu^-e^++\text{h.c.}$ can also be generated, with widths: $\Gamma(\chi\to\mu^-\mu^+)=m_\chi\left(|g^{LL}_{\mu\mu}|^2+|g^{RR}_{\mu\mu}|^2\right)/(24\pi)$ and $\Gamma(\chi\to\mu e)=m_\chi\left(|g^{LL}_{e\mu}|^2+|g^{RR}_{e\mu}|^2\right)/(24\pi)$.

We show in Fig. 4.7 the ratio between $\Gamma(\ell_i\to\ell_j\chi)$ and $\Gamma(\ell_i\to 3\ell_j)$ as a function of m_χ, for a representative case where χ couples only to the R leptons (*i.e.* $q_{L_j}=0$, $q_{e_2}=q_{e_3}=0$, $g_\chi q_{e_1}=2$, and $\tan\theta_{jk_R}=1$) or when χ couples only to the L leptons (*i.e.* $q_{e_j}=0$, $q_{L_2}=q_{L_3}=0$, $g_\chi q_{L_1}=2$, and $\tan\theta_{jk_L}=1$). Again, this result can be understood using the narrow width approximation.

	L_i	e_{R_i}	ϕ	ψ	η
spin	1/2	1/2	0	1/2	0
$SU(2)_L$	2	1	2	1	1
$U(1)_Y$	$-1/2$	-1	$+1/2$	Y_ψ	Y_η
$U(1)_\chi$	q_L	q_e	q_ϕ	q_ψ	q_η

Table 4.5: *Spins and charges under $SU(2)_L \otimes U(1)_Y \otimes U(1)_\chi$ of the particles of the model described in Section 4.4, extended to three generations in Section 4.5.2. All fields are assumed to be singlets under $SU(3)_C$ and the subscript $i = 1\,, 2\,, 3$.*

Under it, the decay rate for $\ell_i \to 3\ell_j$ reads:

$$\Gamma(\ell_i \to 3\ell_j)\Big|_{m_j \to 0} = \frac{m_i m_\chi}{768\pi^2 \Gamma_\chi} \left(|g_{ji}^{LL}|^2 + |g_{ji}^{RR}|^2\right) \left(|g_{jj}^{LL}|^2 + |g_{jj}^{RR}|^2\right) \left(2 + \frac{m_i^2}{m_\chi^2}\right) \left(1 - \frac{m_\chi^2}{m_i^2}\right)^2 + \frac{m_\chi}{64\pi} \left(|g_{jj}^{LL}|^2 |g_{ji}^{LL}|^2 + |g_{jj}^{RR}|^2 |g_{ji}^{RR}|^2\right) \frac{m_\chi}{m_i} \left(1 - 2\frac{m_\chi^2}{m_i^2}\right) . \tag{4.42}$$

Making trivial changes to Eq. (4.14), one reproduces the result $\Gamma(\mu \to e\chi)/\Gamma(\mu \to 3e) \simeq 1$ or $\simeq 17$, and $\Gamma(\tau \to \ell\chi)/\Gamma(\tau \to 3\ell) \simeq 3$ or $\simeq 19$, that we obtained numerically for our two representative scenarios.

4.5.2 $\ell_i \to \ell_j \chi$ at the one loop level

Now we are going to present the model developed in Section 4.4 extended to the three-generation scenario. Table 4.5 summarizes the model's particle content and corresponding spins and charges under $SU(2)_L \otimes U(1)_Y \otimes U(1)_\chi$.

For three-generation case, the Lagrangian that describes the interaction with the massive gauge boson χ has the form:

$$\mathcal{L} \supset - i g_\chi q_L \left(\overline{e}_L \gamma^\nu e_L + \overline{\mu}_L \gamma^\nu \mu_L + \overline{\tau}_L \gamma^\nu \tau_L + \overline{\nu}_{L_1} \gamma^\nu \nu_{L_1} + \overline{\nu}_{L_2} \gamma^\nu \nu_{L_2} + \overline{\nu}_{L_3} \gamma^\nu \nu_{L_3}\right) \chi_\nu - i g_\chi q_e \left(\overline{e}_R \gamma^\nu e_R + \overline{\mu}_R \gamma^\nu \mu_R + \overline{\tau}_R \gamma^\nu \tau_R\right) \chi_\nu - i g_\chi q_\Psi \overline{\Psi} \gamma^\nu \Psi \chi_\nu - i q_\eta g_\chi \left[\eta^* (\partial^\nu \eta) - (\partial^\nu \eta^*) \eta\right] \chi_\nu \,, \tag{4.43}$$

and there also arises a Yukawa coupling to the right-handed leptons $\mathcal{L} \supset h_k \overline{\ell}_{k_R} \eta \psi + \text{h.c.}$ with $\ell_k = e\,, \mu\,, \tau$.

The form factors in Eq. (4.26), as well as, the decay rate in Eq.(4.28), now for the process $\ell_i \to \ell_j \chi$, are still valid making trivial changes to go from the two-generation case to the three-generation one.

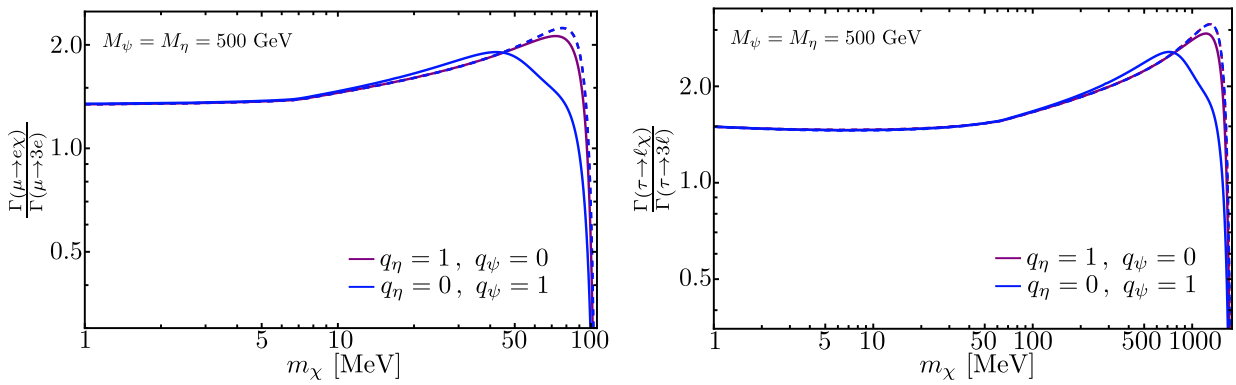

Figure 4.8: *Ratio of rates* $\Gamma(\ell_i \to \ell_j\chi)/\Gamma(\ell_i \to 3\ell_j)$ *as a function of* m_χ *for the one-loop model presented in Section 4.5.2, assuming* $q_L = 1 + q_e$, $h_i h_j = 1$ *and* $g_\chi = 1$. *The solid lines show the full result obtained from Eq. (4.28), while the dashed ones neglect the contribution from* F_1. *The left panel corresponds to the muon channel, and the right panel corresponds to the tau channel.*

As we have pointed out in Section 4.4, in this toy model, $\ell_i^- \to \ell_j^-\ell_j^+\ell_j^-$ arises at one-loop level, through χ-penguin and box diagrams. However, for the three-generation case the wrong-sign decays $\ell_i^- \to \ell_j^-\ell_k^+\ell_j^-$ are also generated, as well as, the decays $\ell_i^- \to \ell_k^-\ell_j^+\ell_j^-$. For the wrong-sign decays, we need two cLFV vertices, so they arise at the one-loop level through χ-penguin topologies and box diagrams. In the χ-penguin-type diagram, each cLFV vertex is similar to those shown in Fig. 4.2 with χ off-shell. The other type of processes is generated through diagrams with a flavor violating interaction vertex and a flavor conserving interaction vertex, plus diagrams with two cLFV vertices, so they arise at the one-loop level through χ-penguin topologies and box diagrams. For simplicity[7], we will only analyze the decays $\ell_i^- \to \ell_j^-\ell_j^+\ell_j^-$ here.

Focusing on the region 1 MeV $\lesssim m_\chi \lesssim m_i$, in the case when $m_i = m_\mu$, the dominant decay modes are $\chi \to e^-e^+\,, \overline{\nu}_{L_1}\nu_{L_1}\,, \overline{\nu}_{L_2}\nu_{L_2}\,, \overline{\nu}_{L_3}\nu_{L_3}$, with width:

$$\Gamma_\chi = \frac{g_\chi^2\, m_\chi}{24\pi}\left(|q_e|^2 + 4|q_L|^2\right)\,, \tag{4.44}$$

and for the $m_i = m_\tau$ case, in addition to the above modes, we must consider the decay mode $\chi \to \mu^-\mu^+$ [8], with width: $\Gamma(\chi \to \mu^-\mu^+) = g_\chi^2\, m_\chi \left(|q_e|^2 + |q_L|^2\right)/(24\pi)$.

We show in Fig. 4.8 the ratio of rates $\Gamma(\ell_i \to \ell_j\chi)/\Gamma(\ell_i \to 3\ell_j)$ as a function of m_χ for two representative choices of charges, $q_\eta = 1$ while $q_\psi = 0$, and $q_\eta = 0$ while $q_\psi = 1$, and a mass choice of 500 GeV for the particles in the loop, M_η and M_ψ. For cases where $M_\eta > M_\psi$ or $M_\psi > M_\eta$

[7] We note that the wrong-sign decays are not suppressed generally, see for instance [127, 128].

[8] The one-loop decay, $\chi \to \mu^-e^+ + \text{h.c.}$, could also be generated in this mass range, however, it is negligible with respect to tree level decays.

(as we analyzed in Section 4.4) the results are analogous. We find that the ratio is ~ 2, for both muon and tau decays. Agains, this result can be understood analytically employing the narrow width approximation. Under it, the decay rate for $\ell_i \to 3\ell_j$ reads

$$\Gamma(\ell_i \to 3\ell_j)\Big|_{m_j\to 0} = \frac{g_\chi^2|q_e|^2}{16\pi}\frac{m_\chi^2}{m_i}\left(1-2\frac{m_\chi^2}{m_i^2}\right)\left(2\left(|F_1(m_\chi^2)|^2 - F_1(m_\chi^2)F_2(m_\chi^2)\right) + |F_2(m_\chi^2)|^2\frac{m_\chi^2}{m_i^2}\right)$$
$$+ \frac{m_i m_\chi g_\chi^2}{96\pi^2\Gamma_\chi}(|q_e|^2+|q_L|^2)\left(1-\frac{m_\chi^2}{m_i^2}\right)^2\left[\left|F_1(m_\chi^2)\frac{m_i}{m_\chi} - F_2(m_\chi^2)\frac{m_\chi}{m_i}\right|^2 + 2|F_1(m_\chi^2)-F_2(m_\chi^2)|^2\right], \tag{4.45}$$

where the term in the second row is dominant for the light boson. Using the Eq. (4.45) and the decay rate in Eq.(4.28) (adapted to the three-generation case), we can obtain the ratio for the cases shown in Fig. 4.8. Also in this scenario, one finds in the limit $m_\chi \to 0$ the rate for $\ell_i \to 3\ell_j$ is finite and comparable to the rate for $\ell_i \to \ell_j\chi$, quite independently of the masses and charges of the particles in the loop.

4.6 Discussion and Conclusions

In previous literature on this topic, in an EFT approach, we find a wrong description of the LFV process $\ell_i \to \ell_j\chi$ when the gauge boson has an ultralight mass. As a result, the decay rate has an unphysical divergence in the limit $m_\chi \to 0$ on account of the term coming from the emission of the longitudinal component of the vector boson.

We have studied in detail the lepton flavor violating process $\ell_i \to \ell_j\chi$, with χ a massive gauge boson arising from the spontaneous breaking of a local $U(1)_\chi$ symmetry. We have constructed the most general effective interaction between two charged leptons with different flavor and a massive gauge boson, and we have calculated the decay rate in terms of the corresponding form factors. The decay rate presents terms inversely proportional to the inverse of the χ-boson mass, corresponding to the decay into the longitudinal component of the χ-boson, which naively lead to an enhancement of the rate when χ is very light.

We have constructed two gauge invariant and renormalizable models where the decay $\mu \to e\chi$ is generated either at tree level or at one-loop level. We have analyzed the behavior of the rate in the limit $m_\chi \ll m_\mu$, and we have explicitly checked that the rate remains finite. We have also calculated the expected rate for the process $\mu \to 3e$, mediated by an off-shell χ.

We have found that for these two models, the ratio of rates of $\mu \to e\chi$ and $\mu \to 3e$ is $\mathcal{O}(1)$ in the range of χ-masses considered. Further, for the tree-level model we find that the decay is dominated by coupling terms proportional to γ^μ and $\gamma^5\gamma^\mu$. On the other hand, for the one-loop model the

decay is mediated by interaction vertices proportional to γ^μ, $\gamma^5\gamma^\mu$, $\sigma^{\mu\nu}p_{\chi\nu}$ and $\gamma^5\sigma^{\mu\nu}p_{\chi\nu}$, although the latter two give the dominant contributions for $m_\chi \to 0$. We have also performed the extension to the three-generation scenario, where the tau channels are generated. This extension does not modify the previous discussion, but rather completes the picture. Correspondingly, and in view of the current limits on $\mu \to 3e$ from the SINDRUM collaboration, it would be necessary an improvement of experiments searching for $\mu \to e\chi$ [129] of at least 5-6 orders of magnitude compared to the TWIST sensitivity in order to observe a signal. Analogous comments apply to $\tau \to (\mu/e)\chi$ in view of the bounds on the $\tau \to 3e, 3\mu, ...$ processes.

A model-independent phenomenological analysis according to the general features found in this chapter (for either tree or loop generated cLFV) is in progress and will be presented elsewhere.

Chapter 5

Indirect upper limits on $\ell_i \to \ell_j\gamma\gamma$ from $\ell_i \to \ell_j\gamma$

5.1 Overview

As we discussed in Chapter 3, the experimental observation of any kind of cLFV would imply the existence of NP even beyond the discovery of neutrino oscillations . The cLFV process $\ell_i \to \ell_j\gamma\gamma$ [130–132] has been less explored than its analogous process with a single photon $\ell_i \to \ell_j\gamma$. For the muon case, the stronger upper limit for $\mu \to e\gamma\gamma$ comes from the Crystal Box detector [133]. This limit is however two orders of magnitude weaker than present $\mu \to e\gamma$ limits, see Table 5.1, since the MEG experiment was optimized for back-to-back topologies and no new dedicated experiment for $\mu \to e\gamma\gamma$ has been carried out since Crystal Box. On the other hand, the tau case, *i.e.* $\tau \to \ell\gamma\gamma$ [134–138] has rarely being searched for. The stronger direct experimental limit we have found in the literature comes from ATLAS after the LHC run-I [139], but there are no direct experimental search exists for its brother channel $\tau \to e\gamma\gamma$. This limit is three orders of magnitude weaker than the current upper limit for $\tau \to \mu\gamma$, as shown in Table 5.1.

Reanalyzing data produced by the BaBar Collaboration for searches of $\tau \to \ell\gamma$ [72], Bryman *et al.* [138] found upper bounds on the branching ratios $\text{BR}(\tau \to \mu\gamma\gamma) < 5.8 \times 10^{-4}$ and $\text{BR}(\tau \to e\gamma\gamma) < 2.5 \times 10^{-4}$ at 90%CL. For this analysis, the authors applied the idea developed by Bowman *et al.* [131], where data from experiments searching $\ell_i \to \ell_j\gamma$ can be used to derive indirect upper limit for $\ell_i \to \ell_j\gamma\gamma$, as some of the events with a single photon would fall into the signal region defined for the double photon channel.

In this chapter, we will develop an analysis on EFT framework of the charged lepton flavor violating processes $\ell_i \to \ell_j\gamma\gamma$ and $\ell_i \to \ell_j\gamma$. Using a low-energy effective Lagrangian we will generate at tree level the local interaction $\bar{\ell}_i\ell_j\gamma\gamma$, which induces to one-loop the $\ell_i \to \ell_j\gamma$ decay. By means of the correlation between the two processes, we will show that the loop corrections can induce large ratios for $\ell_i \to \ell_j\gamma$ deriving in indirect upper limits for $\ell_i \to \ell_j\gamma\gamma$. We will find bounds one order of magnitude stronger than current experimental direct limits for $\mu \to e\gamma\gamma$, and almost three orders of magnitude better than previous considerations for $\tau \to \ell\gamma\gamma$, although the

Decay Mode	Current upper limit on BR (90%CL)	
$\mu \to e\gamma$	4.2×10^{-13}	MEG (2016) [55]
$\mu \to e\gamma\gamma$	7.2×10^{-11}	Crystal Box (1986) [133]
$\tau \to e\gamma$	3.3×10^{-8}	BaBar (2010) [72]
$\tau \to \mu\gamma$	4.2×10^{-8}	Belle (2021) [73]
$\tau \to \mu\gamma\gamma$	1.5×10^{-4}	ATLAS (2017) [139]

Table 5.1: *Experimental upper bounds for the $\ell_i \to \ell_j\gamma(\gamma)$ cLFV decays.*

direct searches for these processes at Belle II could improve these results.

At the lowest order in the EFT, the single photon cLFV decay is induced by a five-dimensional dipole operator, which will also generate $\ell_i \to \ell_j\gamma\gamma$ by radiating an additional photon from either lepton. Nevertheless, being an $\mathcal{O}(\alpha)$ suppressed contribution, we do not expect to learn new information from the latter channel.

In this work, we will not consider flavor conserving interactions, since its effects on NP would be very suppressed with respect to the contributions of QED, known to high precision [140]. We will focus on the correlation between the single-photon channel and the double photon channel in the scenario when the dim-5 operators are suppressed and the main contribution comes from the dim-7 operators. The aim is, through a model-independent EFT analysis, to derive new indirect limits on the double photon channel due to the current experimental bounds on the single-photon channel. In Section 5.2, we present the effective Lagrangian built with seven- and eight-dimensional operators, that describe tree-level interactions $\bar{\ell}_i\ell_j\gamma\gamma$. In Section 5.3, we study the possible EW invariant extensions of the effective Lagrangian. In Section 5.4, we present the indirect upper limits for $\ell_i \to \ell_j\gamma\gamma$ decay from the correlation with $\ell_i \to \ell_j\gamma$. We end in Section 5.6 with the final discussion and conclusions [1].

[1] Note added: This chapter is the basis of [141].

5.2 EFT analysis of $\ell_i \to \ell_j\gamma\gamma$

The most general low-energy effective Lagrangian (QED-invariant) that describes the local interaction of two charged leptons of different flavor and two photons, is given by [131]

$$\begin{aligned}\mathcal{L}_{\text{Int}} = &\left(G_{SR}^{ij}\bar{\ell}_{L_i}\ell_{R_j} + G_{SL}^{ij}\bar{\ell}_{R_i}\ell_{L_j}\right)F_{\mu\nu}F^{\mu\nu} \\ &+ \left(\tilde{G}_{SR}^{ij}\bar{\ell}_{L_i}\ell_{R_j} + \tilde{G}_{SL}^{ij}\bar{\ell}_{R_i}\ell_{L_j}\right)\tilde{F}_{\mu\nu}F^{\mu\nu} \\ &+ \left(G_{VL}^{ij}\bar{\ell}_{L_i}\gamma^{\sigma}\ell_{L_j} + G_{VR}^{ij}\bar{\ell}_{R_i}\gamma^{\sigma}\ell_{R_j}\right)F^{\mu\nu}\partial_{\nu}F_{\mu\sigma} \\ &+ \left(\tilde{G}_{VL}^{ij}\bar{\ell}_{L_i}\gamma^{\sigma}\ell_{L_j} + \tilde{G}_{VR}^{ij}\bar{\ell}_{R_i}\gamma^{\sigma}\ell_{R_j}\right)F^{\mu\nu}\partial_{\nu}\tilde{F}_{\mu\sigma} + \text{h.c.}\,, \end{aligned} \tag{5.1}$$

where the dual tensor is defined by $\tilde{F}_{\mu\nu} = \frac{1}{2}\epsilon_{\mu\nu\sigma\lambda}F^{\sigma\lambda}$ and i, j are generation indices. We note that in this effective Lagrangian we have scalar operators and vector operators. The first are contributions of dimension seven and the second are eight-dimensional, then at low-energy, the vector contributions will be suppressed by a factor $\mathcal{O}(m_i/\Lambda)$ with respect to the scalar operators. Here m_i is the mass of the decaying lepton, Λ the scale of new physics responsible for these interactions and $G_{SR(L)}$, $\tilde{G}_{SR(L)}$, $G_{VR(L)}$, $\tilde{G}_{VR(L)}$ are effective couplings, which have energy dimensions $[G_{SR(L)}] = [\tilde{G}_{SR(L)}] = E^{-3}$ and $[G_{VR(L)}] = [\tilde{G}_{VR(L)}] = E^{-4}$.

In the charged lepton sector it is satisfied that $m_e \ll m_\mu \ll m_\tau$, then m_j will be neglected in the remaining chapter. In the rest frame of the decaying particle, the differential decay rate for $\ell_i \to \ell_j\gamma\gamma$ is given by

$$\frac{\mathrm{d}^2\Gamma(\ell_i \to \ell_j\gamma\gamma)}{\mathrm{d}E_\gamma \mathrm{d}E_{\gamma'}} = \frac{\left|G_{ij}\right|^2}{16\pi^3}\, m_i^2\big(m_i - E_\gamma - E_{\gamma'}\big)\big(m_i - 2(E_\gamma + E_{\gamma'})\big)^2\,, \tag{5.2}$$

where E_γ and $E_{\gamma'}$ are the energies associated with the photons, and we define

$$\begin{aligned}\left|G_{ij}\right|^2 \equiv &\left|G_{SL}^{ij} + \frac{im_iG_{VR}^{ij}}{4}\right|^2 + \left|G_{SR}^{ij} + \frac{im_iG_{VL}^{ij}}{4}\right|^2 \\ &+ \left|\tilde{G}_{SL}^{ij} + \frac{im_i\tilde{G}_{VR}^{ij}}{4}\right|^2 + \left|\tilde{G}_{SR}^{ij} + \frac{im_i\tilde{G}_{VL}^{ij}}{4}\right|^2. \end{aligned} \tag{5.3}$$

We could also generate the process of interest by means of an effective five-dimensional dipole operator [142]

$$\mathcal{L}_{\text{dim-5}} = D_R^{ij}\,\bar{\ell}_{L_i}\sigma_{\mu\nu}\ell_{R_j}F^{\mu\nu} + D_L^{ij}\,\bar{\ell}_{R_i}\sigma_{\mu\nu}\ell_{L_j}F^{\mu\nu} + \text{h.c.}\,, \tag{5.4}$$

plus a photon radiated from either lepton. Here $\sigma_{\mu\nu} = \frac{i}{2}[\gamma^\mu, \gamma^\nu]$ and $D_{R(L)}^{ij}$ are effective couplings with energy dimensions $[D_{R(L)}^{ij}] = E^{-1}$. The corresponding differential decay rate for $\ell_i \to \ell_j\gamma\gamma$

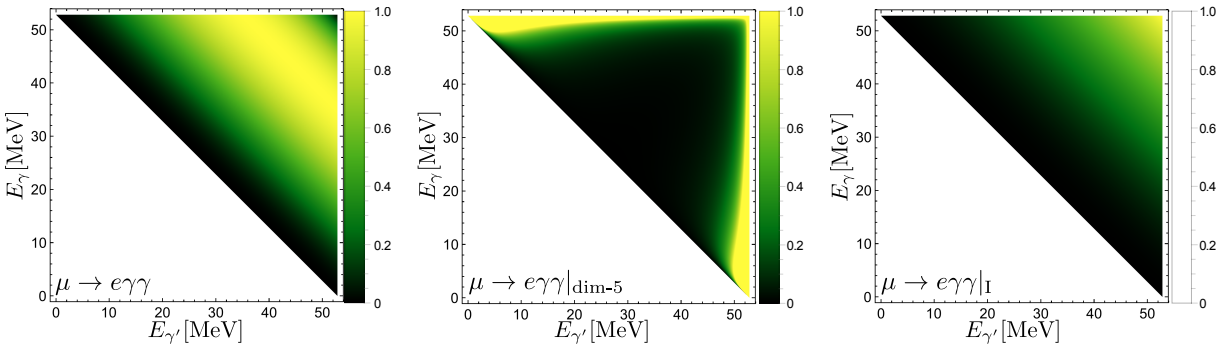

(a) *Local interaction.* (b) *Radiative dipole interaction.* (c) *Interference interaction.*

Figure 5.1: *Normalized Dalitz plot distributions for $\mu \to e\gamma\gamma$ for the local interaction case (left plot), the radiative dipole interaction case (middle plot) and the interference term between the two previous interactions (right plot).*

is given by

$$\left.\frac{\mathrm{d}^2\Gamma(\ell_i \to \ell_j\gamma\gamma)}{\mathrm{d}E_\gamma \mathrm{d}E_{\gamma'}}\right|_{\text{dim-5}} = \frac{\alpha\left(|D_R^{ij}|^2 + |D_L^{ij}|^2\right)}{4E_\gamma E_{\gamma'} + m_i^2 - 2m_i(E_\gamma + E_{\gamma'})} \frac{m_i - 2(E_\gamma + E_{\gamma'})}{4\pi^2 E_\gamma^2 E_{\gamma'}^2} \Big[48E_\gamma^3 E_{\gamma'}^3 - m_i^4(E_\gamma - E_{\gamma'})^2 + 2E_\gamma E_{\gamma'} m_i^2\left(E_\gamma^2 + 6E_\gamma E_{\gamma'} + E_{\gamma'}^2\right) - E_\gamma E_{\gamma'} m_i(E_\gamma + E_{\gamma'})\left(24E_\gamma E_{\gamma'} + m_i^2\right)\Big], \tag{5.5}$$

and the differential decay rate for $\ell_i \to \ell_j\gamma\gamma$ from the interference between the effective local operator and the effective dipole operator contributions reads

$$\left.\frac{\mathrm{d}^2\Gamma(\ell_i \to \ell_j\gamma\gamma)}{\mathrm{d}E_\gamma \mathrm{d}E_{\gamma'}}\right|_{\text{I}} = \frac{e\, m_i^2\big(m_i - 2(E_\gamma + E_{\gamma'})\big)^2}{32\pi^3}\left[D_R^{ij}\left(\tilde{G}_{VR}^{ij} + \frac{8G_{SR}^{ij}}{m_i}\right) - D_L^{ij}\left(\tilde{G}_{VL}^{ij} - \frac{8G_{SL}^{ij}}{m_i}\right)\right]. \tag{5.6}$$

We have described the decay $\ell_i \to \ell_j\gamma\gamma$ using local interaction with the Lagrangian in eq. (5.1) and radiative dipole interaction by Lagrangian in Eq. (5.4). In Fig. 5.1 we show the normalized Dalitz plot distributions for $\mu \to e\gamma\gamma$ for the local interaction case, the radiative dipole interaction case and the interference term between both Lagrangians. Comparing the three figures, we observe clear differences between the local interaction, the dipole interaction with a radiated photon and the interference term between them. The normalized Dalitz plot distributions in Fig. 5.1 show that by means of this observable one could differentiate experimentally the local interaction $\overline{\ell_i}\ell_j\gamma\gamma$ ($\mathcal{L}_{\text{Int}}$), from the dipole operator with one-photon radiation ($\mathcal{L}_{\text{dim}-5}$).

As we pointed out before, the relevant contributions in the effective Lagrangian for the low-energy cLFV observables, are the seven-dimension scalar operators. Consequently, we will neglect

the contribution of the vector operators in the remaining work. In this limit, the effective coupling defined in Eq. (5.3) corresponds to $|G_{ij}|^2 \equiv |G_{SL}^{ij}|^2 + |G_{SR}^{ij}|^2 + |\tilde{G}_{SL}^{ij}|^2 + |\tilde{G}_{SR}^{ij}|^2$. Finally, the partial decay rate for $\ell_i \to \ell_j\gamma\gamma$ reads

$$\Gamma(\ell_i \to \ell_j\gamma\gamma) = \frac{|G_{ij}|^2}{3840\pi^3}\, m_i^7 \,. \tag{5.7}$$

Using the U.L. for the different channels of the $\ell_i \to \ell_j\gamma\gamma$ decay: $\mathrm{BR}(\mu \to e\gamma\gamma) < 7.2 \times 10^{-11}$ [133], $\mathrm{BR}(\tau \to \mu\gamma\gamma) < 1.5 \times 10^{-4}$ [139] and $\mathrm{BR}(\tau \to e\gamma\gamma) < 2.5 \times 10^{-4}$ [143], we can put the following constraints on the effective couplings:

$$\begin{aligned} |G_{\mu e}| &\leq 4.2 \times 10^{-9}\ \mathrm{GeV}^{-3}\,, \\ |G_{\tau e}| &\leq 1.1 \times 10^{-6}\ \mathrm{GeV}^{-3}\,, \\ |G_{\tau\mu}| &\leq 8.5 \times 10^{-7}\ \mathrm{GeV}^{-3}\,, \end{aligned}$$

where the constraint on $|G_{\mu e}|$ is in accordance with the limit obtained by S. Davidson *et. al.* [132].

Unlike the Lagrangian in Eq. (5.1), the effective dipole Lagrangian in Eq. (5.4), contributes to $\ell_i \to \ell_j\gamma$ at the tree level,

$$\Gamma(\ell_i \to \ell_j\gamma)_{\mathrm{dim-5}} = \frac{m_i^3}{4\pi}\left(|D_R^{ij}|^2 + |D_L^{ij}|^2\right)\,, \tag{5.8}$$

and therefore their $\mathcal{O}(\alpha)$ suppressed contribution to $\ell_i \to \ell_j\gamma\gamma$ is expected to lay beyond experimental sensitivities, as we will see in the next section.

5.3 Invariance under the electroweak group

The Lagrangian in Eq. (5.1) is obviously not invariant under the Standard Model (SM) gauge symmetry. However, it is possible to write a Lagrangian for the considered interactions with photons and charged leptons which is manifestly $SU(2)_L \otimes U(1)_Y$ invariant above the EW energy scale. It reads [2]

$$\begin{aligned} \mathcal{L}'_{\mathrm{Int}} = &\left(\frac{g_{SR}^{ij}}{\Lambda^4}\overline{L}_{L_i}\Phi\ell_{R_j} + \frac{g_{SL}^{ij}}{\Lambda^4}\overline{\ell}_{R_i}\Phi^\dagger L_{L_j}\right) B_{\mu\nu}B^{\mu\nu} \\ &+ \left(\frac{g_{VL}^{ij}}{\Lambda^4}\overline{L}_{L_i}\gamma^\sigma L_{L_j} + \frac{g_{VR}^{ij}}{\Lambda^4}\overline{\ell}_{R_i}\gamma^\sigma \ell_{R_j}\right) B^{\mu\nu}D_\nu B_{\mu\sigma}\,, \end{aligned} \tag{5.9}$$

[2] For simplicity we do not write the terms with dual fields but they must be considered.

where $B^{\mu\nu}$ is the hypercharge field, D_ν is the covariant derivative, and Φ is the SM Higgs isodoublet (see chapter 2). Here L_{L_i} stands for the leptonic L isodoublet, the effective couplings $g^{ij}_{SR(L)}$ and $g^{ij}_{VR(L)}$ are dimensionless, and, as we had previously pointed, Λ is the scale of new physics. Working in the unitary gauge, such that

$$\phi = \frac{1}{\sqrt{2}}\begin{pmatrix} 0 \\ v+H \end{pmatrix}, \quad \text{and} \quad L_{L_i} = \begin{pmatrix} \nu_{L_i} \\ \ell_{L_i} \end{pmatrix},$$

one finds after spontaneous electroweak symmetry breaking, in addition to the interest interaction, terms that generate new interactions between the Higgs boson, two charged leptons, and two photons

$$\begin{aligned} \mathcal{L}'_{\text{Int}} =& \frac{1}{\sqrt{2}}\left(\frac{g^{ij}_{SR}}{\Lambda^4}\overline{\ell}_{L_i}\ell_{R_j} + \frac{g^{ij}_{SL}}{\Lambda^4}\overline{\ell}_{R_i}\ell_{L_j}\right)(v+H)\cos^2\theta_w F_{\mu\nu}F^{\mu\nu} \\ &+ \left(\frac{g^{ij}_{VL}}{\Lambda^4}\overline{\ell}_{L_i}\gamma^\sigma\ell_{L_j} + \frac{g^{ij}_{VR}}{\Lambda^4}\overline{\ell}_{R_i}\gamma^\sigma\ell_{R_j}\right)\cos^2\theta_w F^{\mu\nu}\partial_\nu F_{\mu\sigma} + \cdots . \end{aligned} \tag{5.10}$$

Noteworthy, additional processes will also be generated between the Higgs, two charged leptons and two Z bosons, or one Z and one photon, as well as interactions with neutrinos, which are not shown in the Lagrangian in Eq. (5.10).

If we identify

$$\begin{aligned} G^{ij}_{SR} &\equiv \frac{g^{ij}_{SR}}{\Lambda^4\sqrt{2}} v\cos^2\theta_w\,, \\ G^{ij}_{VR} &\equiv \frac{g^{ij}_{VR}}{\Lambda^4}\cos^2\theta_w\,, \end{aligned}$$

and analogously for L coefficients, we may then recover the Lagrangian in Eq. (5.1).

Notice that in Eq. (5.10), if the scale of the process is smaller than the Higgs vacuum expectation value, the operator in the second row, which involves a derivative of the electromagnetic tensor, would be suppressed concerning the operator in the first row. Then, we will only use the dominant operator below.

Particularly interesting could be to analyze the cLFV interactions $H\overline{\ell}_i\ell_j\gamma\gamma$ generated after the SSM, as we present in Eq. (5.10). Using our best upper limits for the coefficients $|G_{ij}|$ in

Eq. (5.14), we can put constrain on the $\mathrm{Br}(H \to \ell_i\ell_j\gamma\gamma)$ [3], as follows [4]

$$\begin{aligned}
\mathrm{Br}(H \to \mu e\gamma\gamma) &\leq 1.4 \times 10^{-11}\,, \\
\mathrm{Br}(H \to \tau e\gamma\gamma) &\leq 2.2 \times 10^{-8}\,, \\
\mathrm{Br}(H \to \tau\mu\gamma\gamma) &\leq 2.9 \times 10^{-8}\,.
\end{aligned}$$

5.4 Upper limits from $\ell_i \to \ell_j\gamma$

The effective operators in Eq. (5.1) were built with the aim of generating a local interaction involving two leptons and two photons. As a result they will not contribute to $\ell_i \to \ell_j\gamma$ at the tree level, and therefore the $\ell_i \to \ell_j\gamma\gamma$ decays can provide new information about these independent operators. Nevertheless, $\ell_i \to \ell_j\gamma$ can be generated at one loop from the same operators, as shown in Fig. 5.2. Notice that there are two additional diagrams where the loop is composed of the two photons in the effective vertex, known as tadpole diagrams, and the photon in the final state is coupled to either lepton. Nonetheless, the integration scale of the tadpole would be the mass of the particles in the loop, and thus these loops vanish for photons.

The amplitudes generated by these diagrams have UV divergent terms, and thus we need to introduce dim-5 and 6 counterterms to absorb them. These are given by

$$\begin{aligned}
\mathcal{L}_{\mathrm{CT}} = {} & C_L\,\bar{\ell}_L\gamma^\alpha\partial^\beta\ell_L F_{\alpha\beta} + C_R\,\bar{\ell}_R\gamma^\alpha\partial^\beta\ell_R F_{\alpha\beta} \\
& + D_R\,\bar{\ell}_L\sigma_{\alpha\beta}\ell_R F^{\alpha\beta} + D_L\,\bar{\ell}_R\sigma_{\alpha\beta}\ell_L F^{\alpha\beta}\,,
\end{aligned} \tag{5.11}$$

where for simplicity, we have omitted generation indices.

Notice that in Eq. (5.11), the first row are six-dimensional operators and the second row are five-dimensional operators. It also highlights the fact that the last row is precisely Eq. (5.4), meaning that quantum corrections generate the dipole operator even if they were suppressed at first. The coefficients of these operators take the values

$$\begin{aligned}
C_L &= \frac{2\,e}{3\epsilon} m_i\,(\tilde{G}_{SR} - iG_{SR})\,, \\
C_R &= -\frac{2\,e}{3\epsilon} m_i\,(\tilde{G}_{SL} - iG_{SL})\,, \\
D_R &= \frac{2\,e}{3\epsilon} m_i^2\,(2i\tilde{G}_{SR} - G_{SR})\,, \\
D_L &= -\frac{2\,e}{3\epsilon} m_i^2\,(2i\tilde{G}_{SL} - G_{SL})\,,
\end{aligned} \tag{5.12}$$

[3] As usual, both charge conjugate channels are included.

[4] We are not considering possible contributions due to operators that generate interactions of the dipolar type.

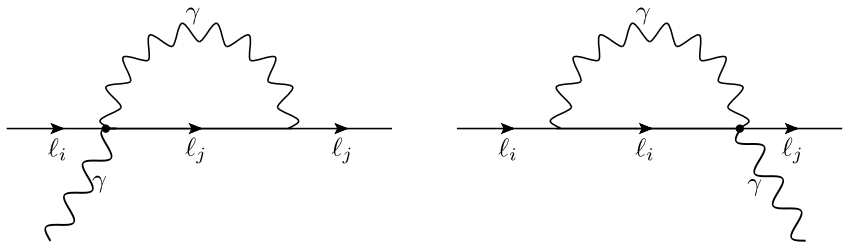

Figure 5.2: *One-loop diagrams contributing to $\ell_i \to \ell_j \gamma$ from the effective operators in eq. (5.1).*

with $D = 4 - 2\epsilon$. Then, in the $\overline{MS}$ scheme, the decay rate for $\ell_i \to \ell_j \gamma$ is given by

$$\begin{aligned}\Gamma(\ell_i \to \ell_j \gamma) \simeq & \frac{\alpha\,|G_{ij}|^2}{144\,\pi^4}\, m_i^7 \left[1 + \frac{3}{4}\log\left(\frac{\mu^2}{m_i^2}\right)\right]^2 \\ \simeq & \frac{80\alpha}{3\pi}\left[1 + \frac{3}{4}\log\left(\frac{\mu^2}{m_i^2}\right)\right]^2 \Gamma(\ell_i \to \ell_j \gamma\gamma)\,. \end{aligned} \tag{5.13}$$

Following this relation and the U.L. on the $\mathrm{BR}(\ell_i \to \ell_j \gamma)$ in table 5.1, we obtained stronger limits for the effective couplings $|G_{ij}|$ (for $\mu = m_i$, which yields the most conservative upper bounds):

$$\begin{aligned} |G_{\mu e}| &\leq 1.3 \times 10^{-9}\ \mathrm{GeV}^{-3}\,, \\ |G_{\tau e}| &\leq 5.9 \times 10^{-8}\ \mathrm{GeV}^{-3}\,, \\ |G_{\tau \mu}| &\leq 5.1 \times 10^{-8}\ \mathrm{GeV}^{-3}\,, \end{aligned} \tag{5.14}$$

where, these constraints lead to indirect upper limits for $\ell_i \to \ell_j \gamma\gamma$,

$$\mathrm{BR}(\mu \to e\gamma\gamma) \leq 6.8 \times 10^{-12}\,, \tag{5.15}$$

$$\mathrm{BR}(\tau \to e\gamma\gamma) \leq 5.3 \times 10^{-7}\,, \tag{5.16}$$

$$\mathrm{BR}(\tau \to \mu\gamma\gamma) \leq 6.8 \times 10^{-7}\,. \tag{5.17}$$

The prediction for $\mathrm{BR}(\mu \to e\gamma\gamma)$ is almost one order of magnitude more restrictive than the experimental constraint from the Crystal Box Detector. Using the expected sensitivity for the $\mu \to e\gamma$ decay in MEG II [144], we would obtain an indirect constraint on $\mathrm{BR}(\mu \to e\gamma\gamma)$ of around one order of magnitude stronger than that shown in Eq. (5.15). Similarly, the prediction for τ decays is around three orders of magnitude more restrictive than the constraint from Bryman *et. al.* [143] and ATLAS [139]. Notice that these upper limits were obtained under the extreme hypothesis of suppressed dim-5 dipole operators with respect dim-7 ones, *i.e.* the most interesting scenario for the double photon channel, and yet they are stronger than current limits, especially

for τ decays. It is also important to mention that, if the main contribution in the Lagrangian of Eq. (5.1) comes from the eight-dimensional operators, for instance in a model where LFV is restricted to the L sector, the limits on the Branching fractions in Eqs. (5.15)-(5.17) are reduced by a factor $\sim [3.5, 4]$.

On the other hand, if the dipole contributions are not suppressed by symmetries in the UV, then they naturally dominate over those in Eq. (5.1) in the IR. However they are strongly constrained by $\ell_i \to \ell_j\gamma$, which they induce already at the tree level, and moreover their contribution to $\ell_i \to \ell_j\gamma\gamma$ has an additional $\mathcal{O}(\alpha)$ suppression. From the description at tree level of $\ell_i \to \ell_j\gamma$ in Eq. (5.8), and using the U.L. for these processes, we obtain

$$\sqrt{|D_R^{\mu e}|^2 + |D_L^{\mu e}|^2} \leq 3.7 \times 10^{-14}\ \text{GeV}^{-1}\,,$$
$$\sqrt{|D_R^{\tau e}|^2 + |D_L^{\tau e}|^2} \leq 4.1 \times 10^{-10}\ \text{GeV}^{-1}\,,$$
$$\sqrt{|D_R^{\tau \mu}|^2 + |D_L^{\tau \mu}|^2} \leq 4.7 \times 10^{-10}\ \text{GeV}^{-1}\,.$$

Consequently, if the dipole is the only source of cLFV, the allowed rates for the double photon emission will be even more constrained:[5]

$$\text{BR}(\mu \to e\gamma\gamma)_{\text{dim}-5} \leq 2.4 \times 10^{-14}\,, \tag{5.18}$$
$$\text{BR}(\tau \to e\gamma\gamma)_{\text{dim}-5} \leq 3.1 \times 10^{-9}\,, \tag{5.19}$$
$$\text{BR}(\tau \to \mu\gamma\gamma)_{\text{dim}-5} \leq 4.2 \times 10^{-9}\,. \tag{5.20}$$

These results follow our discussion above, since we do not expect to learn any new information from the double photon channels if they originate from the same source inducing the single photon one.

Finally, it is worth mentioning that we also considered the processes $\ell_i \to \ell_j\ell_j\bar{\ell}_j$ and $\ell_i \to \ell_j\ell_k\bar{\ell}_k$, which can be generated at one-loop from the Lagrangian in Eq. (5.1). However these decays are $\mathcal{O}(\alpha)$ suppressed compared with the $\ell_i \to \ell_j\gamma$ decays and, since the experimental constraints [55, 57, 72–74] on both types of processes are of the same order, the former restrictions are trivially satisfied when the limits of the latter have been imposed.

5.5 $\ell_i \to \ell_j\gamma$ vs $\ell_i \to \ell_j\gamma\gamma$ in specific model realizations

Whatever NP generates $\ell_i \to \ell_j\gamma$ at measurable rates will also induce the double photon process trivially, by radiation off either charged lepton. This, however, will not be very interesting, since

[5] Here we imposed $E_\gamma > 7\,(50)$ MeV in $\mu\,(\tau)$ decays in order to avoid collinear singularities from bremsstrahlung.

the two-photon process will be $\mathcal{O}(\alpha)$ suppressed with respect to the single-photon one and the experimental upper limit on the former can be, at most, of the same order of magnitude than the bound on the latter.

Situations where the two-photon process really provide an independent handle on the physics underlying cLFV correspond, in the EFT viewpoint, to the case where both decay modes are primarily generated by different operators. For the double photon process to be phenomenologically relevant, one would also need that the dipole operators generating $\ell_i \to \ell_j\gamma$ at lowest order in the low-energy EFT (dimension five) are suppressed, so that the corresponding ones inducing $\ell_i \to \ell_j\gamma\gamma$ (starting at dimension seven) matter. Ultimately, only the experiment will tell what is the process where cLFV is finally discovered. Nonetheless, it seems adequate to motivate experimental searches of the two-photon process by showing a realistic NP model where actually $\ell_i \to \ell_j\gamma\gamma$ can be as relevant as $\ell_i \to \ell_j\gamma$, a question which we study next.

This was pioneered in Ref. [131], finding that charged heavy lepton mediation of the cLFV would GIM-suppress stronger $\ell_i \to \ell_j\gamma$ than $\ell_i \to \ell_j\gamma\gamma$. We examined three different well-motivated scenarios for cLFV: Higgs mediation, axion-like particles (ALPs) and two Higgs doublet models (2HDMs), findind that also within 2HDMs the two-photon decay is relevant phenomenologically. Some more details on each model are given in the following.

Before the improved CMS [145] and ATLAS [81] bounds on $H \to \ell_i\bar{\ell}_j$, there was enough room to allow for interesting Higgs-mediated LFV signatures, as it was shown in Ref. [146]. Therein, the only source of LFV was the Yukawa couplings, which were severely constrained by the most recent LHC measurements. As a result of that, the decay rates with a single photon turns out to be always considerably larger than that of the double photon process.

In the case of ALPs, their cLFV interactions (and also the flavor-conserving ones) were examined in Refs. [106,147]. ALPs were an interesting candidate to study, as they naturally couple to a photon pair. Although ALPs are searched for in a wide range of masses, our interest was restricted here to the case where its mass is larger than the decaying lepton's (otherwise the low-energy EFT needs to be modified to include this ALP, a, as an active degree of freedom; in any case, searches for $\ell_i \to \ell_j a$ would be more interesting, see e.g. Ref. [148]). Applying the known bounds on ALP couplings, again the two-photon process is quite suppressed compared to the single photon one.

Finally, results are much more promising within 2HDMs. In this case, the $\ell_i \to \ell_j\gamma$ decays are allowed at one loop, but thrice helicity suppressed, which makes the two loop Barr-Zee type of diagram the dominant contribution. As the one-loop $\ell_i \to \ell_j\gamma\gamma$ process is not suppressed, it seems *a priori* possible that the two-photon channel be relevant. In the heavy Higgs limit, both

decays are related by

$$\mathrm{BR}(\ell_i \to \ell_j \gamma) \backsimeq \frac{15\alpha}{\pi}\left[\log\left(\frac{m_i^2}{m_H^2}\right)\right]^2 \mathrm{BR}(\ell_i \to \ell_j \gamma\gamma)\,, \tag{5.21}$$

where H stands for the heaviest neutral scalar (the contribution from h, with $m_h \sim 125$ GeV, vanishes in the alignment limit, which is favored by data [41]; and that of the pseudoscalar boson, A, is suppressed for the two photon mode as it does not couple to W bosons at tree level). As a result of eq. (5.21), $\mathrm{BR}(\ell_i \to \ell_j \gamma) \sim \mathrm{BR}(\ell_i \to \ell_j \gamma\gamma)$ for both $i = \mu, \tau$, enhancing the case for searches of the di-photon mode at MEG II and Belle-II.

5.6 Discussion and Conclusions

We have studied in an EFT framework the local cLFV interaction $\bar{\ell}_i \ell_j \gamma\gamma$ and its correlation with the $\ell_i \to \ell_j \gamma$ decay. In the scenario where seven-dimensional dominate over five-dimensional operators, we derived model-independent upper limits for $\ell_i \to \ell_j \gamma\gamma$ decay, presented in Eqs. (5.15)-(5.17). These limits have been obtained indirectly from the $\ell_i \to \ell_j \gamma$ decay induced at one-loop for the effective Lagrangian in Eq. (5.1). In the situation where these processes are generated through the dipole operator, we obtained stronger upper bounds than the constraints shown in Eqs. (5.15)-(5.17), whereby these upper bounds could be considered as the most conservative limits.

The upper limits found are stronger than the current limits on these decays. For the muon case, the limit found here improves by one order of magnitude the direct search by the Crystal Box detector. While the limits for the less explored channel $\tau \to \ell\gamma\gamma$ are almost three orders of magnitude stronger than previous analyses. Future searches of the single-photon channel in experiments like MEG II [56] and Belle II [76] will improve these upper limits in one order of magnitude, approximately.

Naively assuming that Belle II could achieve the same sensitivity for double photon process as for single photon process, the experiment could probe the $\ell_i \to \ell_j \gamma\gamma$ decays up to $\mathcal{O}(10^{-9})$, thus improving our indirect limits in Eqs. (5.16) and (5.17). Moreover, Belle II could even access the bounds induced by the dipole operators, Eqs. (5.19) and (5.20), however, we stress that it is better to prove the dipole operators through single-photon decays.

The cLFV decays $\ell_i \to \ell_j \gamma\gamma$ are not the golden channels for LFV searches, consequently having been less explored than analogous processes such as the single-photon channel or $\ell_i \to 3\ell_j$. A motivation to be interested in these processes comes from an EFT point of view, where these channels allow to probe new independent effective operators, and thus they will help cover directions in the NP space. On the other side, the model building point of view is less trivial.

Naively, we could expect that any UV complete theory leading to $\ell_i \to \ell_j \gamma\gamma$ would first induce the single-photon channel, however, there could be models where the opposite occurs. We have seen that within two Higgs double models it is possible that both decay channels have similar probabilities. This would be a well-motivated scenario that illustrates the potential of $\ell_i \to \ell_j \gamma\gamma$ decays in the search for NP. We are currently refining our work in this direction [6].

[6] A more detailed account will be given in Fabiola Fortuna's Ph. D. Thesis, next year. Therein, the relevance of the LFV two-photon vertex in LFV conversions in nuclei will also be discussed.

Chapter 6

Conclusions and Perspectives

The motivation behind the studies performed in this thesis is the possible existence of physics beyond the Standard Model in experimental searches for charged lepton flavor violation. Besides that and their intrinsic interest, we were motivated by the possibility to contribute from a phenomenological point of view in the experimental search for these signals. In this thesis, we report our results and phenomenological analysis on the analysis of some selected cLFV processes, which may be useful in experimental searches for NP. In this Chapter, we summarized the main conclusions and results presented in this work, developed in the central chapters of this thesis: Chapters 4 and 5. We also present the perspectives and works in progress which are extensions of the main material covered in this thesis.

Experimental searches for cLFV decays, including, or mediated by, invisible states (χ) have been developed since the mid-1980s. In $\ell_i \to \ell_j \chi$ decays, the strongest upper limit for muon to electron transition comes from the TWIST collaboration in 2015, while for tau modes comes from the ARGUS collaboration in 1995. The best limits for these processes are orders of magnitude poorer than current limits from cLFV decays where all final state particles are detected. This fact has triggered studies in the BaBar and Belle(-II) collaborations to search for these processes and also MEG-II intends to improve TWIST limits.

One of the possible scenarios for cLFV decay including invisible states, is when the invisible state has spin one, which admits a rigorous QFT understanding when χ is a gauge boson. In the simplest EFT description, using an effective Lagrangian $\mathcal{L}_{\text{eff}} = g\bar{\ell}_i \gamma^\rho \chi_\rho \ell_j + \text{h.c.}$, an unphysical divergence in the limit $m_\chi \to 0$ is found. This divergence corresponds to the emission of the longitudinal component of the vector boson.

In Chapter 4, we show that the divergence in the limit $m_\chi \to 0$ for the $\ell_i \to \ell_j \chi$ decay, arises as a consequence of a naive first EFT approach. We presented two gauge invariant and renormalizable models where the decay $\ell_i \to \ell_j \chi$ is generated either at tree- or at one-loop level. After a detailed analysis of the behavior of the rate in the limit $m_\chi \ll m_i$, we find that, as a result of gauge invariance, the decay rate is finite and well behaved in the limit $m_\chi \to 0$, so that,

Type of model	f^M	g^M	f^D	g^D
Tree level	c_1	c_2	0	0
One loop	$c_3 \frac{m_\chi^2}{\Lambda^2}$	f^M	$c_4 \frac{m_\mu}{\Lambda^2}$	$-f^D$

Table 6.1: *Dominant behaviour of the monopole and dipole couplings in eq. (6.1) according to the LFV $\mu - e - \chi$ transition being generated at tree level or one loop, as found in Chapter 4. Generic dimensionless couplings are represented as c_i and Λ stands for the heavy NP scale suppressing these effective interactions. Analogous couplings for the LFV $\tau - e/\mu - \chi$ transitions are found in the same chapter.*

the decay $\ell_i \to \ell_j \chi$ matches the well studied $\ell_i \to \ell_j \gamma$ decay. As well, we analyzed the $\ell_i \to 3\ell_j$ decay mediated by an off-shell χ, also getting a finite decay rate in the limit $m_\chi \to 0$.

From the analysis developed, we learned that great care should be taken in the study on cLFV decay including a spin-one boson χ, on an EFT framework, for ensuring the finiteness of observables in the massless χ limit. As a perspective of this work, we are developing a model-independent phenomenological analysis for cLFV transitions including a gauge boson. The realizations to tree-level and one-loop level are summarized in the following effective Lagrangian with monopole (M) and dipole (D) operators

$$\mathcal{L}_{\text{eff}} = f^M_{e\mu} \bar{e} \gamma^\alpha \chi_\alpha \mu + g^M_{e\mu} \bar{e} \gamma^\alpha \gamma_5 \chi_\alpha \mu + f^D_{e\mu} \bar{e} \sigma^{\alpha\beta} \chi_{\alpha\beta} \mu + g^D_{e\mu} \bar{e} \sigma^{\alpha\beta} \gamma_5 \chi_{\alpha\beta} \mu + \text{h.c.}\,, \tag{6.1}$$

where $\chi_{\alpha\beta}$ is the abelian field-strength tensor including the Proca field χ_α, and the $\tau \to e/\mu$ transitions can be obtained by trivial modifications. Tree level generated LFV transitions only include renormalizable monopolar interactions, while LFV transitions arising at one loop include both monopolar and dipolar interactions. Couplings $\{f/g\}^{D/M}$ differ among the tree and one-loop cases as shown in table 6.1 (the flavour indices are omitted). Using this effective Lagrangian we will analyze the phenomenological consequences of the cLFV interactions, focusing on the two-body decays $\ell_i \to \ell_j \chi$, as well as, processes mediated by a virtual χ. We will also study the implications of our results in the experimental searches at MEG-II and Belle-II.

One of the golden channels in the experimental search for cLFV is the $\ell_i \to \ell_j \gamma$ decay, but its analogous process $\ell_i \to \ell_j \gamma\gamma$ has been much less explored. The best upper limits found in the literature on the BR($\ell_i \to \ell_j \gamma\gamma$) are two orders of magnitude weaker than the present limits for muon to electron and photon decay, and four orders of magnitude weaker for tau modes, $\tau \to \ell\gamma$.

In Chapter 5, we present an EFT analysis of the cLFV processes $\ell_i \to \ell_j \gamma\gamma$ and $\ell_i \to \ell_j \gamma$ through a low-energy effective Lagrangian that describes the local interaction of two charged

leptons of different flavor and two photons. Using the correlation between the $\ell_i \to \ell_j\gamma\gamma$ and the $\ell_i \to \ell_j\gamma$ decays, we derive new indirect limits on the double photon channel. We find that our bounds are one order of magnitude stronger than current experimental direct limits for $\mu \to e\gamma\gamma$, and almost three orders of magnitude better than previous considerations for $\tau \to \ell\gamma\gamma$.

Searches for $\ell_i \to \ell_j\gamma\gamma$ decays are well-motivated from an EFT and a model-building point of view. The former due to the fact that these channels allow probing new independent effective operators, thus covering a wider parameter space in the search for NP. The latter because there could exist some UV complete theories where the double-photon channel has a branching ratio higher or similar than the single-photon channel. One of these scenarios is the two Higgs doublet model, where it is possible that both decay channels have similar probabilities, as we have shown.

S. Davidson *et al.* [132] discussed the contributions of LFV two-photon vertex on the $\mu \to e$ conversions in nuclei. They found that the constraints obtained from $\mu \to e$ conversion in nuclei are one order of magnitude stronger than the ones stemming from $\mathrm{BR}(\mu \to e\gamma\gamma)$. One of the perspectives of this work is to analyze the contributions of the local interaction of two charged leptons of different flavors and two photons on the $\ell \to \tau$ conversion processes. Using our limits on the effective couplings of the LFV two-photon vertex we shall bind the $\ell \to \tau$ conversion processes and compare these with the expected sensitivity of the NA-64 experiment [149].

Summarizing, in this thesis, we presented our contributions made on the charged lepton flavor violation topic. In the first work, we corrected earlier descriptions, using in our case an EFT approach and two complementary UV complete realizations, for the behavior at ultralight gauge boson mass in the $\ell_i \to \ell_j\chi$ decays. We presented two gauge invariant and renormalizable models, either at tree or loop level, where we have explicitly checked that the decay rate remains finite in the limit $m_\chi \to 0$. In the second work, we analyzed the local interaction of two charged leptons of different flavors and two photons and found, indirectly, the strongest upper limits on $\mathrm{BR}(\ell_i \to \ell_j\gamma\gamma)$. We also motivated from an EFT and model-building point of views, the possible relevance of the search for these decay channels.

Bibliography

[1] S. L. Glashow, "Partial Symmetries of Weak Interactions," *Nucl. Phys.*, vol. 22, pp. 579–588, 1961.

[2] S. Weinberg, "A Model of Leptons," *Phys. Rev. Lett.*, vol. 19, pp. 1264–1266, 1967.

[3] A. Salam, "Weak and Electromagnetic Interactions," *Conf. Proc. C*, vol. 680519, pp. 367–377, 1968.

[4] Y. Fukuda *et al.*, "Evidence for oscillation of atmospheric neutrinos," *Phys. Rev. Lett.*, vol. 81, pp. 1562–1567, 1998.

[5] Q. R. Ahmad *et al.*, "Measurement of the rate of $\nu_e + d \rightarrow p + p + e^-$ interactions produced by ^8B solar neutrinos at the Sudbury Neutrino Observatory," *Phys. Rev. Lett.*, vol. 87, p. 071301, 2001.

[6] Q. R. Ahmad and *et al.*, "Direct evidence for neutrino flavor transformation from neutral current interactions in the Sudbury Neutrino Observatory," *Phys. Rev. Lett.*, vol. 89, p. 011301, 2002.

[7] E. P. Hincks and B. Pontecorvo, "Search for gamma-radiation in the 2.2-microsecond meson decay process," *Phys. Rev.*, vol. 73, pp. 257–258, Feb 1948. [Online]. Available: https://link.aps.org/doi/10.1103/PhysRev.73.257

[8] J. Steinberger and H. B. Wolfe, "Electrons from Muon Capture," *Phys. Rev.*, vol. 100, no. 5, p. 1490, 1955.

[9] G. Arnison *et al.*, "Further Evidence for Charged Intermediate Vector Bosons at the SPS Collider," *Phys. Lett. B*, vol. 129, pp. 273–282, 1983.

[10] P. Bagnaia *et al.*, "Evidence for $Z^0 \rightarrow e^+e^-$ at the CERN $\bar{p}p$ Collider," *Phys. Lett. B*, vol. 129, pp. 130–140, 1983.

[11] S. Abachi *et al.*, "Observation of the top quark," *Phys. Rev. Lett.*, vol. 74, pp. 2632–2637, 1995.

[12] F. Abe *et al.*, "Observation of top quark production in $\bar{p}p$ collisions," *Phys. Rev. Lett.*, vol. 74, pp. 2626–2631, 1995.

[13] K. Kodama *et al.*, "Observation of tau neutrino interactions," *Phys. Lett. B*, vol. 504, pp. 218–224, 2001.

[14] S. Chatrchyan *et al.*, "Observation of a New Boson at a Mass of 125 GeV with the CMS Experiment at the LHC," *Phys. Lett. B*, vol. 716, pp. 30–61, 2012.

[15] G. Aad *et al.*, "Observation of a new particle in the search for the Standard Model Higgs boson with the ATLAS detector at the LHC," *Phys. Lett. B*, vol. 716, pp. 1–29, 2012.

[16] F. Englert and R. Brout, "Broken Symmetry and the Mass of Gauge Vector Mesons," *Phys. Rev. Lett.*, vol. 13, pp. 321–323, 1964.

[17] P. W. Higgs, "Broken Symmetries and the Masses of Gauge Bosons," *Phys. Rev. Lett.*, vol. 13, pp. 508–509, 1964.

[18] Q. R. Ahmad and *et al.*, "Direct evidence for neutrino flavor transformation from neutral-current interactions in the sudbury neutrino observatory," *Phys. Rev. Lett.*, vol. 89, p. 011301, Jun 2002. [Online]. Available: https://link.aps.org/doi/10.1103/PhysRevLett.89.011301

[19] N. Cabibbo, "Unitary Symmetry and Leptonic Decays," *Phys. Rev. Lett.*, vol. 10, pp. 531–533, 1963.

[20] M. Kobayashi and T. Maskawa, "CP Violation in the Renormalizable Theory of Weak Interaction," *Prog. Theor. Phys.*, vol. 49, pp. 652–657, 1973.

[21] W. Buchmuller and D. Wyler, "Effective Lagrangian Analysis of New Interactions and Flavor Conservation," *Nucl. Phys. B*, vol. 268, pp. 621–653, 1986.

[22] D. B. Kaplan, "Effective field theories," in *7th Summer School in Nuclear Physics Symmetries*, 6 1995.

[23] A. Pich, "Effective field theory: Course," in *Les Houches Summer School in Theoretical Physics, Session 68: Probing the Standard Model of Particle Interactions*, 6 1998, pp. 949–1049.

[24] M. B. Einhorn and J. Wudka, "The Bases of Effective Field Theories," *Nucl. Phys. B*, vol. 876, pp. 556–574, 2013.

[25] R. Penco, "An Introduction to Effective Field Theories," 6 2020.

[26] S. Weinberg, "Phenomenological Lagrangians," *Physica A*, vol. 96, no. 1-2, pp. 327–340, 1979.

[27] S. Mihara, J. P. Miller, P. Paradisi, and G. Piredda, "Charged Lepton Flavor-Violation Experiments," *Ann. Rev. Nucl. Part. Sci.*, vol. 63, pp. 531–552, 2013.

[28] S. L. Glashow, J. Iliopoulos, and L. Maiani, "Weak Interactions with Lepton-Hadron Symmetry," *Phys. Rev. D*, vol. 2, pp. 1285–1292, 1970.

[29] B. Pontecorvo, "Inverse beta processes and nonconservation of lepton charge," *Zh. Eksp. Teor. Fiz.*, vol. 34, p. 247, 1957.

[30] G. Feinberg, "Decays of the mu Meson in the Intermediate-Meson Theory," *Phys. Rev.*, vol. 110, pp. 1482–1483, 1958.

[31] Z. Maki, M. Nakagawa, and S. Sakata, "Remarks on the unified model of elementary particles," *Prog. Theor. Phys.*, vol. 28, pp. 870–880, 1962.

[32] A. Gando *et al.*, "Reactor On-Off Antineutrino Measurement with KamLAND," *Phys. Rev. D*, vol. 88, no. 3, p. 033001, 2013.

[33] K. Abe *et al.*, "Solar Neutrino Measurements in Super-Kamiokande-IV," *Phys. Rev. D*, vol. 94, no. 5, p. 052010, 2016.

[34] F. P. An *et al.*, "New measurement of θ_{13} via neutron capture on hydrogen at Daya Bay," *Phys. Rev. D*, vol. 93, no. 7, p. 072011, 2016.

[35] K. Abe *et al.*, "Atmospheric neutrino oscillation analysis with external constraints in Super-Kamiokande I-IV," *Phys. Rev. D*, vol. 97, no. 7, p. 072001, 2018.

[36] D. Adey *et al.*, "Measurement of the Electron Antineutrino Oscillation with 1958 Days of Operation at Daya Bay," *Phys. Rev. Lett.*, vol. 121, no. 24, p. 241805, 2018.

[37] G. Bak *et al.*, "Measurement of Reactor Antineutrino Oscillation Amplitude and Frequency at RENO," *Phys. Rev. Lett.*, vol. 121, no. 20, p. 201801, 2018.

[38] M. A. Acero *et al.*, "First Measurement of Neutrino Oscillation Parameters using Neutrinos and Antineutrinos by NOvA," *Phys. Rev. Lett.*, vol. 123, no. 15, p. 151803, 2019.

[39] C. D. Shin *et al.*, "Observation of reactor antineutrino disappearance using delayed neutron capture on hydrogen at RENO," *JHEP*, vol. 04, p. 029, 2020.

[40] K. Abe *et al.*, "Constraint on the matter–antimatter symmetry-violating phase in neutrino oscillations," *Nature*, vol. 580, no. 7803, pp. 339–344, 2020, [Erratum: Nature 583, E16 (2020)].

[41] P. A. Zyla *et al.*, "Review of Particle Physics," *PTEP*, vol. 2020, no. 8, p. 083C01, 2020.

[42] H. de Kerret *et al.*, "Double Chooz θ_{13} measurement via total neutron capture detection," *Nature Phys.*, vol. 16, no. 5, pp. 558–564, 2020.

[43] R. N. Mohapatra *et al.*, "Theory of neutrinos: A White paper," *Rept. Prog. Phys.*, vol. 70, pp. 1757–1867, 2007.

[44] S. T. Petcov, "The Processes $\mu \to e + \gamma, \mu \to e + \overline{e}, \nu' \to \nu + \gamma$ in the Weinberg-Salam Model with Neutrino Mixing," *Sov. J. Nucl. Phys.*, vol. 25, p. 340, 1977, [Erratum: Sov.J.Nucl.Phys. 25, 698 (1977), Erratum: Yad.Fiz. 25, 1336 (1977)].

[45] J. I. Illana and T. Riemann, "Charged lepton flavor violation from massive neutrinos in Z decays," *Phys. Rev. D*, vol. 63, p. 053004, 2001.

[46] E. Arganda, A. M. Curiel, M. J. Herrero, and D. Temes, "Lepton flavor violating Higgs boson decays from massive seesaw neutrinos," *Phys. Rev. D*, vol. 71, p. 035011, 2005.

[47] G. Hernández-Tomé, G. López Castro, and P. Roig, "Flavor violating leptonic decays of τ and μ leptons in the Standard Model with massive neutrinos," *Eur. Phys. J. C*, vol. 79, no. 1, p. 84, 2019, [Erratum: Eur.Phys.J.C 80, 438 (2020)].

[48] V. Barger, D. Marfatia, and K. Whisnant, "Progress in the physics of massive neutrinos," *Int. J. Mod. Phys. E*, vol. 12, pp. 569–647, 2003.

[49] A. Y. Smirnov, "Neutrino physics: Open theoretical questions," *Int. J. Mod. Phys. A*, vol. 19, pp. 1180–1200, 2004.

[50] S. T. Petcov, "Towards complete neutrino mixing matrix and CP-violation," *Nucl. Phys. B Proc. Suppl.*, vol. 143, pp. 159–166, 2005.

[51] S. Weinberg, "Baryon- and lepton-nonconserving processes," *Phys. Rev. Lett.*, vol. 43, pp. 1566–1570, Nov 1979. [Online]. Available: https://link.aps.org/doi/10.1103/PhysRevLett.43.1566

[52] J. Schechter and J. W. F. Valle, "Neutrino masses in su(2) $\bigotimes$ u(1) theories," *Phys. Rev. D*, vol. 22, pp. 2227–2235, Nov 1980. [Online]. Available: https://link.aps.org/doi/10.1103/PhysRevD.22.2227

[53] R. N. Mohapatra and G. Senjanovic, "Neutrino Mass and Spontaneous Parity Nonconservation," *Phys. Rev. Lett.*, vol. 44, p. 912, 1980.

[54] A. de Gouvea and P. Vogel, "Lepton Flavor and Number Conservation, and Physics Beyond the Standard Model," *Prog. Part. Nucl. Phys.*, vol. 71, pp. 75–92, 2013.

[55] A. M. Baldini *et al.*, "Search for the lepton flavour violating decay $\mu^+ \to \mathrm{e}^+\gamma$ with the full dataset of the MEG experiment," *Eur. Phys. J. C*, vol. 76, no. 8, p. 434, 2016.

[56] A. M. Baldini and *et al.*, "The Search for $\mu^+ \to e^+\gamma$ with $10-14$ Sensitivity: The Upgrade of the MEG Experiment," *Symmetry*, vol. 13, no. 9, p. 1591, 2021.

[57] U. Bellgardt *et al.*, "Search for the Decay $\mu^+ \to e^+e^+e^-$," *Nucl. Phys. B*, vol. 299, pp. 1–6, 1988.

[58] W. H. Bertl *et al.*, "A Search for muon to electron conversion in muonic gold," *Eur. Phys. J. C*, vol. 47, pp. 337–346, 2006.

[59] A. Flores-Tlalpa, G. López Castro, and P. Roig, "Five-body leptonic decays of muon and tau leptons," *JHEP*, vol. 04, p. 185, 2016.

[60] R. M. Djilkibaev and R. V. Konoplich, "Rare Muon Decay $\mu^+ \to e^+e^-e^+\nu_e\bar{\nu}_\mu$," *Phys. Rev. D*, vol. 79, p. 073004, 2009.

[61] P. M. Fishbane and K. J. F. Gaemers, "Calculation of the Decay $\mu^- \to e^-e^+e^-\nu_\mu\bar{\nu}_e$," *Phys. Rev. D*, vol. 33, p. 159, 1986.

[62] A.-K. Perrevoort, "Sensitivity Studies on New Physics in the Mu3e Experiment and Development of Firmware for the Front-End of the Mu3e Pixel Detector," Ph.D. dissertation, U. Heidelberg (main), 2018.

[63] W. Honecker *et al.*, "Improved limit on the branching ratio of $\mu \to e$ conversion on lead," *Phys. Rev. Lett.*, vol. 76, pp. 200–203, 1996.

[64] J. Kaulard *et al.*, "Improved limit on the branching ratio of $\mu^- \to e^+$ conversion on titanium," *Phys. Lett. B*, vol. 422, pp. 334–338, 1998.

[65] J. Aysto *et al.*, "Physics with low-energy muons at a neutrino factory complex," pp. 259–306, 9 2001.

[66] D. Ambrose *et al.*, "New limit on muon and electron lepton number violation from $K_L^0 \to \mu^\pm e^\mp$ decay," *Phys. Rev. Lett.*, vol. 81, pp. 5734–5737, 1998.

[67] L. Willmann *et al.*, "New bounds from searching for muonium to anti-muonium conversion," *Phys. Rev. Lett.*, vol. 82, pp. 49–52, 1999.

[68] R. Aaij *et al.*, "Search for the lepton-flavor violating decays $B_s^0 \to e^\pm\mu^\mp$ and $B^0 \to e^\pm\mu^\mp$," *Phys. Rev. Lett.*, vol. 111, p. 141801, 2013.

[69] L. Calibbi and G. Signorelli, "Charged Lepton Flavour Violation: An Experimental and Theoretical Introduction," *Riv. Nuovo Cim.*, vol. 41, no. 2, pp. 71–174, 2018.

[70] Y. S. Amhis *et al.*, "Averages of b-hadron, c-hadron, and τ-lepton properties as of 2018," *Eur. Phys. J.*, vol. C81, p. 226, 2021, updated results and plots available at https://hflav.web.cern.ch/.

[71] A. Dainese, M. Mangano, A. B. Meyer, A. Nisati, G. Salam, and M. A. Vesterinen, Eds., *Report on the Physics at the HL-LHC,and Perspectives for the HE-LHC*, ser. CERN Yellow Reports: Monographs. Geneva, Switzerland: CERN, 2019, vol. 7/2019.

[72] B. Aubert *et al.*, "Searches for Lepton Flavor Violation in the Decays $\tau^\pm \to e^\pm\gamma$ and $\tau^\pm \to \mu^\pm\gamma$," *Phys. Rev. Lett.*, vol. 104, p. 021802, 2010.

[73] A. Abdesselam *et al.*, "Search for lepton-flavor-violating tau-lepton decays to $\ell\gamma$ at Belle," *JHEP*, vol. 10, p. 19, 2021.

[74] K. Hayasaka *et al.*, "Search for Lepton Flavor Violating Tau Decays into Three Leptons with 719 Million Produced Tau+Tau- Pairs," *Phys. Lett. B*, vol. 687, pp. 139–143, 2010.

[75] J. P. Lees *et al.*, "Limits on tau Lepton-Flavor Violating Decays in three charged leptons," *Phys. Rev. D*, vol. 81, p. 111101, 2010.

[76] W. Altmannshofer *et al.*, "The Belle II Physics Book," *PTEP*, vol. 2019, no. 12, p. 123C01, 2019, [Erratum: PTEP 2020, 029201 (2020)].

[77] M. Ablikim *et al.*, "Search for the lepton flavor violation processes $J/\psi \to \mu\tau$ and $e\tau$," *Phys. Lett. B*, vol. 598, pp. 172–177, 2004.

[78] B. Aubert *et al.*, "Searches for the decays $B^0 \to \ell^\pm\tau^\mp$ and $B^+ \to \ell^+\nu$ (l=e, μ) using hadronic tag reconstruction," *Phys. Rev. D*, vol. 77, p. 091104, 2008.

[79] R. Aaij *et al.*, "Search for the lepton-flavour-violating decays $B_s^0 \to \tau^\pm\mu^\mp$ and $B^0 \to \tau^\pm\mu^\mp$," *Phys. Rev. Lett.*, vol. 123, no. 21, p. 211801, 2019.

[80] G. Aad *et al.*, "Search for the Higgs boson decays $H \to ee$ and $H \to e\mu$ in pp collisions at $\sqrt{s} = 13$ TeV with the ATLAS detector," *Phys. Lett. B*, vol. 801, p. 135148, 2020.

[81] G. Aad and *et al.*, "Searches for lepton-flavour-violating decays of the Higgs boson in $\sqrt{s} = 13$ TeV pp collisions with the ATLAS detector," *Phys. Lett. B*, vol. 800, p. 135069, 2020.

[82] G. Aad and *et al.*, "Search for the lepton flavor violating decay $Z \to e\bar{\mu}$ in pp collisions at $\sqrt{s}$ TeV with the ATLAS detector," *Phys. Rev. D*, vol. 90, no. 7, p. 072010, 2014.

[83] M. Aaboud and *et al.*, "A search for lepton-flavor-violating decays of the Z boson into a τ-lepton and a light lepton with the ATLAS detector," *Phys. Rev. D*, vol. 98, p. 092010, 2018.

[84] M. K. Gaillard and B. W. Lee, "Rare Decay Modes of the K-Mesons in Gauge Theories," *Phys. Rev. D*, vol. 10, p. 897, 1974.

[85] J. Jaeckel and A. Ringwald, "The Low-Energy Frontier of Particle Physics," *Ann. Rev. Nucl. Part. Sci.*, vol. 60, pp. 405–437, 2010.

[86] R. Bayes *et al.*, "Search for two body muon decay signals," *Phys. Rev. D*, vol. 91, no. 5, p. 052020, 2015.

[87] A. Jodidio *et al.*, "Search for Right-Handed Currents in Muon Decay," *Phys. Rev. D*, vol. 34, p. 1967, 1986, [Erratum: Phys.Rev.D 37, 237 (1988)].

[88] H. Albrecht *et al.*, "A Search for lepton flavor violating decays $\tau \to e\alpha\,, \tau \to \mu\alpha$," *Z. Phys. C*, vol. 68, pp. 25–28, 1995.

[89] M. Marín, "Análisis de signaturas genéricas para un proceso de violación de sabor leptónico $\tau \to \ell\chi(\gamma)$," Master's thesis, Cinvestav, Cinvestav, 2016.

[90] P. Roig, "Effective Field Theory Analysis for Lepton-flavor Violating Interactions in Presence of a Boson," *Acta Phys. Polon. B*, vol. 50, pp. 1965–1970, 2019.

[91] L. B. Okun and Y. B. Zeldovich, "PARADOXES OF UNSTABLE ELECTRON," *Phys. Lett. B*, vol. 78, pp. 597–600, 1978.

[92] L. B. Okun and M. B. Voloshin, "ON THE ELECTRIC CHARGE CONSERVATION," *JETP Lett.*, vol. 28, p. 145, 1978.

[93] M. Suzuki, "SLIGHTLY MASSIVE PHOTON," *Phys. Rev. D*, vol. 38, p. 1544, 1988.

[94] F. Wilczek, "Axions and Family Symmetry Breaking," *Phys. Rev. Lett.*, vol. 49, pp. 1549–1552, 1982.

[95] B. Grinstein, J. Preskill, and M. B. Wise, "Neutrino Masses and Family Symmetry," *Phys. Lett. B*, vol. 159, pp. 57–61, 1985.

[96] Z. G. Berezhiani and M. Y. Khlopov, "Cosmology of Spontaneously Broken Gauge Family Symmetry," *Z. Phys. C*, vol. 49, pp. 73–78, 1991.

[97] J. L. Feng, T. Moroi, H. Murayama, and E. Schnapka, "Third generation familons, b factories, and neutrino cosmology," *Phys. Rev. D*, vol. 57, pp. 5875–5892, 1998.

[98] M. Hirsch, A. Vicente, J. Meyer, and W. Porod, "Majoron emission in muon and tau decays revisited," *Phys. Rev. D*, vol. 79, p. 055023, 2009, [Erratum: Phys.Rev.D 79, 079901 (2009)].

[99] J. Jaeckel, "A Family of WISPy Dark Matter Candidates," *Phys. Lett. B*, vol. 732, pp. 1–7, 2014.

[100] A. Celis, J. Fuentes-Martín, and H. Serodio, "An invisible axion model with controlled FCNCs at tree level," *Phys. Lett. B*, vol. 741, pp. 117–123, 2015.

[101] A. Celis, J. Fuentes-Martín, and H. Serôdio, "A class of invisible axion models with FCNCs at tree level," *JHEP*, vol. 12, p. 167, 2014.

[102] I. Galon, A. Kwa, and P. Tanedo, "Lepton-Flavor Violating Mediators," *JHEP*, vol. 03, p. 064, 2017.

[103] L. Calibbi, F. Goertz, D. Redigolo, R. Ziegler, and J. Zupan, "Minimal axion model from flavor," *Phys. Rev. D*, vol. 95, no. 9, p. 095009, 2017.

[104] Y. Ema, K. Hamaguchi, T. Moroi, and K. Nakayama, "Flaxion: a minimal extension to solve puzzles in the standard model," *JHEP*, vol. 01, p. 096, 2017.

[105] F. Björkeroth, E. J. Chun, and S. F. King, "Flavourful Axion Phenomenology," *JHEP*, vol. 08, p. 117, 2018.

[106] M. Bauer, M. Neubert, S. Renner, M. Schnubel, and A. Thamm, "Axionlike Particles, Lepton-Flavor Violation, and a New Explanation of a_μ and a_e," *Phys. Rev. Lett.*, vol. 124, no. 21, p. 211803, 2020.

[107] J. Heeck and H. H. Patel, "Majoron at two loops," *Phys. Rev. D*, vol. 100, no. 9, p. 095015, 2019.

[108] C. Cornella, P. Paradisi, and O. Sumensari, "Hunting for ALPs with Lepton Flavor Violation," *JHEP*, vol. 01, p. 158, 2020.

[109] L. Calibbi, D. Redigolo, R. Ziegler, and J. Zupan, "Looking forward to lepton-flavor-violating alps," *Journal of High Energy Physics*, vol. 2021, no. 9, Sep 2021. [Online]. Available: http://dx.doi.org/10.1007/JHEP09(2021)173

[110] Y. Farzan and I. M. Shoemaker, "Lepton Flavor Violating Non-Standard Interactions via Light Mediators," *JHEP*, vol. 07, p. 033, 2016.

[111] J. Heeck, "Lepton flavor violation with light vector bosons," *Phys. Lett. B*, vol. 758, pp. 101–105, 2016.

[112] Y. Farzan and J. Heeck, "Neutrinophilic nonstandard interactions," *Phys. Rev. D*, vol. 94, no. 5, p. 053010, 2016.

[113] A. Ibarra, M. Marín, and P. Roig, "Flavor violating muon decay into an electron and a light gauge boson," *Phys. Lett. B*, vol. 827, p. 136933, 2022.

[114] P. Pal, *An Introductory Course of Particle Physics*. Taylor & Francis, 2014. [Online]. Available: https://books.google.com.co/books?id=2Tf6AwAAQBAJ

[115] W. J. Marciano and A. I. Sanda, "Exotic Decays of the Muon and Heavy Leptons in Gauge Theories," *Phys. Lett. B*, vol. 67, pp. 303–305, 1977.

[116] B. W. Lee and R. E. Shrock, "Natural Suppression of Symmetry Violation in Gauge Theories: Muon - Lepton and Electron Lepton Number Nonconservation," *Phys. Rev. D*, vol. 16, p. 1444, 1977.

[117] J. M. Cornwall, D. N. Levin, and G. Tiktopoulos, "Derivation of Gauge Invariance from High-Energy Unitarity Bounds on the s Matrix," *Phys. Rev. D*, vol. 10, p. 1145, 1974, [Erratum: Phys.Rev.D 11, 972 (1975)].

[118] C. E. Vayonakis, "Born Helicity Amplitudes and Cross-Sections in Nonabelian Gauge Theories," *Lett. Nuovo Cim.*, vol. 17, p. 383, 1976.

[119] B. W. Lee, C. Quigg, and H. B. Thacker, "Weak Interactions at Very High-Energies: The Role of the Higgs Boson Mass," *Phys. Rev. D*, vol. 16, p. 1519, 1977.

[120] M. S. Chanowitz and M. K. Gaillard, "Multiple Production of W and Z as a Signal of New Strong Interactions," *Phys. Lett. B*, vol. 142, pp. 85–90, 1984.

[121] A. M. Sirunyan *et al.*, "Search for supersymmetric partners of electrons and muons in proton-proton collisions at $\sqrt{s} = 13$ TeV," *Phys. Lett. B*, vol. 790, pp. 140–166, 2019.

[122] G. Aad *et al.*, "Search for electroweak production of charginos and sleptons decaying into final states with two leptons and missing transverse momentum in $\sqrt{s} = 13$ TeV pp collisions using the ATLAS detector," *Eur. Phys. J. C*, vol. 80, no. 2, p. 123, 2020.

[123] A. Abada, M. E. Krauss, W. Porod, F. Staub, A. Vicente, and C. Weiland, "Lepton flavor violation in low-scale seesaw models: SUSY and non-SUSY contributions," *JHEP*, vol. 11, p. 048, 2014.

[124] A. Ibarra, M. Marín, and P. Roig, "Flavor violating ℓ_i decay into ℓ_j and a light gauge boson," *SciPost*, vol. XX, p. YY, (to be published in SciPost, within the proceedings of the 16th International Workshop on TAU lepton Physics), 2022.

[125] E. De La Cruz-Burelo, M. Hernández-Villanueva, and A. De Yta-Hernández, "New method for beyond the Standard Model invisible particle searches in tau lepton decays," *Phys. Rev. D*, vol. 102, no. 11, p. 115001, 2020.

[126] F. Tenchini, M. García-Hernández, T. Kraetzschmar, P. K. Rados, E. De La Cruz-Burelo, A. De Yta-Hernández, I. Heredia de la Cruz, and A. Rostomyan, "First results and prospects for tau LFV decay $\tau \to e + \alpha$(invisible) at Belle II," *PoS*, vol. ICHEP2020, p. 288, 2021.

[127] G. Hernández-Tomé, J. I. Illana, M. Masip, G. López Castro, and P. Roig, "Effects of heavy Majorana neutrinos on lepton flavor violating processes," *Phys. Rev. D*, vol. 101, no. 7, p. 075020, 2020.

[128] I. Pacheco and P. Roig, "Lepton flavor violation in the Littlest Higgs Model with T parity realizing an inverse seesaw," *JHEP*, vol. 02, p. 054, 2022.

[129] M. Aiba *et al.*, "Science Case for the new High-Intensity Muon Beams HIMB at PSI," 11 2021.

[130] J. Dreitlein and H. Primakoff, "Possible neutrinoless decay modes of the muon," *Phys. Rev.*, vol. 126, pp. 375–378, Apr 1962. [Online]. Available: https://link.aps.org/doi/10.1103/PhysRev.126.375

[131] J. D. Bowman, T. P. Cheng, L.-F. Li, and H. S. Matis, "New Upper Limit for $\mu \to e\gamma\gamma$," *Phys. Rev. Lett.*, vol. 41, pp. 442–445, 1978.

[132] S. Davidson, Y. Kuno, Y. Uesaka, and M. Yamanaka, "Probing $\mu e\gamma\gamma$ contact interactions with $\mu \to e$ conversion," *Phys. Rev. D*, vol. 102, no. 11, p. 115043, 2020.

[133] D. Grosnick *et al.*, "Search for the Rare Decay $\mu^+ \to e^+\gamma\gamma$," *Phys. Rev. Lett.*, vol. 57, p. 3241, 1986.

[134] A. Gemintern, S. Bar-Shalom, G. Eilam, and F. Krauss, "Lepton flavor violating decays $L \to \ell\gamma\gamma$ as a new probe of supersymmetry with broken R parity," *Phys. Rev. D*, vol. 67, p. 115012, 2003.

[135] A. Cordero-Cid, G. Tavares-Velasco, and J. J. Toscano, "Implications of a very light pseudoscalar boson on lepton flavor violation," *Phys. Rev. D*, vol. 72, p. 117701, 2005.

[136] J. I. Aranda, F. Ramírez-Zavaleta, J. J. Toscano, and E. S. Tututi, "Higgs mediated lepton flavor violating tau decays $\tau \to \mu\gamma$ and $\tau \to \mu\gamma\gamma$ in effective theories," *Phys. Rev. D*, vol. 78, p. 017302, 2008.

[137] J. I. Aranda, A. Flores-Tlalpa, F. Ramírez-Zavaleta, F. J. Tlachino, J. J. Toscano, and E. S. Tututi, "Effective Lagrangian description of Higgs mediated flavor violating electromagnetic transitions: Implications on lepton flavor violation," *Phys. Rev. D*, vol. 79, p. 093009, 2009.

[138] D. A. Bryman, S. Ito, and R. Shrock, "Upper limits on branching ratios of the lepton-flavor-violating decays $\tau \to \ell\gamma\gamma$ and $\tau \to \ell X$," *Phys. Rev. D*, vol. 104, no. 7, p. 075032, 2021.

[139] I. Angelozzi, "In pursuit of lepton flavour violation : A search for the $\tau \to \mu\gamma\gamma$ decay with ATLAS at $\sqrt{s}$ =8 TeV," Ph.D. dissertation, U. Amsterdam, IHEF, 2017.

[140] S. Actis *et al.*, "Quest for precision in hadronic cross sections at low energy: Monte Carlo tools vs. experimental data," *Eur. Phys. J. C*, vol. 66, pp. 585–686, 2010.

[141] F. Fortuna, A. Ibarra, X. Marcano, M. Marín, and P. Roig, "Indirect upper limits on $\ell_i \to \ell_j\gamma\gamma$ from $\ell_i \to \ell_j\gamma$," 10 2022.

[142] A. Celis, V. Cirigliano, and E. Passemar, "Model-discriminating power of lepton flavor violating τ decays," *Phys. Rev. D*, vol. 89, no. 9, p. 095014, 2014.

[143] D. A. Bryman, S. Ito, and R. Shrock, "Upper limits on branching ratios of the lepton-flavor-violating decays $\tau \to \ell\gamma\gamma$ and $\tau \to \ell X$," *Phys. Rev. D*, vol. 104, no. 7, p. 075032, 2021.

[144] P. W. Cattaneo and A. Schöning, "MEG II and Mu3e status and plan," *EPJ Web Conf.*, vol. 212, p. 01004, 2019.

[145] A. M. Sirunyan *et al.*, "Search for lepton flavour violating decays of the Higgs boson to $\mu\tau$ and eτ in proton-proton collisions at $\sqrt{s} = 13$ TeV," *JHEP*, vol. 06, p. 001, 2018.

[146] R. Harnik, J. Kopp, and J. Zupan, "Flavor Violating Higgs Decays," *JHEP*, vol. 03, p. 026, 2013.

[147] M. Bauer, M. Neubert, S. Renner, M. Schnubel, and A. Thamm, "The Low-Energy Effective Theory of Axions and ALPs," *JHEP*, vol. 04, p. 063, 2021.

[148] L. Calibbi, D. Redigolo, R. Ziegler, and J. Zupan, "Looking forward to lepton-flavor-violating ALPs," *JHEP*, vol. 09, p. 173, 2021.

[149] S. Gninenko, S. Kovalenko, S. Kuleshov, V. E. Lyubovitskij, and A. S. Zhevlakov, "Deep inelastic $e-\tau$ and $\mu-\tau$ conversion in the NA64 experiment at the CERN SPS," *Phys. Rev. D*, vol. 98, no. 1, p. 015007, 2018.